Assessing storm energy reduction by the vegetated salt marsh platform in Newbury, MA: A background to enhancing natural protection by the living shoreline

Municipal Vulnerability Preparedness Grant Program

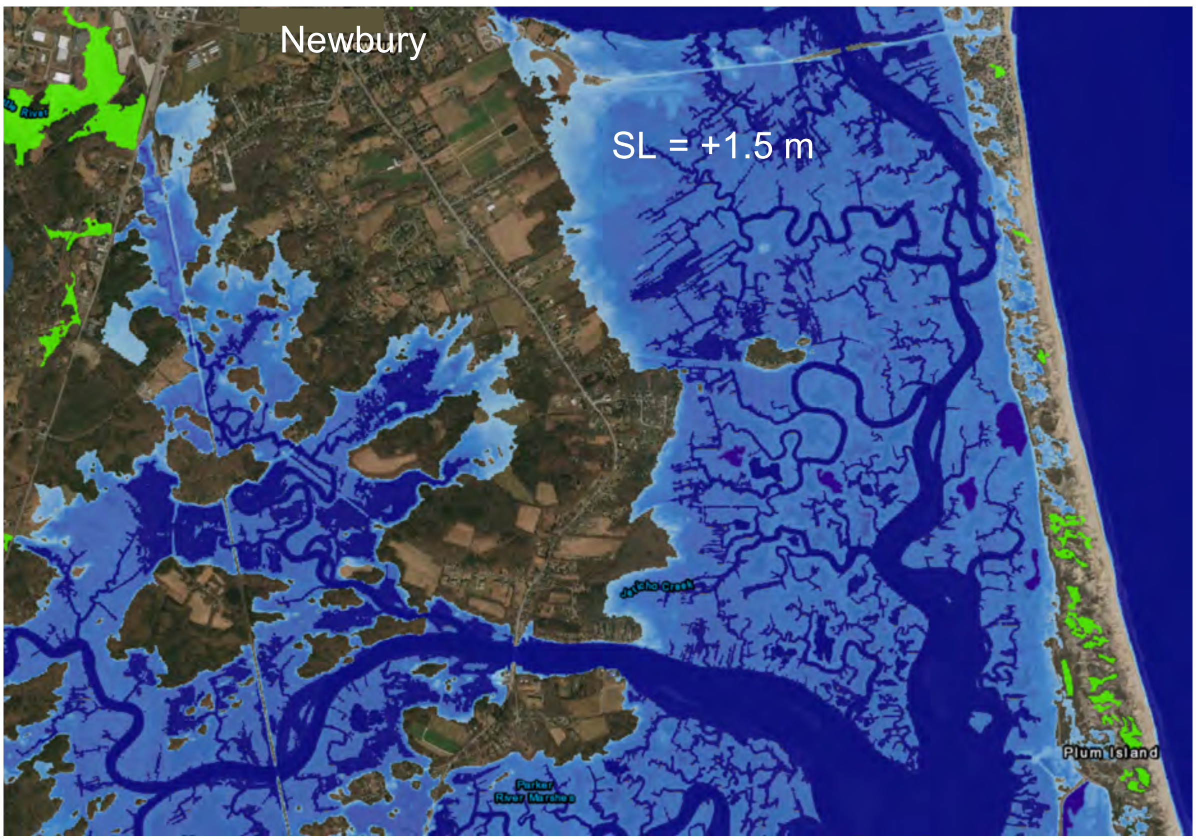

NOAA inundation map of Newbury, MA for a 1.5 m rise in sea level.

January 2020

Boston University: *Duncan FitzGerald, Zoe Hughes, & Alyssa Novak*

University of New Orleans: *Ioannis Georgiou, Madeline Foster-Martinez, & Md Mohuiddin Sakib*

Town of Newbury: *Geoffrey Walker*

Executive Summary

Winter storms along the North Shore and throughout Massachusetts are increasingly causing widespread flooding and wave erosion, particularly during periods of large astronomic tides coupled with the passage of powerful extra-tropical storms. Like many coastal communities along the North Shore, the Town of Newbury is vulnerable to the effects of global warming and climate change, conditions leading to an increase in the rate of sea-level rise (SLR) and a greater frequency and magnitude of coastal storms. One of the major appealing characteristics of Newbury is that beautiful marshes, estuaries, and tidal flats surround much of the town. However, because of Newbury's coastal setting and extensive marshlands, many landowners abut the marsh and are susceptible to flooding during intense northeasters. Studies of hurricane impacts along the Gulf coast have demonstrated that regions having expansive wetlands, such as those comprising the Louisiana coast, can significantly reduce storm surges and wave energy. The impetus of this study was to analyze if platform marshes bordering Newbury would provide the same reduction in storm energy along its shoreline.

To evaluate the capacity of the saltmarsh to attenuate storm surge and waves and assess its vulnerability of Newbury to future sea-level rise, we simulated several selected storms using a coupled flow and wave model based on Delft3D modeling suite. We validated the model for flow and tides using previous measurements in Plum Island Sound that were collected in 2015 and new data obtained in a major instrument deployment during the Fall 2019 - Winter 2020 period. The topography of the marsh surface was determined from LiDAR data and detailed RTK surveys. For the model runs, roughness of the marsh surface was determined from data collected along three marsh transects. Detailed measurement included elevation, percentage of type of vegetation, and stem density. Existence of salt pannes, pools, tidal creeks, and other features were also noted.

The primary storms influencing Newbury are northeasters, but the region is also impacted by less frequent southwesterly extra-tropical cyclones and occasional hurricanes. We identified four storm scenarios (most frequent direction and intensity) based on the combined storm analyses conducted by the WHG during their modeling of Plum Island for Hurricane Sandy 1 project as well as the Wave Information Study (WIS). The selected storms were then used in the final simulations for present conditions, and for future conditions under scenarios of sea level rise identified in the proposal (see Kopp et al., 2017). Wave height and storm surge attenuation were evaluated at seven different sites throughout the Newbury marsh and shoreline. The characteristic of the marsh were manipulated to simulate 1. different roughness of the marsh occurring during the growth season (robust plants) and the winter (ice flattened), 2. different plant types, 3. conversion to tidal flat, 4. ditch filling, 5. addition of oyster reefs, and 6. sea level rise scenarios.

One of the major findings in our modeling is the importance of vegetation in attenuating wave storm energy. Reducing drag by removing vegetation in the model produced dramatically different results. Without vegetation only 35% of the transects reached complete attenuation, whereas with vegetation 85% reached complete attenuation across all four storms simulated. In the absence of vegetation, only drag due to topography reduces wave height. Modeling showed that for the largest wave in each of the simulated storms (at spring high tide) waves were completely attenuated before reaching the upland surrounding the marsh. There were two minor exceptions to this pattern (e.g., reduced from 0.53 m to 0.05 m), but these occurred where waves were propagating across a relatively narrow marsh (< 600 m).

Our regional modeling suggests that the topography of the marsh platform, with or without vegetation, does little to attenuate the storm surge, meaning that the water elevation along the shoreline during the storm is almost the same as it is in open water areas, such as in upper Plum Island Sound. During major storms, the entire backbarrier behaves as a large open-water pond. Although some attenuation does occur as flooding from the sound enters the tidal creeks, once the marsh platform is flooded, storm winds push water against the upland topography encompassing most of Newbury. Thus, sea-level rise will not appreciably increase storm surge height. However, as the marsh surface lowers, the surge will impact the upland shoreline sooner during major storms.

TABLE OF CONTENTS

LIST OF ILLUSTRATIONS

INTRODUCTION

Winter storms along the North Shore and throughout Massachusetts are increasingly causing extensive flooding and wave erosion, particularly during periods of large astronomic tides coupled with the passage of intense extra-tropical storms. For example, slow moving storms in January and March of 2018 contained gale-forces winds with gusts greater than 60 mph, producing two of the three highest storm surges ever-recorded in Boston Harbor and was felt throughout all the coastal communities surrounding the Great Marsh. Kurt Schwartz, director of the Massachusetts Emergency Management Agency described these storms as resembling: “damage caused by a Category 1 hurricane.” The clear imprint of these storms was observed by the loss of beach, dune scarping, and overwash along Castle Neck, Plum Island, and Salisbury Beach. Inland areas also suffered from extensive flooding including waves crashing over the Plum Island Turnpike (Figure 1), standing water affecting sewer systems, and impacts to Plum Island Shellfish Purification Plant (Wade, 2018). Numerous roadways in Newbury became impassible, including Pine Island Road, Newman Road, and portions of Cottage Road and Hay Street. These conditions present an obvious impediment and danger for rescue and service vehicles (Figure 1).

Like many coastal communities along the North Shore, the Town of Newbury is vulnerable to the effects of global warming and climate change, conditions that are leading to an increase in the rate of sea-level rise (SLR) and a greater frequency and magnitude of coastal storms. The record winter northeasters of 2018 and size and influence of Hurricane Sandy in 2012 portend the ferocity of the future storm climate in New England. The increasing frequency of flooding in downtown Boston and in other coastal cities is a direct consequence of rising sea level. Predicted SLR and increased storm surge elevations have the potential to significantly and negatively impact Newbury’s coastal economy, facilities, and infrastructure upon which the community relies.

At a Municipal Vulnerability Preparedness Workshop held for the Town of Newbury in May of 2018 at the Parker River National Wildlife Refuge, town officials and other attendees listed seven priority actions. The highest priority centered on the Great Marsh and included measures to improve resiliency, erosion and hydrology management, and continue protection efforts among other actions. Additionally, the third highest priority focused on emergency access roads, including Plum Island Turnpike, Northern Boulevard, Hanover Street, and Pine Island Road, emphasizing the need for plans to reduce flooding, raise roadways, and improve drainage. Given the town’s identification of these top priorities, the proposed project is aimed at quantifying how the existing marsh system reduces storm surge elevation and wave energy and will investigate measures to enhance marsh resiliency utilizing “living shoreline” concepts (NOAA, 2017; WHG, 2017).

The Town of Newbury’s goals are directly aligned with MVP’s grant objective: *Detailed Vulnerability and Risk Assessment,* which includes projects that map and evaluate vulnerable community facilities, vulnerable populations, natural resources and/or infrastructure using best available techniques and climate projections are eligible. Thus, the impetus for this research study was to:

1. Provide maps depicting marsh elevation, marsh vegetation types and morphological units
2. Produce time series of wave heights and tidal elevation conditions during a variety of storm and non-storm conditions.
3. Analyze vegetation versus marsh elevation

4. Describe how seal level rise and storm scenarios were chosen
5. Examine input parameters for Delft3D and SWAN modeling
6. Interpret modeling results
7. Discuss how vegetation on Newbury marshes reduces wave energy and storm surge elevation
8. Relate how future increases in SLR and increased storminess will affect the Newbury shoreline and uplands

Figure 1 Photos during and following the Bomb Cyclone of 4 January 2018, providing a glimpse of the vulnerability of this coastal community. A. Water Street, B. Plum Island Turnpike, C. Pine Island Road, and D. Plum Island.

Background

Saltmarsh and waterways comprise and or define much of the east, south, and western borders of the Town of Newbury, including portions of the Great Marsh, Parker River National Wildlife Refuge, and state Wildlife Management Areas. In fact, marshes comprise 30% of the town's acreage. Newbury is fronted by Plum Island, which has a high residence density and region prone to storm erosion and flooding. Using FEMA's most recent 2014 Flood Insurance Rate Map, MVPC (2016) determined that Newbury has 7,825 acres (12.3 mi^2) of land, including salt marsh that is located within the 100-year floodplain. This represents 47% of town land, which is therefore susceptible to flooding during a 100-event (Figure 2). This is the highest acreage and percentage of town land of the 15 communities comprising the Merrimack Valley region (MVPC, 2016). The Parker River and its major tributary, the Little River, and their subordinate tributaries spread far inland and extend east-west across Newbury connecting to Plum Island Sound. This channel system is entirely tidal, which means that during periods of significant storms, tidal surges extend far inland. It also means that freshwater moving downstream in tributaries during high precipitation events may back-up where these streams enter tidal channels. Together these conditions are responsible for flooding roadways and endangering town facilities and infrastructure.

In the present regime of accelerating SLR and increase storm magnitude and frequency, the sustainability of coastal protection is of growing importance, including for small coastal communities (Figure 2 & Figure 3). The magnitude of storm surges and wave energy that reach a coastline are two of the most important criteria in designing coastal defenses. It is widely recognized that salt marshes are able to significantly attenuate wave energy (Möller 2006, Yang et al 2012, Wu et al 2013). As waves propagate across a marsh, they lose energy by moving vegetation and performing work, which directly results in smaller wave heights. The amount of wave reduction is related to width and elevation of the marsh, the type and density of vegetation, depth of water, and wave characteristics (Yang et al 2012, Wu et al 2013). For example, as seen in Figure 1, waves broke across Water Street during 4 March 2018 storm at a site where the marsh is less than 100 yards wide. In contrast, nearby wider breadths of marsh experienced some flooding but no breaking waves. Like wave energy, storm surges produced by hurricanes and large extratropical storms can also be lessened by an expanse of wetlands. Marshes impart an overall roughness to the landward propagating bulge of water comprising a storm surge thereby decreasing its height. Studies in the Netherlands (Stark et al, 2015) and in Louisiana (Fischbach et al 2015) demonstrate that the degree of reduction is dependent on marsh elevation and morphology, its relief, and type of marsh vegetation.

Given that 47% of the Town of Newbury is within the 100-yr floodplain (Figure 2) and witnessing the flooding that occurred twice during this past winter throughout much of the town, the importance of preserving and enhancing the saltmarsh is a recognized goal of Newbury's Municipality Preparedness Plan, receiving its highest priority. This decision is justified because the town fully recognizes that SLR is accelerating, as has been demonstrated from the Boston Harbor tide gage data (NOAA, 2018). This trend and increasing storm impacts have also been discussed in detailed in the exhaustive Climate Ready Boston report (Boston Ready Advisory Group, 2016; Duncan FitzGerald and Zoe Hughes were part of this scientific team and co-authored the report). This project uses field data as inputs to a hydrodynamic and wave model to quantify how much wave energy and storm surge reduction occurs from wind and waves approaching the shoreline from different directions (and therefore different marsh widths, elevation, types of vegetation, etc.) and for given storm surge elevations (and higher SLR positions).

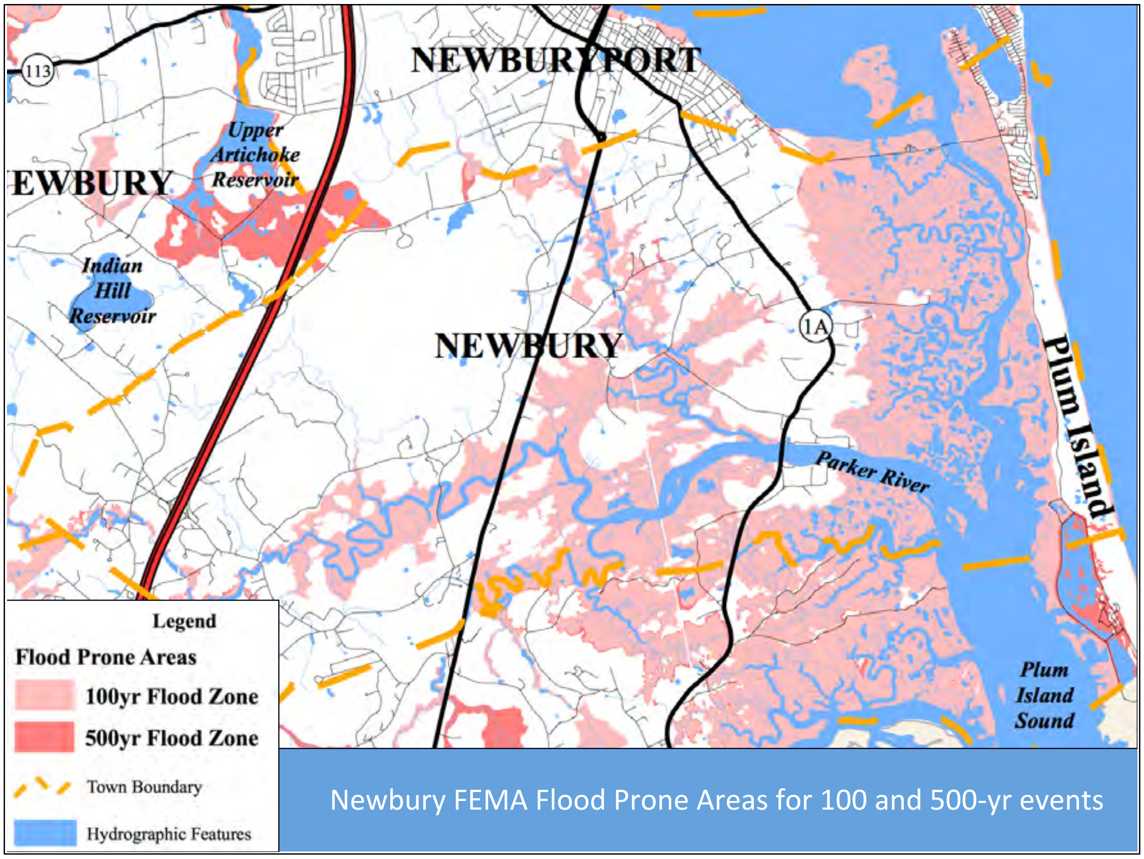

Figure 2. Federal Emergency Management Agency flood zones.

The results of these analyses are used to explore (from a modeling standpoint) the viability of modifying and/or expanding the marsh where possible to further increase marsh resiliency and decrease storm impacts. For example, tidal flats immediately adjacent to the marsh edge can be modified to support *Spartina alterniflora,* thereby building a wider marsh system that would further reduce wave energy. Other possible living shoreline defenses to explore would include: 1) thin layer deposition, 2) changing upland grass/shrubbery species to better absorb wave energy (i.e., planting *Phragmites* along north side of the Plum Island Turnpike) 3) installing oyster or mussel reefs, and 4) encouraging vegetation that adds greater roughness that would reduce wave heights. The findings of this project should aid the Town in planning and managing is assets. The results help identify what portions of the Town are most vulnerable to storm surge and breaking waves, what measures can be taken to increase marsh resiliency and improve the marsh's ability to reduce storm impacts, and how to prioritize Town resources.

Need for Assistance

A study of vulnerability of the Great Marsh region by MVPC (2016) demonstrates that the town has 799 residential, commercial, industrial, and institutional structures within the 100-year floodplain. Based the 2014 Assessor's records, these structures collectively are valued at \$124.9 million with *Residential* structures accounting for \$114.8 million, *Commercial* at \$3.9 million,

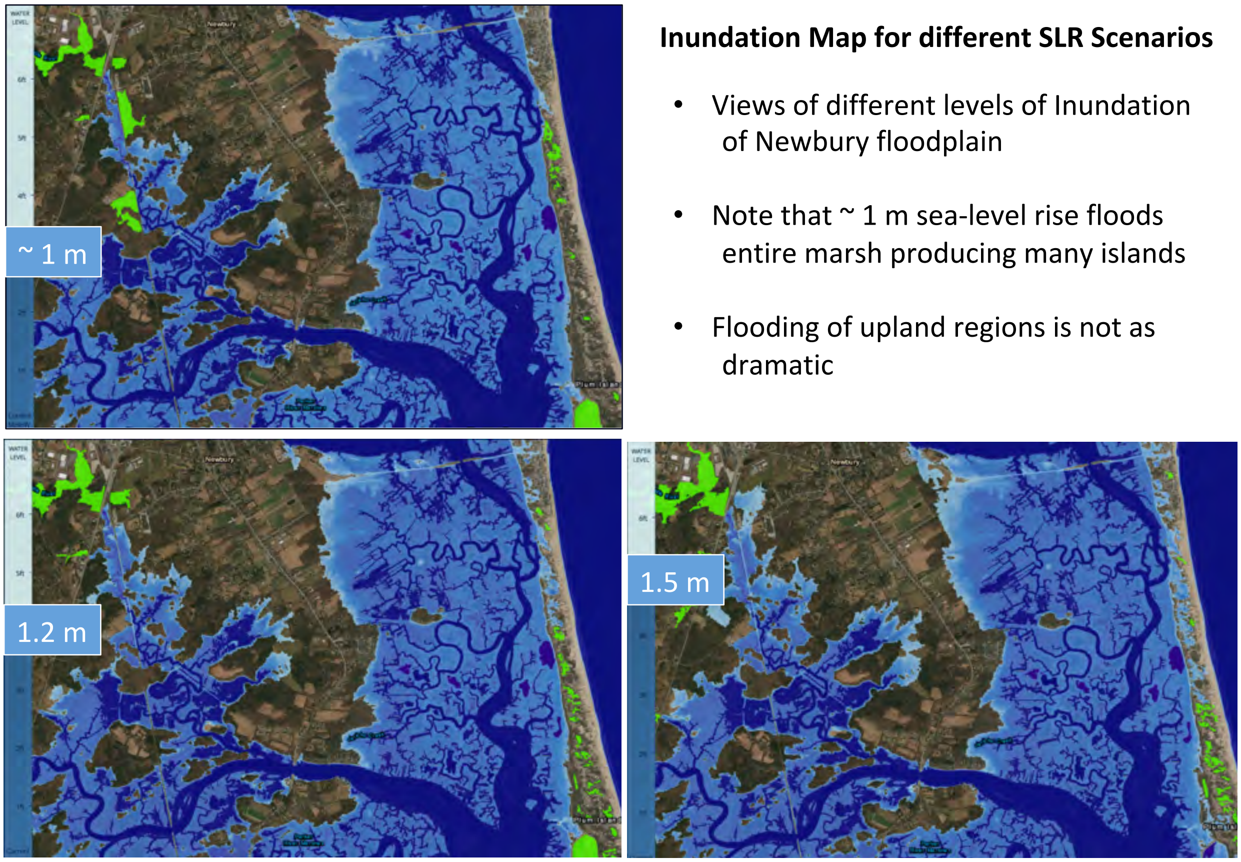

Figure 3. Newbury inundation maps for different SLR scenarios (from NOAA, 2018).

Institutional at $5.8 million, and *Industrial* at $322,800. There are 443 flood insurance policies for properties within FIRM flood hazard areas with a combined insurance value of $118.4million (National Flood Insurance Program [NFIP] Policy Statistics for Massachusetts, 2014). The town is highly proactive in flood plain management activities and is in compliance with NFIP requirements. Most of these activities have involved updating bylaws, training sessions, inspections, adopting revised flood maps, etc. One of the town's *Projects in Development* as part of their Mitigation Action Plan is to incorporate climate change/sea level rise scenarios for future hazard mitigation planning and implementation. The results of this study will be helping to provide important information for implementing the Town's plan.

It should be noted that Newbury is a small rural residential community (pop. ~6800) and its operating budget is heavily funded by the residential property tax and excise tax (82%). Consequently, funding studies and implementing structural projects to respond to and better quantify flooding and future climate changes have been an increased burden to residential taxpayers. Thus, it was necessary for this project to be financially supported by Municipality Vulnerability Preparedness program, as Newbury has no other source of funding. Particularly, given that the town is part of a large system – all of which needs to be considered in the study in order to inform the towns decisions. Due to the similarities in setting the results of this project will be directly transferable to other nearby towns and will be of use to State and federal organizations working in the Great Marsh. All of our results and data will be made available to groups, such as Fish and Wildlife Service and the NSF funded PIE-LTER.

There are very few coastal communities in MA with environmental justice populations, particularly those fronted by barrier islands and marshes. However, data from the 2000 Census indicates that in contrast to its neighbors, Newbury has a higher percentage of lower income households and a lower percentage of high-income households. It also has a notably high percentage of senior residents, and, thus, a larger than normal vulnerable population.

Physical Setting

The Merrimack Embayment in northern Massachusetts is a formerly glaciated terrain now fronted by a 34-km long, mixed-energy barrier island system (sensu, Hayes 1979). The central barrier along this coast is Plum Island bordered to the north by the Merrimack River estuary, the second largest freshwater discharge into the Gulf of Maine. The other tidal inlets along the chain are associated with diminutive estuaries having small drainage basins (FitzGerald 1993). Inlets are anchored next to bedrock outcrops or occur between resistant drumlin landforms (FitzGerald and van Heteren 1999). Stabilization of the landward migrating proto-Plum Island barrier occurred circa 3.6 ka (Hein et al 2012) leading to the development of Plum Island Sound and evolution of the contiguous Great Marsh. The Great Marsh is an internationally-recognized Important Bird Area, and a region that supports dozens of federal trust species, as well as state and federally designated Critical Natural Landscapes.

The backbarrier of Plum Island is dominated by an elongate, north-southward trending shallow lagoonal estuary floored by ubiquitous intertidal and subtidal sand bodies (Figure 4). Mean depth along the thalweg gradually deepens from < 2 m proximal to the upper Parker River to > 10 m at the estuary mouth. The wetlands of Newbury form the northern portion of this system extending from just south of the Parker River north to the Merrimack River estuary. This region experiences semi-diurnal tides with a mean range of 2.8 m, increasing to more than 3.7 m during perigean spring tidal conditions (NOAA 2019). The vast majority of the backbarrier tidal prism (32×10^6 m^3; Valiano and Hopkinson 1998) is exchanged through Plum Island Sound inlet at the southern end of Plum Island, with some additional tidal water discharged into the Merrimack Estuary through Plum Island creek (2.3×10^6 m^3; Zhao et al 2010).

Newbury consists of broad platform marshes dissected by several major channels including the Parker and Plum Island Rivers and several smaller creeks such as Little River, Plumbush, Pine Island Creek, Little Pine Island Creek, and Jericho Creek (Figure 5). The high marsh is dominated by *Spartina patens* and *Distichlis spicata*, and the less extensive low marsh is vegetated by short-form *Spartina alterniflora*. Long- and short- form *Spartina alterniflora* are typically found along creek banks and in poorly drained areas, respectively (Wilson et al 2014). Low marsh areas have an average elevation of 0.98 m above mean sea level; high marshes are ~40 cm higher and flood only during spring tides (Valentine and Hopkinson 2005; Millette et al 2010). Tidal channels and anthropogenic ditches dissect the entire marsh and numerous large and small salt pannes and ponds spot the high marsh surface. More detailed information concerning the vegetation is given in Vegetation Transects section of the report.

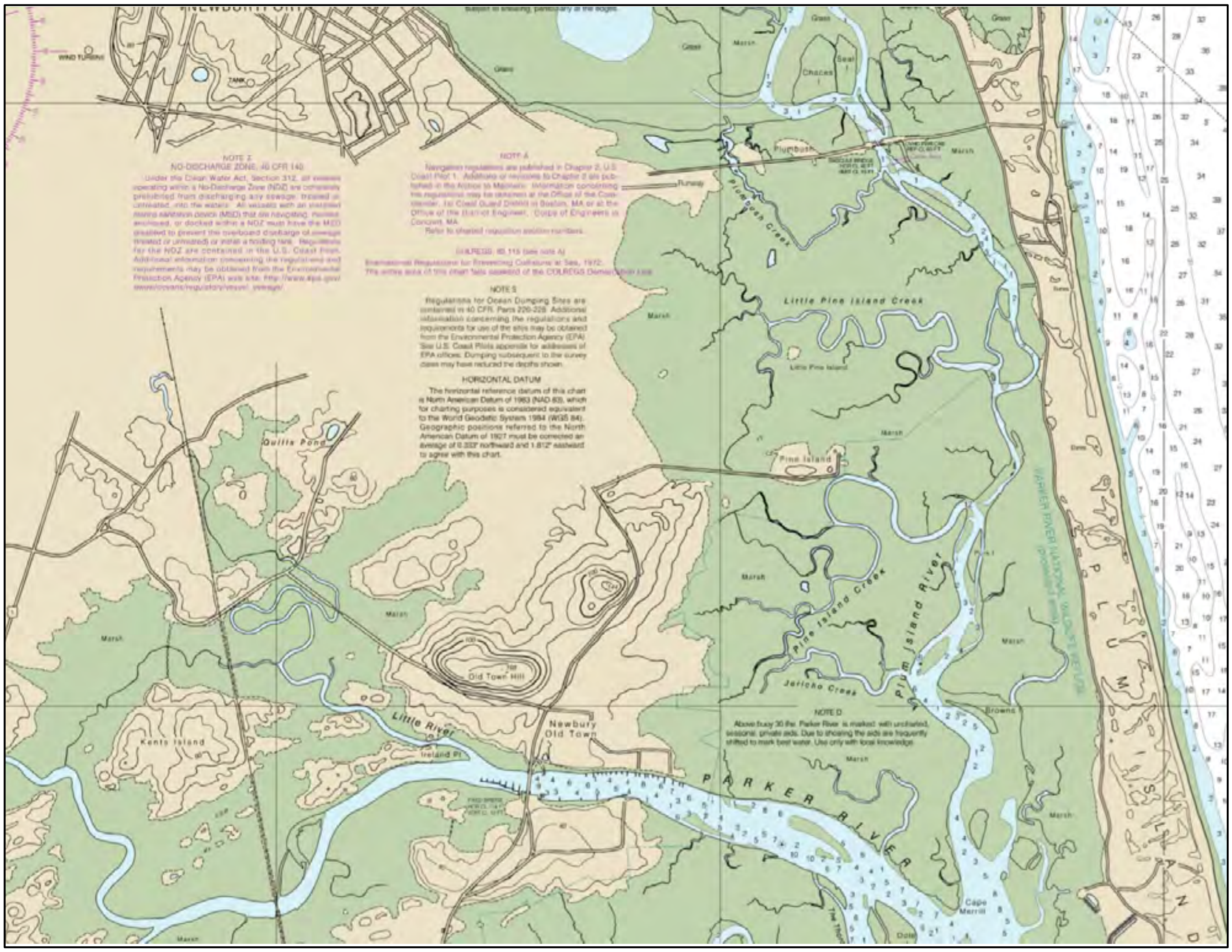

Figure 4. NOAA coastal chart of the northern (Newbury Sector) of Plum Island Sound and Great Marsh region.

The Great Marsh and Plum Island Sound are fed by several small rivers (Zhao et al 2010) draining coastal lowlands dominated glacial and paraglacial deposits (Stone et al., 2006; Hein et al., 2014, 2014). Of these, the Rowley and the Eagle Hill rivers are nearly entirely tidal and have negligible freshwater inputs, whereas the Parker and Ipswich rivers have small freshwater catchments of 167 km^2 (annual discharge: 0.033 km^3) and 402 km^2 (annual discharge: 0.056 km^3), respectively (Sammel, 1967; Simcox, 1992). The largest contribution of freshwater and suspended sediment to the coastal ocean is the Merrimack River, which has a watershed area of 12,885 km^2, an average discharge of 6.5 km^3/yr, and total suspended sediment load of 74,880 MT/yr (Shawler et al 2019). Circulation models demonstrate that suspended sediment from the Merrimack River can enter Plum Island Sound either directly through the Plum Island creek or

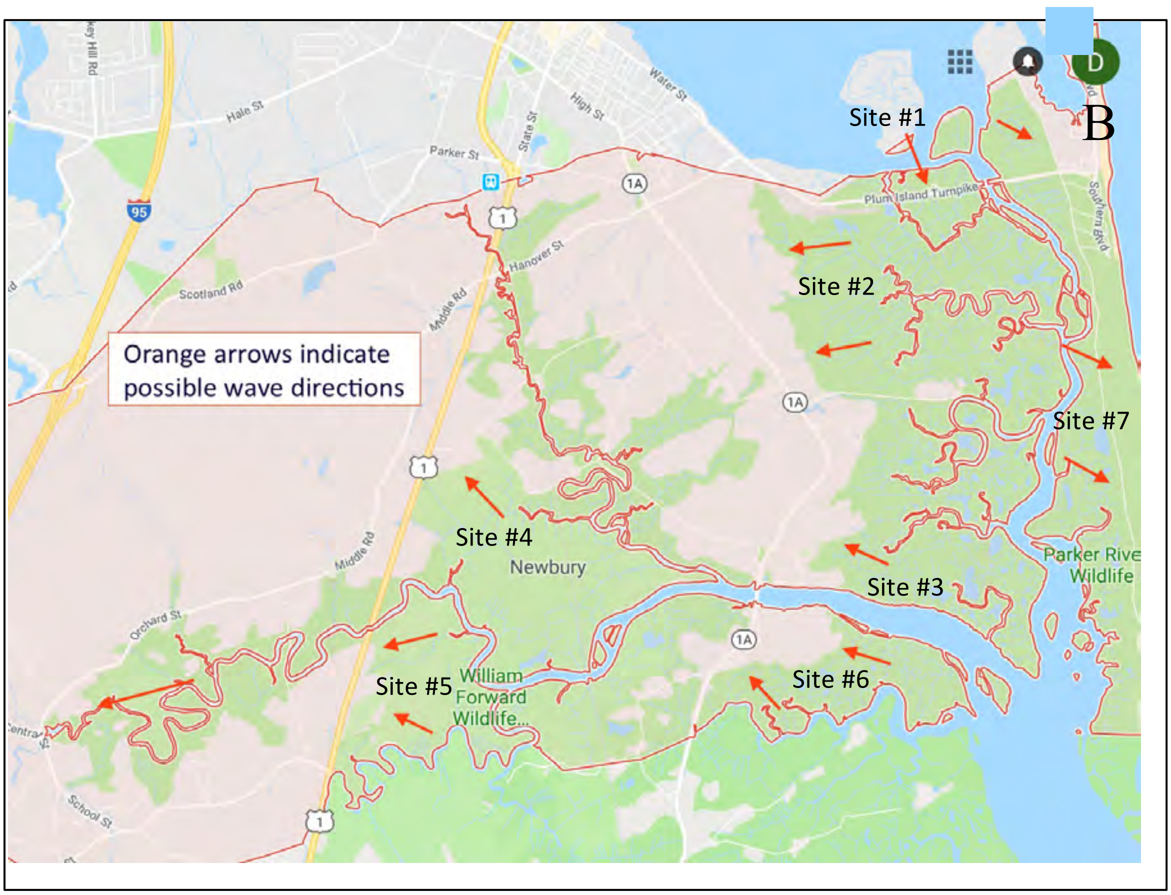

Figure 5. Map of Newbury: A. Boundaries showing major tidal rivers and tidal creeks; green areas showing flooding. B. Areas within the Town of concern and named throughout this report by these numbers.

via the coastal ocean through the Plum Island Sound Inlet (Zhao et al., 2010). A sediment budget for the Great Marsh by Hopkinson et al (2018) estimates that the total quantity of sediment entering the estuary via streams (primarily Parker and Essex) is 3,210 MT/yr, consisting 43% organic and 57% mineral matter. They determined that an additional 10,032 MT/yr of sediment is released to the estuary via marsh edge erosion. Together these sources accounted for only 41% of the sediment required to build the marsh vertically in the present regime of RSLR. Thus, they reasoned that the 59% of the sediment must be coming from the coastal ocean and erosion of tidal flats. The study demonstrates the Great Marsh is in a cannibalistic state.

METHODS

Vegetation Surveys

Modeling storm surge and wave propagation across the marsh requires information on the amount of frictional resistance that is imparted to the bulge of surging water and the waves. This parameter (C_D, roughness) is a function of vegetation type, stem density, stem width, and canopy height, and its impact changes with changing water level. To assess the roughness parameter, vegetation was mapped along 3 transects at each site with a Trimble model 5800 real time kinematic (RTK) differential GPS. The sites included: The Plum Island Turnpike, Kent Island, and Parker River (see Figure 18). At each site, one transect was oriented to run from the edge of a creek/water body toward the upland border with sampling occurring at 100 m intervals. At each sampling location, a GPS point and an elevation measurement was recorded. In addition, vegetation attributes (species composition, percent cover, canopy height, and stem density) were collected using a 0.5 m^2 quadrat and the habitat type (e.g., creek edge, low marsh, high marsh, pool, panne, or upland) was described. All areas along the transect containing > 1.0 m^2 of invasive vegetation (e.g., *Leipidium densiflorum, Phragmites australis*) were delineated, as well as areas experiencing changes in species composition due to increased tidal inundation. Vegetation clipped from 0.0625 m^2 plots (25 cm quadrat) were taken back to the lab. The information collected during the vegetation surveys was used to calculate roughness as well as to inform the storm models (see below).

Hydrodynamic Field Measurements

Instruments were deployed along three cross-shore transects to directly measure the wave height transformation across the marsh. These transects were oriented to capture wave activity due to wind from three directions: north (Transect #1), east (Transect #2), and south (Transect #3). Each transect was arranged in the same manner. Wave gauges were placed at the seaward edge of the marsh (flats station), at the edge of the marsh (shore station), and landward into the marsh (inland station). The east and south transects were oriented such that they inland station was shared between them (Figure 6).

The wave gauges used were RBR Solos, RBR TWRs, and one RBR Duo. These devices take bursting pressure measurements, meaning they take a set number of measurements at a given time interval. The RBR Solos were programmed to turn on, or "burst," every 5 minutes and take 4096 measurements at 16 Hz. The RBR TWRs took 1024 measurements at 4 Hz every 15 minutes, and the RBR Duo took 2048 measurements at 6 Hz every 10 minutes. The instruments were deployed on November 27, 2018, and took measurements until January 7, 2019. The readings from simultaneous measurements were used to determine how wave heights transform over the marsh in different conditions. This data was used to calculate the roughness parameter.

via the coastal ocean through the Plum Island Sound Inlet (Zhao et al., 2010). A sediment budget for the Great Marsh by Hopkinson et al (2018) estimates that the total quantity of sediment entering the estuary via streams (primarily Parker and Essex) is 3,210 MT/yr, consisting 43% organic and 57% mineral matter. They determined that an additional 10,032 MT/yr of sediment is released to the estuary via marsh edge erosion. Together these sources accounted for only 41% of the sediment required to build the marsh vertically in the present regime of RSLR. Thus, they reasoned that the 59% of the sediment must be coming from the coastal ocean and erosion of tidal flats. The study demonstrates the Great Marsh is in a cannibalistic state.

METHODS

Vegetation Surveys

Modeling storm surge and wave propagation across the marsh requires information on the amount of frictional resistance that is imparted to the bulge of surging water and the waves. This parameter (C_D, roughness) is a function of vegetation type, stem density, stem width, and canopy height, and its impact changes with changing water level. To assess the roughness parameter, vegetation was mapped along 3 transects at each site with a Trimble model 5800 real time kinematic (RTK) differential GPS. The sites included: The Plum Island Turnpike, Kent Island, and Parker River (see Figure 18). At each site, one transect was oriented to run from the edge of a creek/water body toward the upland border with sampling occurring at 100 m intervals. At each sampling location, a GPS point and an elevation measurement was recorded. In addition, vegetation attributes (species composition, percent cover, canopy height, and stem density) were collected using a 0.5 m^2 quadrat and the habitat type (e.g., creek edge, low marsh, high marsh, pool, panne, or upland) was described. All areas along the transect containing > 1.0 m^2 of invasive vegetation (e.g., *Leipidium densiflorum, Phragmites australis*) were delineated, as well as areas experiencing changes in species composition due to increased tidal inundation. Vegetation clipped from 0.0625 m^2 plots (25 cm quadrat) were taken back to the lab. The information collected during the vegetation surveys was used to calculate roughness as well as to inform the storm models (see below).

Hydrodynamic Field Measurements

Instruments were deployed along three cross-shore transects to directly measure the wave height transformation across the marsh. These transects were oriented to capture wave activity due to wind from three directions: north (Transect #1), east (Transect #2), and south (Transect #3). Each transect was arranged in the same manner. Wave gauges were placed at the seaward edge of the marsh (flats station), at the edge of the marsh (shore station), and landward into the marsh (inland station). The east and south transects were oriented such that they inland station was shared between them (Figure 6).

The wave gauges used were RBR Solos, RBR TWRs, and one RBR Duo. These devices take bursting pressure measurements, meaning they take a set number of measurements at a given time interval. The RBR Solos were programmed to turn on, or "burst," every 5 minutes and take 4096 measurements at 16 Hz. The RBR TWRs took 1024 measurements at 4 Hz every 15 minutes, and the RBR Duo took 2048 measurements at 6 Hz every 10 minutes. The instruments were deployed on November 27, 2018, and took measurements until January 7, 2019. The readings from simultaneous measurements were used to determine how wave heights transform over the marsh in different conditions. This data was used to calculate the roughness parameter.

Hydrodynamic and Wave Modeling

To evaluate and assess storm surge and wave attenuation along the Great Marsh fronting the Town of Newbury, we used a hydrodynamic and wave modeling suite (Delft3D; Lesser et al., 2004), which has been used successfully to study storm surge and wave dynamics throughout the world. We leveraged previously funded efforts (e.g. Hurricane Sandy NFWF study in Plum Island Sound – FitzGerald et al., 2017) during which time hydrodynamic data were collected throughout Plum Island Sound. The model, which was validated for tidally-induced currents, was supplemented with waves. This approach enabled us to assess wave propagation throughout the great marsh with dynamic coupling during storm conditions, to better evaluate changes in waves heights throughout the basin.

The Delft3D hydrodynamics and wave modeling suite is a numerical process-based model that is capable of resolving hydrodynamics, sediment transport, and resulting morphology under the combined effects of currents and waves (Lesser et al 2004). The Delft3D suite can be used to simulate flow and wave propagation in coastal and deltaic marsh environments, including fine-scale circulation and over-marsh flow in saltmarsh (e.g., Caldwell et al 2014; Hanegan and Georgiou 2015; Sullivan et al 2015) and was recently employed to investigate hurricane storm surge and resulting sedimentation on Louisiana wetlands during Hurricane Gustav (Liu et al 2018; Sullivan et al 2015).

Model domain and grid development

The resolution of the flow grid for Plum Island Sound model (PIS-Delft3D) varies from 200m offshore of Plum Island to 20-40 m in the vicinity of tidal inlets and throughout the backbarrier. The coupled wave grid has similar resolution offshore but then reduces to 60 m in the vicinity of tidal inlets and across the marsh. In the focus areas surrounding the Town of Newbury we used a different modeling approach using a higher resolution transect model (~1 m) to better study the effects of vegetation, bathymetry transitions oyster reefs and other alternatives (see section Marsh Transect Wave Attenuation Model for more detail).

Initial conditions

The model bathymetry utilizes the most recent bathymetry available for the area: (1) regional bathymetry for the coastal ocean based on the Coastal Relief Model from NOAA, (2) regional LiDAR obtained from the US Army Corps of Engineers in 2014, and (3) additional RTK data taken during the Hurricane Sandy NFWF study in Plum Island Sound 2015 to resolve smaller tidal channels and marsh edge topography. Future marsh surface elevations for future SLR scenarios were determined using projections of the marsh surface using accretion measurements also derived from Hurricane Sandy NFWF study, where 15 cores throughout the Great Marsh were collected and analyzed for accretion using Pb^{210} and Cs^{137}.

Boundary conditions

Tides and Storm Surge: For tidal conditions at the open marine boundary we used tidal constituents from the East Coast tidal database (Mukai et al 2002). For the selected storms used in the analysis, we used time-series of storm surge, from the North Atlantic Coastal Study (NACS) as well as re-analysis of storms from the Wave Information Study (WIS) from the US Army Corps of Engineers.

Winds and Waves: Similarly, we used storm surge from the (NACS) supplemented with wave heights, wave periods from the Wave Information Study (WIS) from the US Army Corps of Engineers. Storm waves were simulated using the third-generation wave model SWAN (Booij et al 1999). Time-dependent waves at the open boundary followed NACS and WIS derived conditions. The wind-generation module within SWAN was activated, including water-level setup (increase storm surge elevation) due to waves to better determine water level setup due to waves.

Vegetation: Rather than parameterizing vegetation through the Delft3D module, we decided to assess the effects of vegetation in attenuating waves on a much finer scale, and thus used the transect model which has a 1 m resolution to do so. The transect data were used to characterize drag on the flow field and dampen wave energy over the marsh platform using a vegetation-enhanced friction term (see Marsh Transect Wave Attenuation Model for more detail).

Calibration/Validation

The model was validated using data collected under non-storm conditions by leveraging existing observations collected by the PIs in 2015 which includes a nearshore (~10 m) deployment northeast of the tidal inlet in Plum Island. During our 2015 campaign, instrument tripods were deployed throughout PIS and hydrodynamic data were collected simultaneously. Wave data were not collected at that time, so we used the deployments under this effort to validate waves in Plum Island Sound. Model was tuned to reproduce observed conditions by adjustment of the bottom friction term.

Storm Characterization and analysis

To quantify the effectiveness of the present-day marsh system in reducing storm impacts, we characterized the types of storms that impact Newbury. This information is also be needed to evaluate how potential marsh modifications may help to reduced wave and surge conditions for future sea level positions. The primary storms influencing Newbury are normally northeasters, but there are less frequent southwesterly extra-tropical cyclones as well as the infrequent hurricanes. We utilized the storm analysis conducted by the WHG during their modeling of Plum Island for Hurricane Sandy 1 project, as well as the storm analysis conducted under the Wave Information Study (WIS) to identify 4 scenarios from the record produced. We have identified several dominant events, both in terms of most frequent in terms of direction and intensity. The selected storms were then used in the final simulations for present conditions, and for future conditions under scenarios of sea level rise identified in the proposal (e.g. Kopp et al., 2017).

Data Processing

Vegetation data

Vegetation samples from 0.0625 m^2 plots (25 cm quadrats) were collected for further measurements. Stem widths were calculated from the stem counts and bundle diameters (i.e. the vegetation bundled together). Elevation data from the RTK survey was matched with the corresponding vegetation quadrat data. It was then imported to ArcMap for spatial analysis and Matlab for computation analysis.

Figure 6. Site of the w ave and current meter sensors that helped to calibrate and validate the wave model. Deployments were made along Transects #1-3.

Data storage

The data has been converted to Network Common Data Form (netCDF). NetCDF is a common format for storing data in public repositories because it does not require proprietary software to access. Metadata was collected and written into the files (e.g. project information, instrument specs and locations, etc). Including the metadata ensures the data will be both accessible and interpretable for future users.

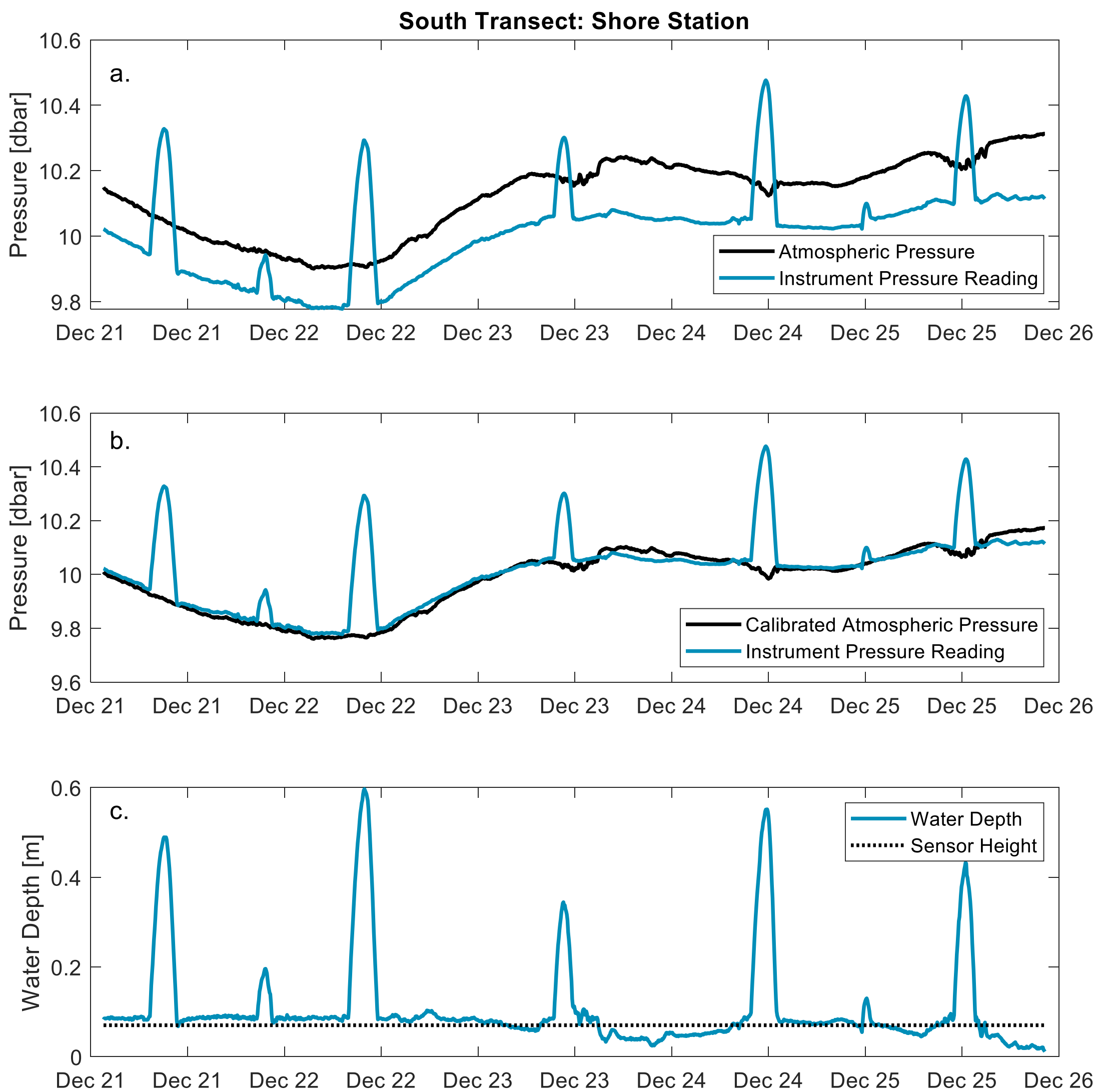

Figure 7. Steps in processing from raw pressure data to water depth at the shore station in the south instrument transect (Transect #3). a) Atmospheric pressure and raw instrument pressure readings. b) Calibrated atmospheric pressure (offset removed) and raw instrument pressure + sensor height).

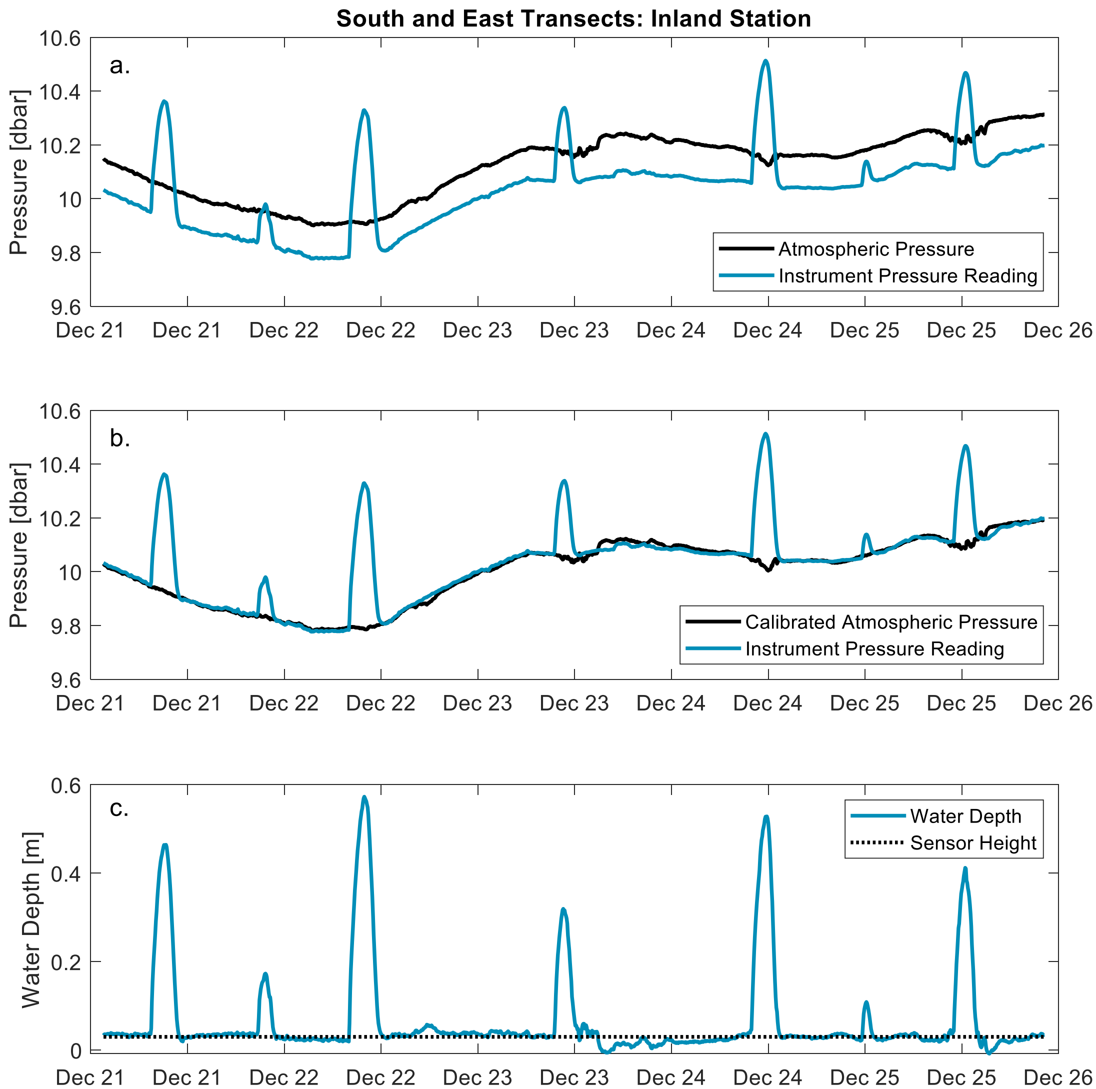

Figure 8. Steps in processing from raw pressure data to water depth at the inland station in the south and east instrument transects (Transects #2&3). a) Atmospheric pressure and raw instrument pressure readings. b) Calibrated atmospheric pressure (offset removed) and raw instrument pressure readings. c) Water depth (raw pressure reading – calibrated atmospheric pressure + sensor height).

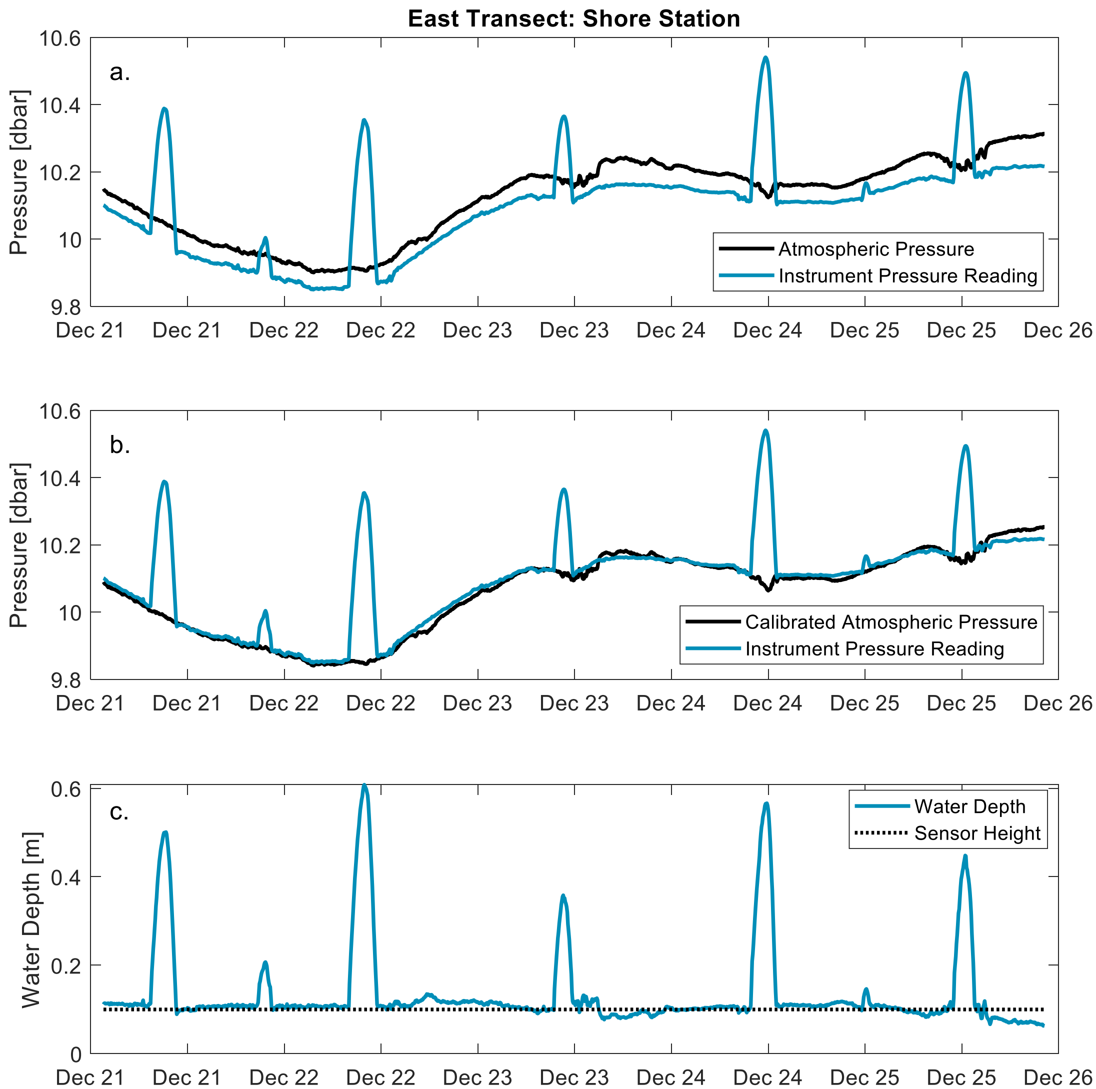

Figure 9. Steps in processing from raw pressure data to water depth at the shore station in the east instrument transect (Transect #2). a) Atmospheric pressure and raw instrument pressure readings. b) Calibrated atmospheric pressure (offset removed) and raw instrument pressure readings. c) Water depth (raw pressure reading – calibrated atmospheric pressure + sensor height).

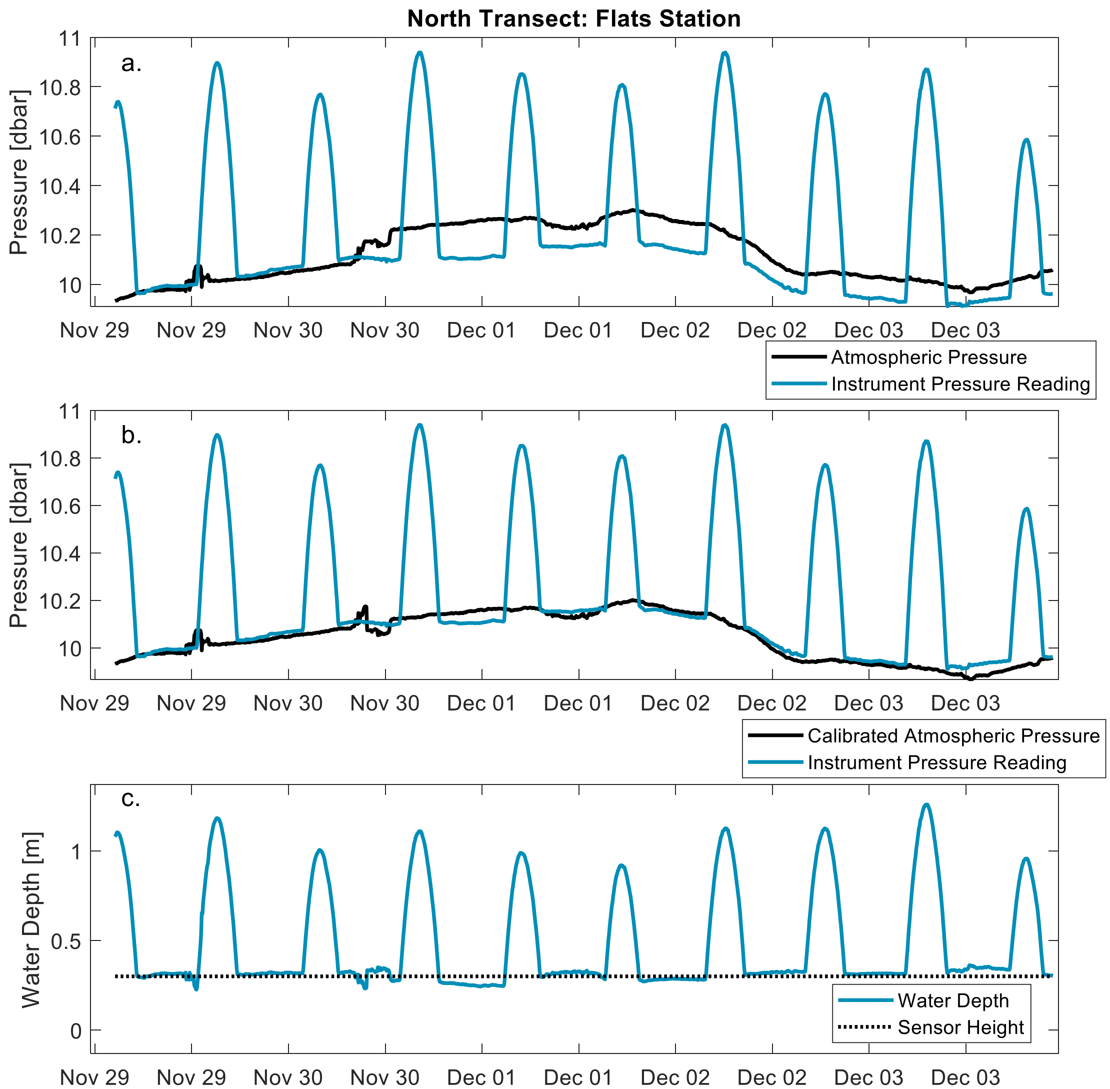

Figure 10. Steps in processing from raw pressure data to water depth at the flats station in the north transect (Transect #1). a) Atmospheric pressure and raw instrument pressure readings. b) Calibrated atmospheric pressure (offset removed) and raw instrument pressure readings. c) Water depth (raw pressure reading – calibrated atmospheric pressure + sensor height).

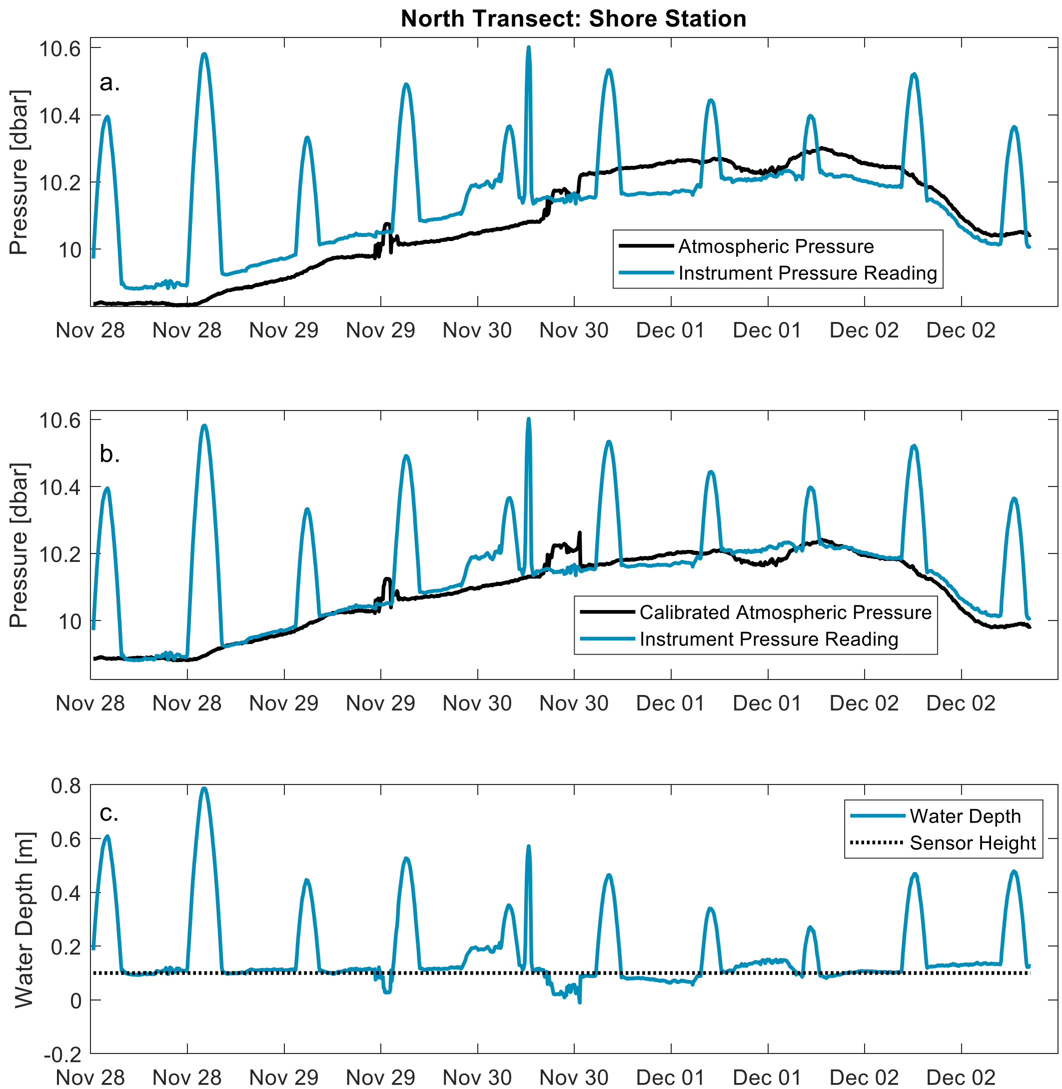

Figure 11. Steps in processing from raw pressure data to water depth at the shore station in the north transect (Transect #1). a) Atmospheric pressure and raw instrument pressure readings. b) Calibrated atmospheric pressure (offset removed) and raw instrument pressure readings c) Water depth (raw pressure reading – calibrated atmospheric pressure + sensor height).

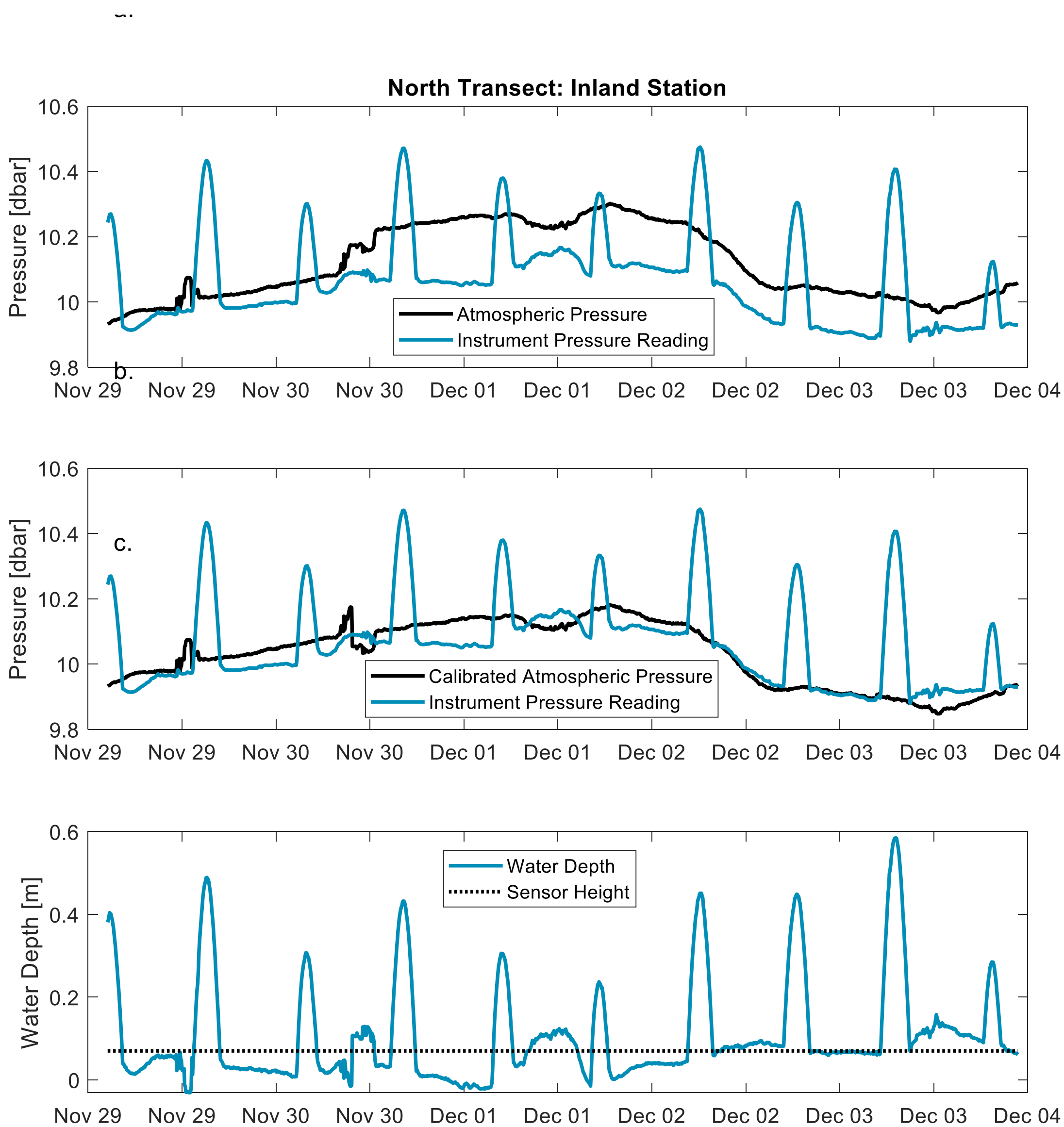

Figure 12. Steps in processing from raw pressure data to water depth at the inland station in the north transect (Transect #1). a) Atmospheric pressure and raw instrument pressure readings. b) Calibrated atmospheric pressure (offset removed) and raw instrument pressure reading. c) Water depth (raw pressure reading – calibrated atmospheric pressure + sensor height).

Wave Statistics

Data from the nine pressure sensors were processed to produce information on how waves transform across the marsh (Figure 6). The first processing step was to remove atmospheric pressure from the signal. A sensor was deployed above the water surface to measure atmospheric pressure. There was a steady offset between the pressure sensors and the atmospheric data (Figure 7a, Figure **8**a, Figure **9**a, Figure **10**a, Figure **11**a, Figure **12**a). To calibrate the data, this offset is determined by comparing the data when all sensors are dry. Examples of the calibrated atmospheric pressure readings and the instruments pressure readings can be seen in Figure 7c, Figure **8**c, Figure **9**c, Figure **10**c, Figure **11**c, Figure **12**c.

Wave statistics, namely significant wave height (H_s) and the root mean square of wave height (H_{RMS}), were calculated from the high frequency pressure sensors following the methods of Wiberg and Sherwood (2008). Modeling the wave heights as a Rayleigh distribution, H_s and H_{RMS} are calculated as:

$$H_{RMS} = \frac{H_s}{\sqrt{2}} = 2\sqrt{2m_0} = 2\sqrt{2\int S_\eta(f)df} = \sqrt{2\sum_i S_{\eta,i}\,\Delta f_i} \qquad (Eq. 1)$$

where $S_\eta\ (f)$ is the spectral density of the water surface elevation with corrections for the height of the pressure sensor. The peak wave period, T_p, is the period with the most energy in the spectrum, S_η. The wavenumber, k_p, is determined by iteration from the dispersion relation. The bottom orbital velocity is calculated as:

$$u_b = \sqrt{2}\left(\sum_i \left[\frac{4\pi^2}{T_i^2 \sinh^2(k_i h)} S_{\eta,i}\Delta f_i\right]\right)^{1/2} \qquad (Eq. 2)$$

Values for H_{RMS}, T_p, k_p, and u_b were calculated for each burst of measurements. Results from simultaneous bursts were compared then compared to assess wave transformation. Water depth, h, was calculated as the average pressure across the whole burst of measurements.

Wave attenuation

There are two common models for wave attenuation across a vegetated surface (*i.e.* marsh), exponential decay and form drag. Exponential decay is the simpler of the two, as it is not

process-based; the model is as follows (Kobayashi et al., 1993):

$$\frac{H_{RMS}}{H_{0,RMS}} = e^{-k_i x} \qquad (Eq. 3)$$

where H_{RMS} is the wave height farther landward, $H_{0,RMS}$ is the incident wave height (*i.e.* wave height seaward), and x is the distance between these points. We used the H_{RMS} values for each burst to calculate the decay constant, k_i, which was then used to compare the attenuation between stations.

Modeling vegetation as a form drag is processed-based and requires additional information on the wave climate and vegetation characteristics. Wave energy dissipated due to vegetative drag is modeled as:

$$\frac{\partial E c_g}{\partial x} = \frac{\partial\left(\frac{1}{8}\rho g H_{rms}^2\right) c_g}{\partial x} = -\langle\epsilon_{\mathrm{v}}\rangle \qquad (Eq. 4)$$

Where E is the wave energy density, c_g is group velocity, ρ is water density, and g is the gravitational constant. The dissipation due to vegetative drag is modeled as (Mendez and Losada, 2004):

$$-\langle\epsilon_{\mathrm{v}}\rangle = -\left(\frac{2}{3\pi}\right)\rho C_D b_v N \left(\frac{g k_p}{2\sigma_p}\right)^3 \frac{\sinh^3 k_p \alpha h + 3\sinh k_p \alpha h}{3k_p \cosh k_p h}\frac{3\sqrt{\pi}}{4} H_{rms}^3 \qquad (Eq. 5)$$

Where b_v is the diameter if the vegetation stem (m), N is the number of vegetation stems in a square meter (m^{-2}), α is the ratio of the water depth to the vegetation height (h_v/h), and C_D is the coefficient of drag. Substituting Eq. 5 into Eq. 4 and applying boundary conditions of H_{RMS} at $x = 0$ is $H_{RMS,0}$ gives:

$$H_{rms} = \frac{H_{0,rms}}{1 + \tilde{\beta} x} \qquad (Eq. 6)$$

Where:

$$\tilde{\beta} = \frac{1}{3\sqrt{\pi}} C_D b_v N H_{0,rms} k_p \frac{\sinh^3 k_p \alpha h + 3\sinh k_p \alpha h}{\left(\sinh 2k_p h + 2k_p h\right)\sinh k_p h} \qquad (Eq. 7)$$

All quantities in this equation besides the drag coefficient or roughness parameter, C_D, were measured by the pressure sensors, calculated from pressure data, or measured during the vegetation survey. Therefore, C_D, is directly solved for each burst of measurements.

The drag coefficient is often found to vary with the Reynolds number (Re), a non-dimensional value that indicates the level of turbulence. Here, a stem Reynolds number is calculated as:

$$Re = \frac{u_b b_v}{\nu} \qquad (Eq. 8)$$

Where ν is kinematic viscosity. Previous studies have found the following relation between C_D and Re:

$$C_D = a + \left(\frac{b}{Re}\right)^c \qquad (Eq. 9)$$

Using the measured and calculated values of C_D and Re, this equation was fit to the data, and the constants ($a, b,$ and c) were determined.

Marsh Transect Wave Attenuation Model

A marsh transect wave attenuation (MTWA) model was built to understand the level of protection provided by the Newbury marsh in different conditions. The MTWA model operates on a shore-normal transect, similar to the setup for the field deployments. It tracks wave height along the transect as it progresses from open water, over the marsh edge, and across the marsh platform. The MTWA model has four processes, which transform the wave height: shoaling, drag from bottom roughness, drag from vegetation, and interaction with scarps. The model does not include wave setup or wave regeneration due to wind, which could cause greater wave propagation. The MTWA model evaluates cell by cell, where a cell is a 1 m in length. It is a one-dimensional model (*i.e.* the cell does not have a width). The criteria for determining the process at work in a given cell is given in Figure 15 and stepped through in detail below.

Inputs: There are three sources of data input to the MTWA model: Army Corps of Engineering LiDAR dataset (2014), results from the vegetation surveys conducted as part of this study, and Delft 3D model output. The Delft 3D model output contains all the wave and depth information for the particular storm and tide condition being modeled.

Processes

Interactions with Scarps and Shoaling: If the cell is inundated, the elevation change between previous cell and current cell is checked. If the elevation difference between these two cells exceeds 0.6 m, it is determined to be a scarp. If the ratio of the cell depth to the scarp height is less than 0.4, the following relationship is applied:

$$H = H_0 * 2.366 * \left(\frac{h}{h_{scarp}}\right)^{1.698} \qquad (Eq. 10)$$

Where h_{scarp} is the height of the scarp, H_0 is the wave height in the previous cell, and H is the wave height in the current cell. This empirical relationship was formulated from the wave data collected in this study (Figure 13).

If ratio of the cell depth to the scarp height is greater than 0.4, shoaling is applied following Green's law (Dean and Dalrymple, 1991):

$$H = H_0 \left(\frac{h_0}{h}\right)^{\frac{1}{4}} \qquad (Eq. 11)$$

Where h_0 is the depth in the previous (seaward) cell.

Bottom Roughness: If the elevation of the cell is less than 0.1 m NAVD88, and it was determined to not be a scarp, then drag from bottom roughness is applied. The drag from bottom roughness is calculated for a flat bottom slope following Dean and Dalrymple (1991):

$$K_f = \left[1 + \frac{8f_w}{6\pi} \frac{k^2 H_{rms,0} \Delta x}{(2kh + \sinh(2kh)) \sinh(kh)}\right]^{-1} \qquad (Eq. 12)$$

Where k is the wave number, and f_w is the wave friction factor defined as (Nielsen 1992):

$$f_w = exp\left[5.213\left(\frac{2\pi\, k_b}{T\, u_B}\right)^{0.194} - 5.977\right] \qquad (Eq. 13)$$

Where k_b is the roughness length scale, which was set to 0.01, and T is the wave period. The wave height is then calculated as:

$$H = H_0 K_f \qquad (Eq. 14)$$

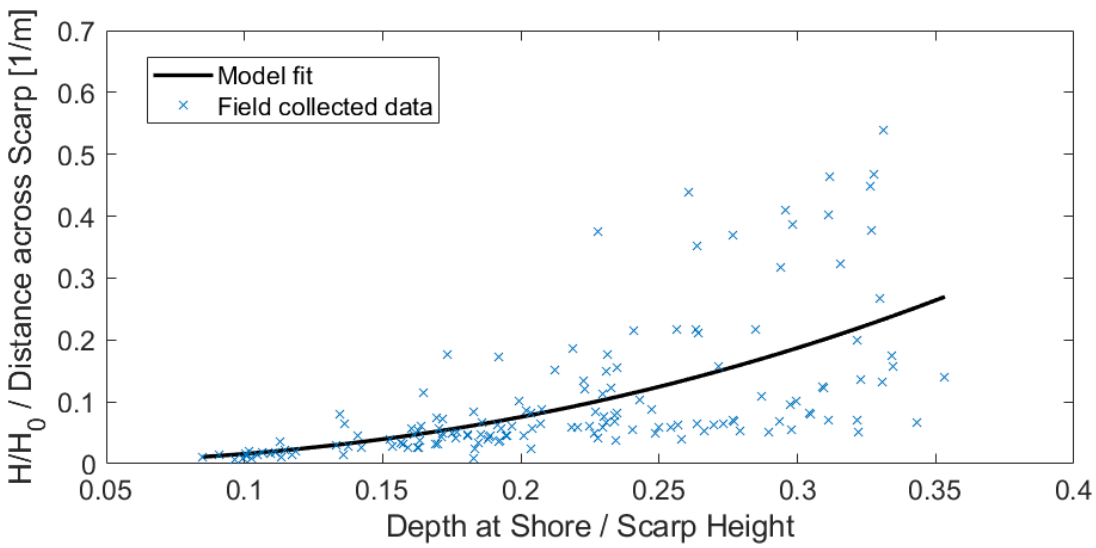

Figure 13. Empirical model used for wave transformation over a marsh scarp

Drag due to Vegetation: If the elevation is greater than 0.1 m NAVD88, and it was determined to not be a scarp, then it is considered vegetated (*i.e.* marsh). First, the Reynolds number, Re, is calculated from the inputs from Delft 3D and the vegetation survey. The drag coefficient, C_D, is calculated as follows:

$$C_D = -0.528 + \left(\frac{222.4}{Re}\right)^{0.804} \qquad (Eq. 15)$$

This relationship is used for values of Re near the range of those observed during the field (Figure 13). For Re below 21, C_D is set to 6, and for those above 390, it is set to 0.2. The drag coefficient is then used in Eq 6 and 7 to calculate the wave height in the given cell.

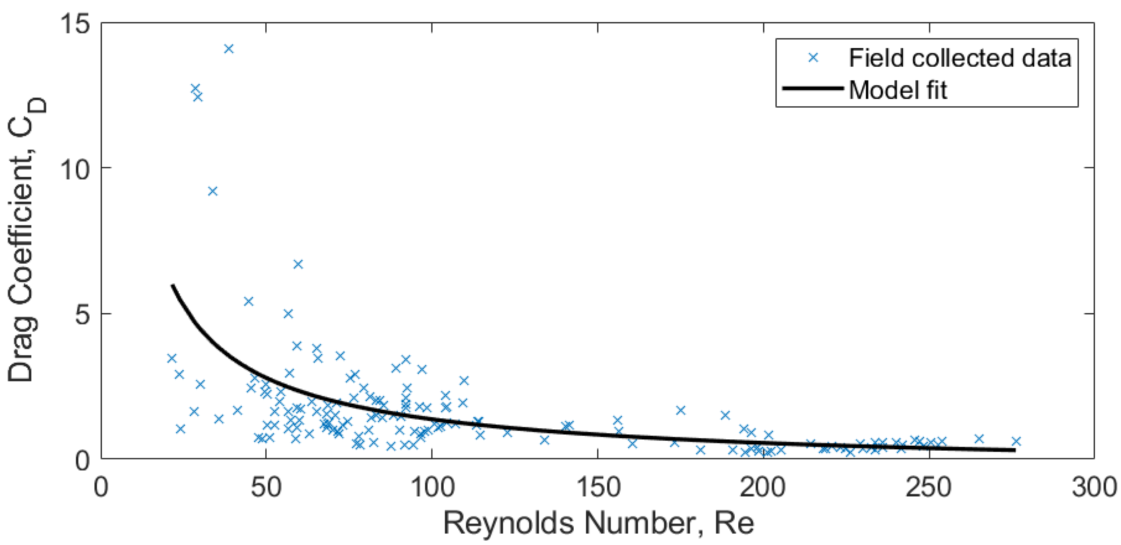

Figure 14. Relationship between Reynolds number, Re, and drag coefficient, C_D. As the Re gets larger, the drag coefficient decreases. For values of Re outside of these bounds, constant values are used. The lowest C_D value measured was 0.21, and the largest was 14.

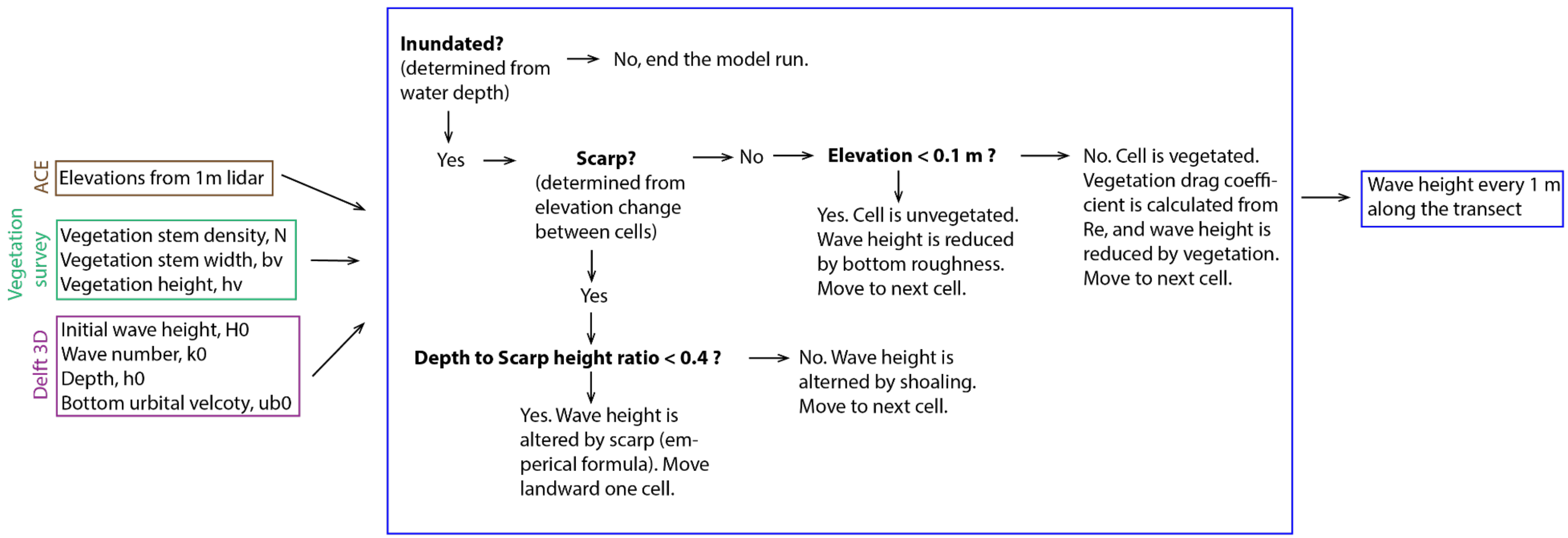

Figure 15. Conceptual diagram of the Marsh Transect Wave Attenuation model. The items in the boxes to the left are the data inputs grouped by source of data (Army Corps of Engineers, Vegetation survey, and Delft 3D). The steps in the blue box are repeated for every cell in the transect until it reaches a cell that is not inundated. The model output is a value of wave height for every cell in the transect.

Transects

Transects were generated using ArcMap in each of the seven sites, (see yellow boxes Figure **16**). In each area of interest, three shore normal transects 1 km long were generated. Each transect starts at the -0.5 m NAVD88 isobath (red lines in Figure 17). We are using the 2014 LiDAR dataset from the Army Corps of Engineers with a resolution of 1 m. The points along the transects are 1 m apart. The elevation is extracted at each of these points and used in the MTWA model.

Exploration of Conditions

The characteristics along the transects were manipulated to reflect specific conditions, as outlined in Task 5. The following changes were made to simulate the conditions.

Different Marsh Vegetation

Vegetation parameters in the vegetation drag model were altered to reflect *S. patens* (greater stem density, N, and smaller stem width, b_v) and *S. alterniflora* (less stem density, N, and larger stem width, b_v).

Conversion to Tidal Flat

The model was run without the vegetation drag model to simulate no vegetation. In subsequent runs of the model, the marsh platform was lowered by 10% with and without vegetation.

Ditch Filling

Elevations were manipulated before inputting into the model. Cells with elevation less than 0.8 m NAVD88 on the marsh platform where raised to the average elevation of the cells 3 m away in both the seaward and landward directions. If more than three consecutive cells were below 0.8 m NAVD88, it was identified as a channel, and the elevation was not changed. This elevation, 0.8 m NAVD88, was identified as being the threshold for ditches (blue lines in Figure 17).

Addition of Oyster Reefs

A new process was added to the MTWA model to simulate the impact of oyster reefs in adjacent channels. These model runs were performed on select transects in areas deemed suitable for oyster reef placement. The oyster reefs simulated are 3 m wide and 0.5 m tall and run parallel to the marsh edge in long sections. Waves travelling over the oyster reefs were transformed as a function of incoming wave height according to two empirical relationships derived by Wiberg et al., 2019. The first is for depths less than 1 m:

$$H = 0.28 * H_0 + 0.003 \qquad (Eq. 16)$$

And the second is for times when the reef is inundated greater than 1 m:

$$H = 0.85 * H_0 + 0.015 \qquad (Eq. 17)$$

This change in wave height occurs over a 40 m distance in the channel before reaching the marsh platform. These relationships were derived from field measurements of wave transformation over a constructed reef consisting of staggered rows of interlocking oyster castle spat blocks. It was constructed by the Nature Conservancy in *Man and Boy Marsh* in Virginia (Wiberg et al., 2019).

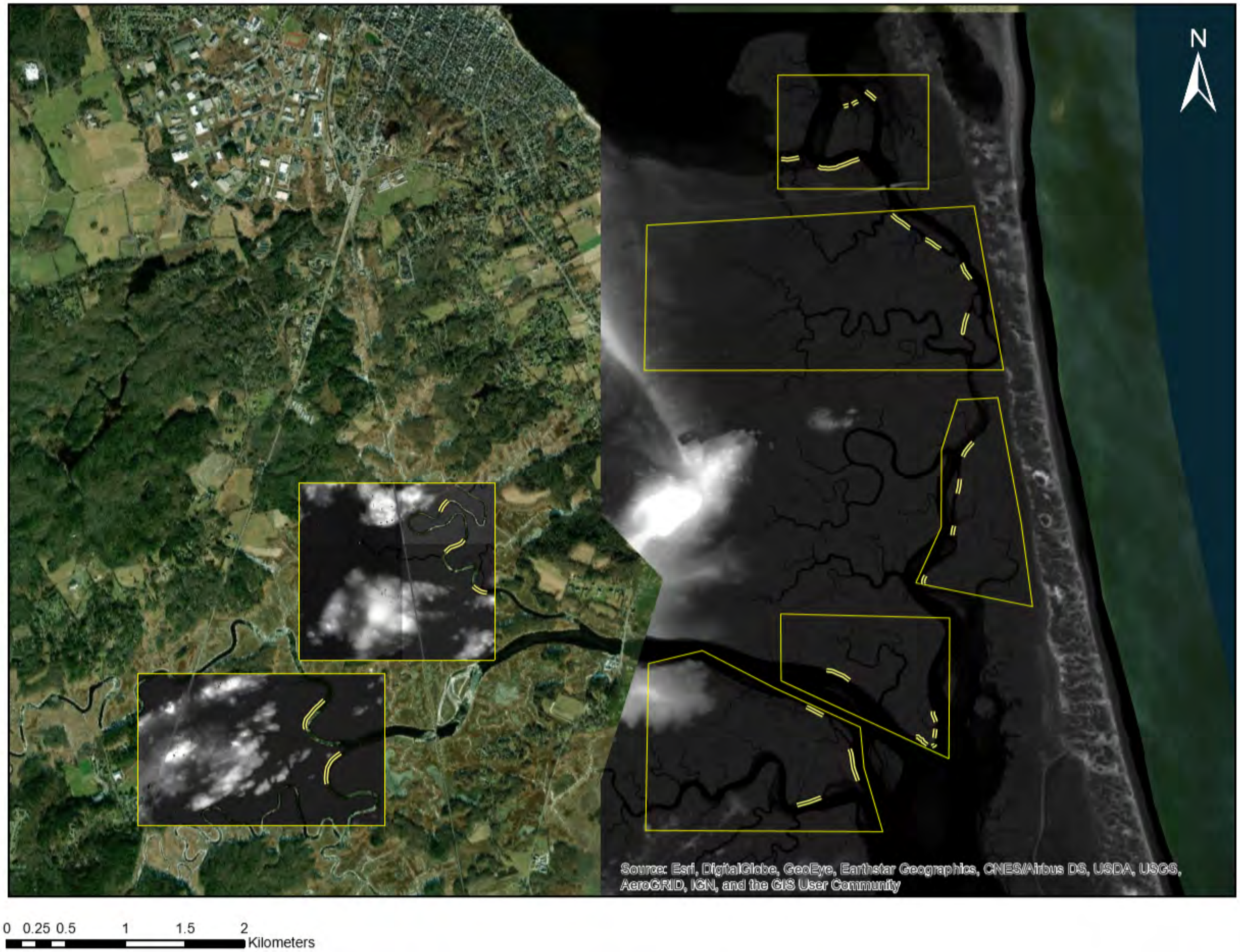

Figure 16. Map of sites of interest (yellow boxes) highlighting the portions of the shorelines (yellow lines) where transects have been generated. The MTWA model runs using inputs from along these transect

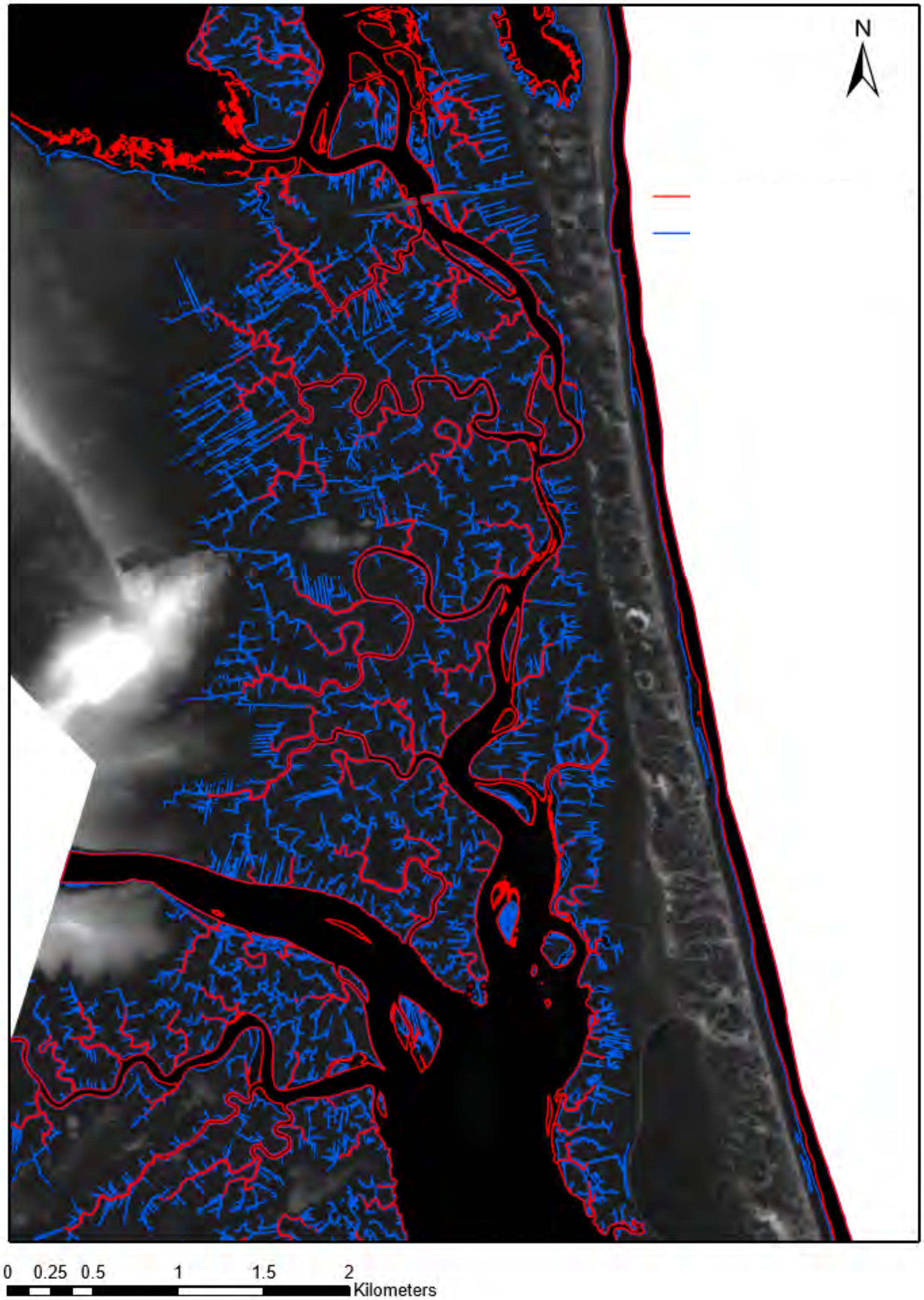

Figure 17. Image from the 2014 LiDAR topography survey by the Army Corps of Engineers. Redlines indicate the -0.5 m NAVD88 isobath, and blue show the +0.8 m NAVD88 isobath.

RESULTS

Vegetation Surveys

Vegetation information was collected at three sites (Figure 17). All sites showed a high diversity of vegetation types characteristic of healthy high and low marshes. However, the marsh at Kent Island site showed evidence of increased decomposition, evidenced by a hummocky topography and bare patches, a habitat characteristic of saltmarshes in early stages of submergence.

Vegetation Types

Plum Island Turnpike: Vegetation observed at this site included: *Phragmites australis* (Pa); *Iva frutescens* (If); *Spartina alterniflora* (Sa); *Spartina patens* (Sp); *Distichilis spicata* (Ds); *Solidago sempervirens* (Ss); *Glaux maritima* (Gm); *Jucus geradii* (Jg); *Salicornia spp*. (Sal). *Spartinia alterniforn and patens* were the dominant vegetation at this site (Table XX).

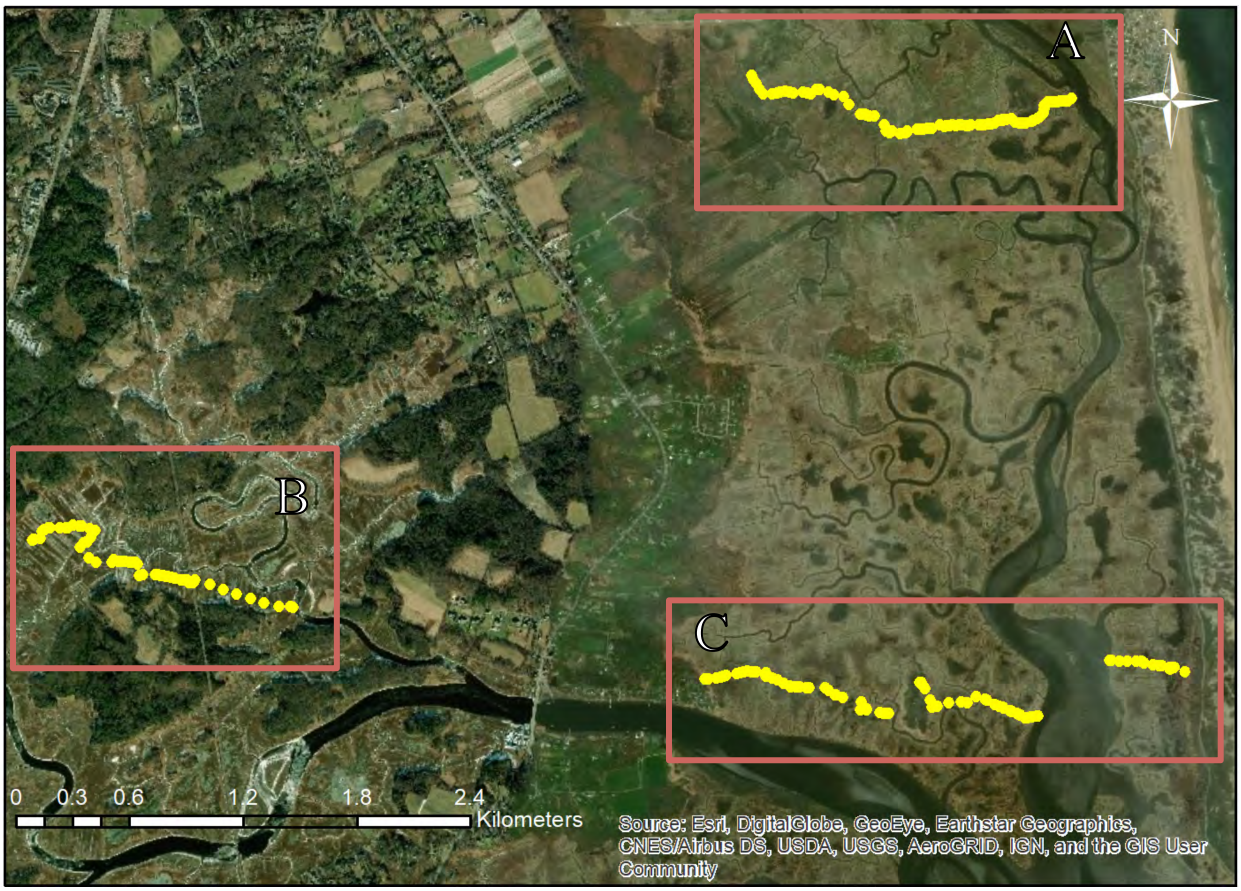

Figure 17. Map showing the location of vegetation surveys. The three vegetation survey transects A. Plum Island Turnpike, B. Kent Island, and C. Parker River are shown in orange boxes. Each yellow circle indicates the location of a vegetation quadrat.

Kent Island: Vegetation observed at this site included: *Phragmites australis* (Pa); *Iva frutescens* (If); *Spartina alterniflora* (Sa); *Spartina patens* (Sp); *Distichilis spicata* (Ds); *Solidago sempervirens* (Ss). *Distichilis spicata* was the dominant vegetation at this site (Table 1).

Parker River: Vegetation observed at this site included: *Phragmites australis* (Pa) at the upland edge; *Iva frutescens* (If); *Spartina alterniflora* (Sa); *Spartina patens* (Sp); *Distichilis spicata* (Ds); *Limonium carolinianum* (Lc); *Solidago sempervirens* (Ss); *Salicornia spp*. (Sal). *Distichilis spicata* was the dominant vegetation at this site (Table 1).

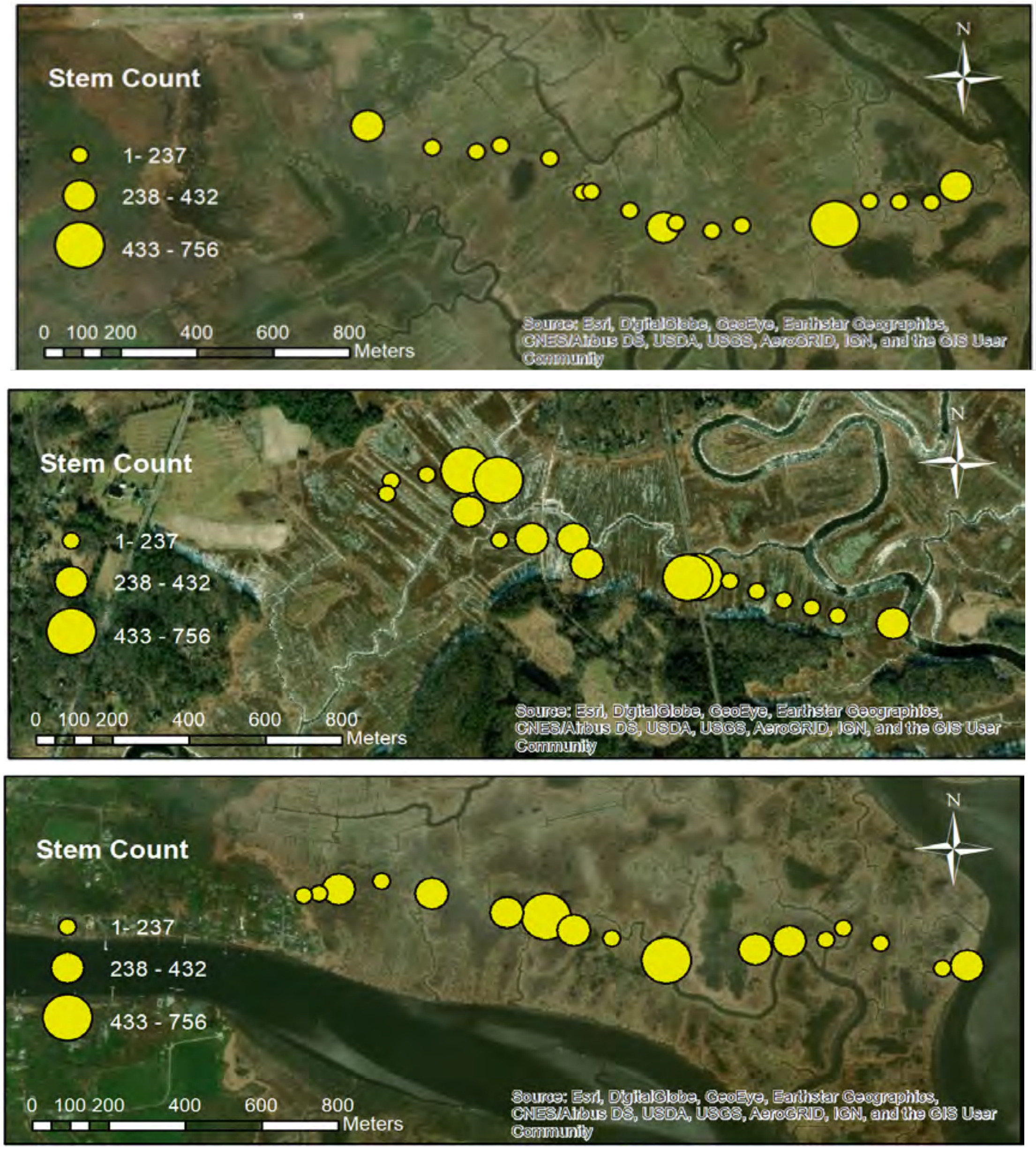

Figure 18. Stem counts for the three vegetation surveys: Plum Island Turnpike (top), Kent Island (middle), and Parker River (bottom). All stem counts are per 0.0625 m2. The larger circles indicate a greater density of stems, as indicated in the legend on the left.

Vegetation Attributes

Variability in stem count and vegetation height was observed within and among sites, with stem counts ranging from 1 to 756 shoots/0.0625m^2 and vegetation height ranging from 0.1 m to 1.2 (Figures 18 and 19; Table 1). Note that a spatial relationship between stem elevation and density and proximity to open water or uplands does not exist. This likely indicates that the plants are responding to a variety of additional forcings, including elevation, hydroperiod, nutrient loading, peat characteristics, and others.

Elevation Relationships

Because saltwater and brackish vegetation are closely related to hydroperiod, we examined the relationship between elevation and percent coverage of *S. Patens*. *S. patens* is a supratidal halophytic plant that can only withstand limit saltwater inundation. In the Great Marsh, this plant community is only inundated by spring high tides and storm surges, which occur several times a month. Thus, we hypothesized that *S. patens* coverage would correlate with elevation, which is a proxy for hydroperiod. However, when the entire dataset was plotted, no apparent correlation was found identified. Plots for the individual transects are shown in Figures 19-22. Only vegetation along the Parker River transect shows any significant trend (Figure 19), but even this correlation explains only 30% of the data, meaning that other variables also control vegetation type.

Parker River Transect

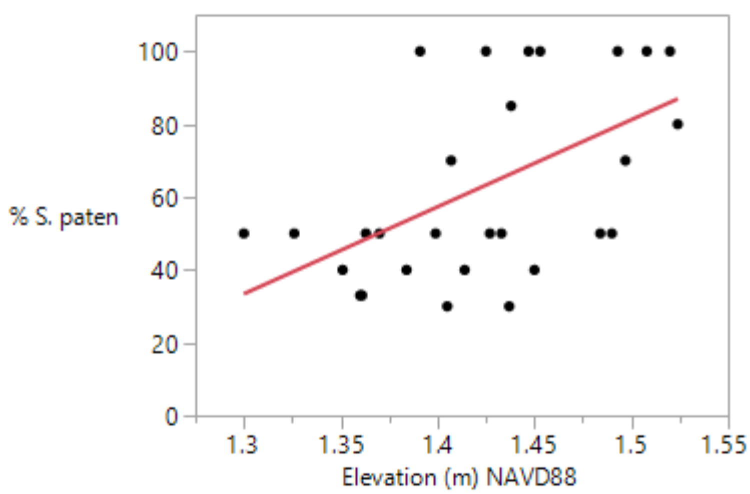

Figure 19. A positive relationship was observed between elevation and percent cover of S. patens at Parker River (R^2 = .29, $F(1, 27) = 11.32$, p = .0023). Note: the R^2 value indicates that the parameter elevation explains thirty percent of the variability in *S.patens* percent cover at this site. The remaining seventy percent is explained by other variables.

Kent Island Transect

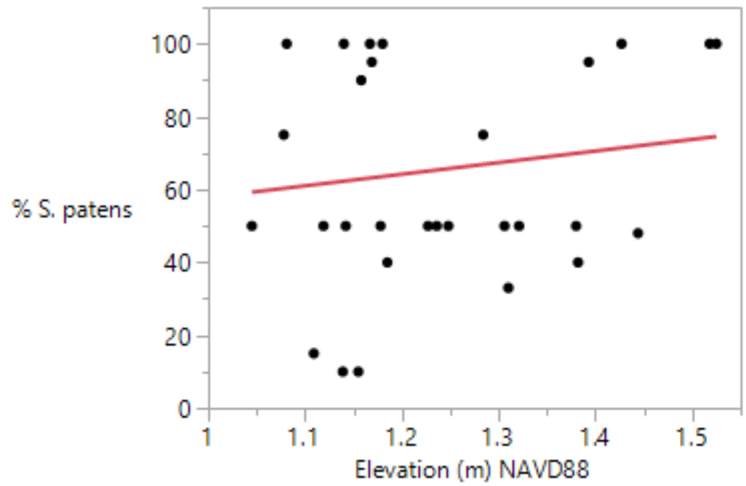

Figure 20. No relationship was observed between elevation and percent cover of *S. patens* at Kent Island (R^2 = .02, F(1, 29) = 0.58, p = 0.45).

Plum Island Turnpike

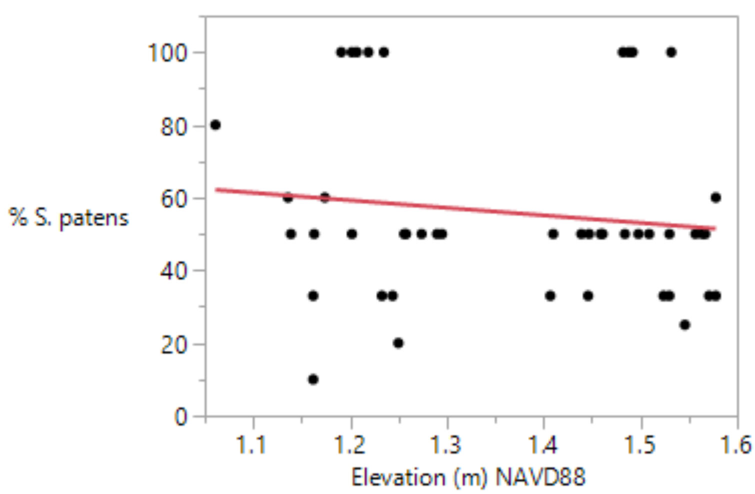

Figure 21. No relationship was observed between elevation and percent cover of *S. patens* at the Plum Island Turnpike site (R^2 = .02, F(1, 43) = 0.75, p = 0.39).

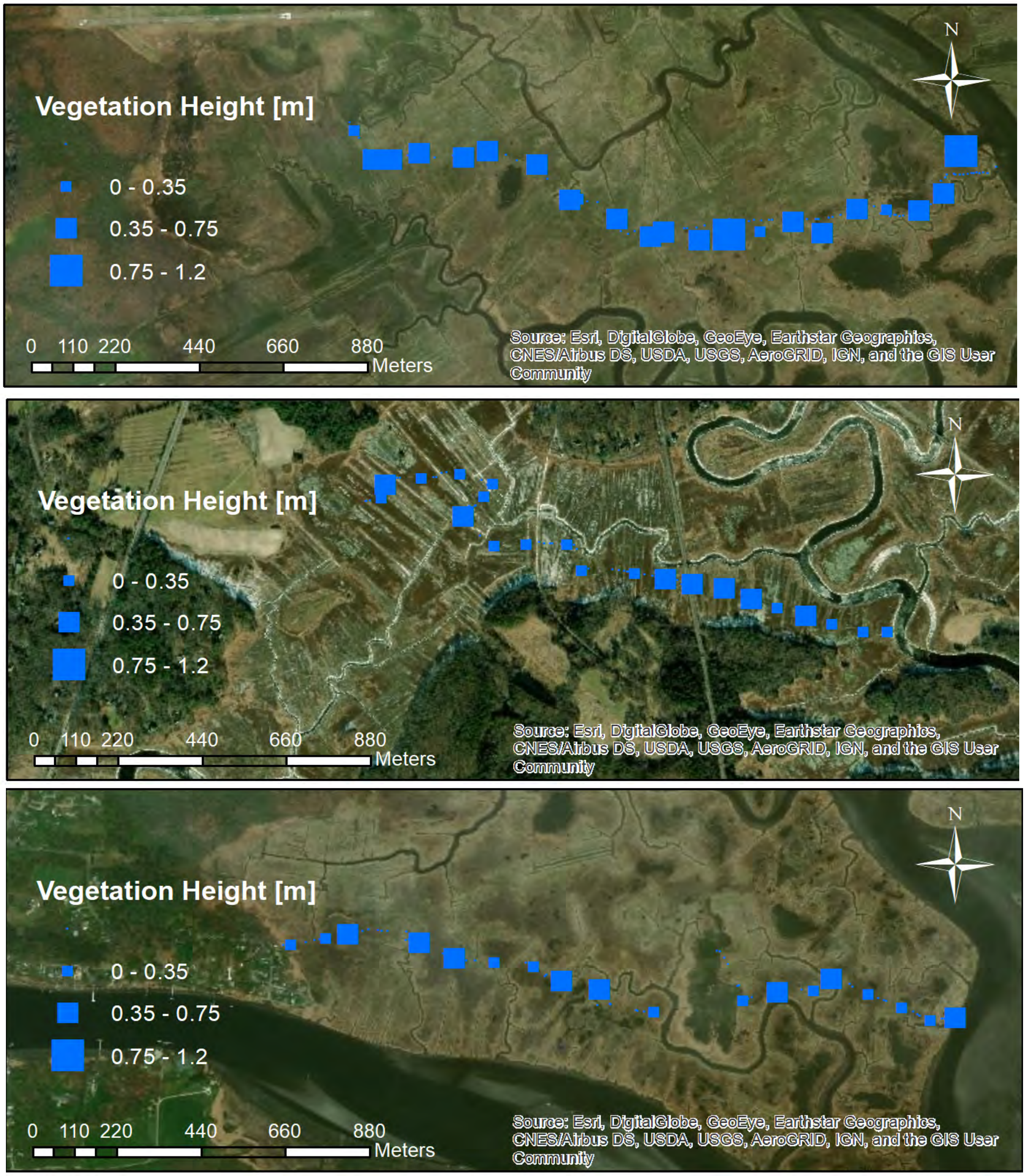

Figure 22. Vegetation height (m) for the three vegetation surveys: Plum Island Turnpike top), Kent Island (middle), and Parker River (bottom).

Table 1. Vegetation characteristics along transects where wave data was collected, including mean shoot density (number/m^2) stem width (mm), and height (m).

Site	Shoot Density [#/m^2]	Stem width [mm]	Shoot height [m]	Dominant vegetation type
Plum Island Turnpike	5900	2.6	0.27	*Distichilis spicata*
Kent Island	3153	2.6	0.27	*Distichilis spicata*
Parker River	3153	1.0	0.20	Short-form Spartina alterniflora and *Spartina patens*

Hydrodynamic and Wave Modeling

To assess the vulnerability of Newbury from storm surge and waves, and evaluate the attenuation capacity of saltmarshes, we simulated several selected storms (see storm characterization and analysis) using our coupled flow and wave model based on Delft3D modeling suite. We validated the model for flow/tides using previous observations in Plum Island Sound collected in 2015 (FitzGerald et al., 2017). The selected storms, with corresponding wave height, wave period, wind speed, and wind direction, along with chosen inundations regime coinciding with the low, intermediate, and high tide, were conducted for four storms, which represent typical events with high return intervals. We simulated these storms for present conditions and repeated for future scenarios with sea-level rise. Figure 23 and Figure 24 show hydrodynamic results (water level inundation and significant wave heights) from the regional Delft3D simulations for storm C6 and C5 respectively under present and future conditions. Results show that inundation from the storm for marshes fronting Newbury increases for each storm, compared to present conditions, by 5-40%, with ~0.3-0.4m more surge reaching the perimeter of the town. Corresponding with the inundation results, wave height propagation from the sound to the marsh edge where our transect modeling starts, wave heights increased by 15-25% depending on location with 0.05-0.2 m larger waves for future conditions. The most significant areas that experience increased inundation and larger exposure to waves in Newbury port, near Joppa flats, where wave heights increase by at least 40%.

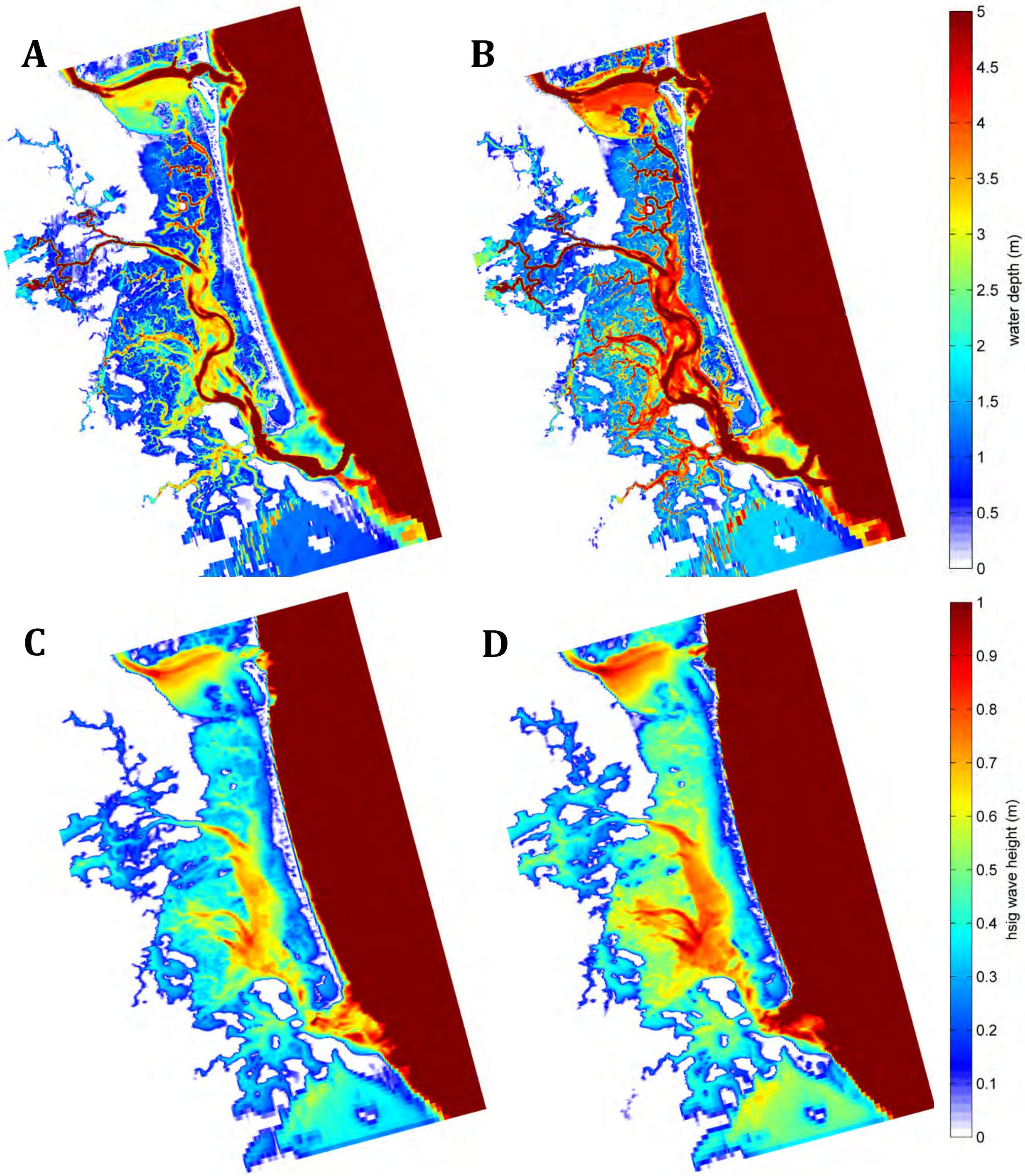

Figure 23. Hydrodynamic results from the regional Delft3D simulations for storm C6 showing inundation for present conditions (A) and for SRL scenario RCP8.5 (B). Similarly, bottom panels show significant wave heights through Plum Island for present conditions (C) and for the same SRL scenario (D).

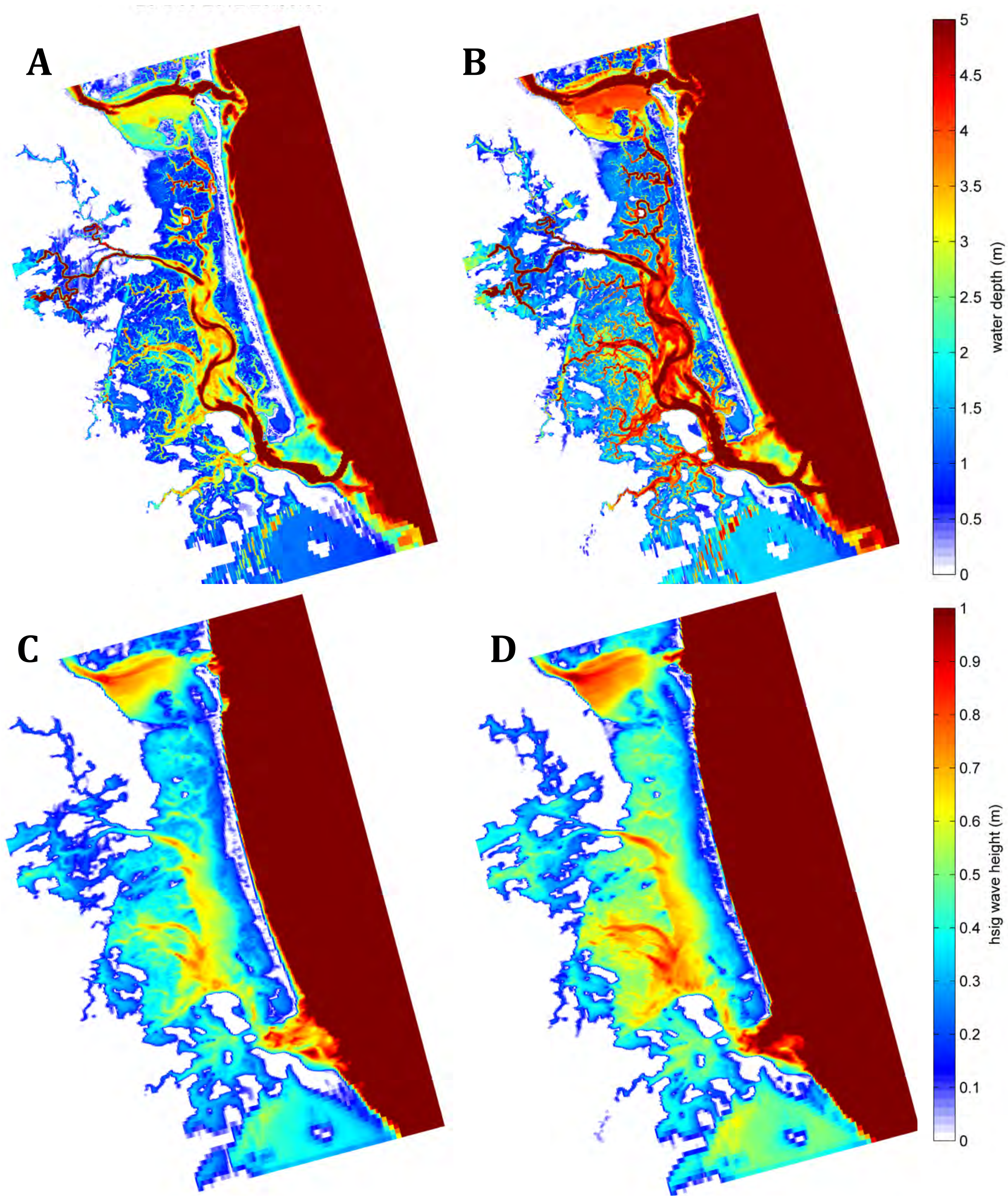

Figure 24. Hydrodynamic results from the regional Delft3D simulations for storm C5 showing inundation for present conditions (A) and for SRL scenario RCP8.5 (B). Similarly, bottom panels show significant wave heights through Plum Island for present conditions (C) and for the same SRL scenario (D).

Future Bathymetry Adjustment due to Sea Level Rise

Forward projection indicates a very likely 21st century Global Sea Level (GSL) rise of around 135 cm under maximum range across all RCPs and calibrations scenario (Kopp et al., 2016) (Figure 1). We have updated our existing bathymetry (Figure 2) by incorporating extreme projection of 21st century GSL rise to evaluate future sea level rise impact on plum island backbarrier marsh. Average marsh accretion in Plum Island (~15 cores using ^{210}Pb and ^{137}Cs) is ~2.8 mm/yr based on measurements obtained during an earlier study (FitzGerald et al., 2017). GSL rise rate at Plum Island is 2.85 mm/yr. We have calculated time varying acceleration rate for the extreme sea level rise projection from the below graph. We found a constant acceleration rate on global sea level rise. We also added that acceleration rate on both GSL rise as well as marsh accretion rate. We considered hundred percent of that constant acceleration for each of future year projection of GSL rise and only seventy percent acceleration on marsh accretion. We assumed that marsh of Plum island could accrete maximum 7 mm/yr in future. We assumed marsh will accrete five times more than open water body and also considered it in our updated bathymetry calculation. The equation we have used to update our bathymetry shown below:

For Marsh or any land:

$$Z_{final} = Z_i + (GSLR + Acr) \qquad (Eq. 18)$$

For Open Water body:

$$Z_{final} = Z_i + (GSLR + Acr / 5) \qquad (Eq. 19)$$

Where,
$Z_{final} = Final\ depth$
$Z_i = Initial\ depth$
$GSLR = Global\ Sea\ Level\ Rise\ rate\ in\ meter/yr$
$Acr = Accretion\ rate\ in\ meter/yr$
Note: Acceleration was incorporated for both GSLR and Accretion rate.

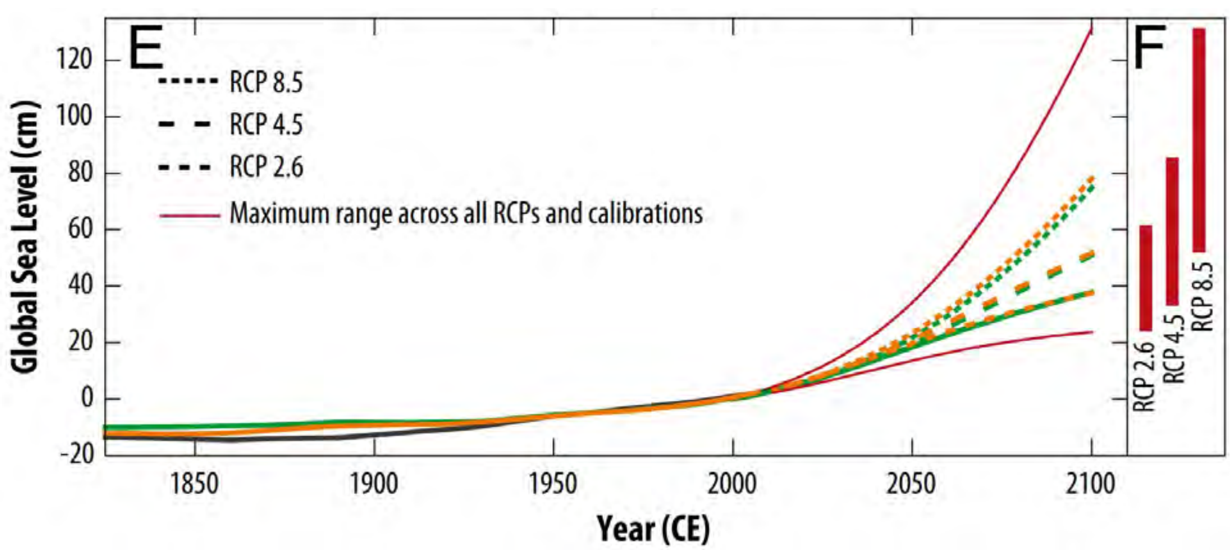

Figure 25. 21st Century Global Sea Level (GSL) rise projection for numerous scenarios (Kopp et al., 2016)

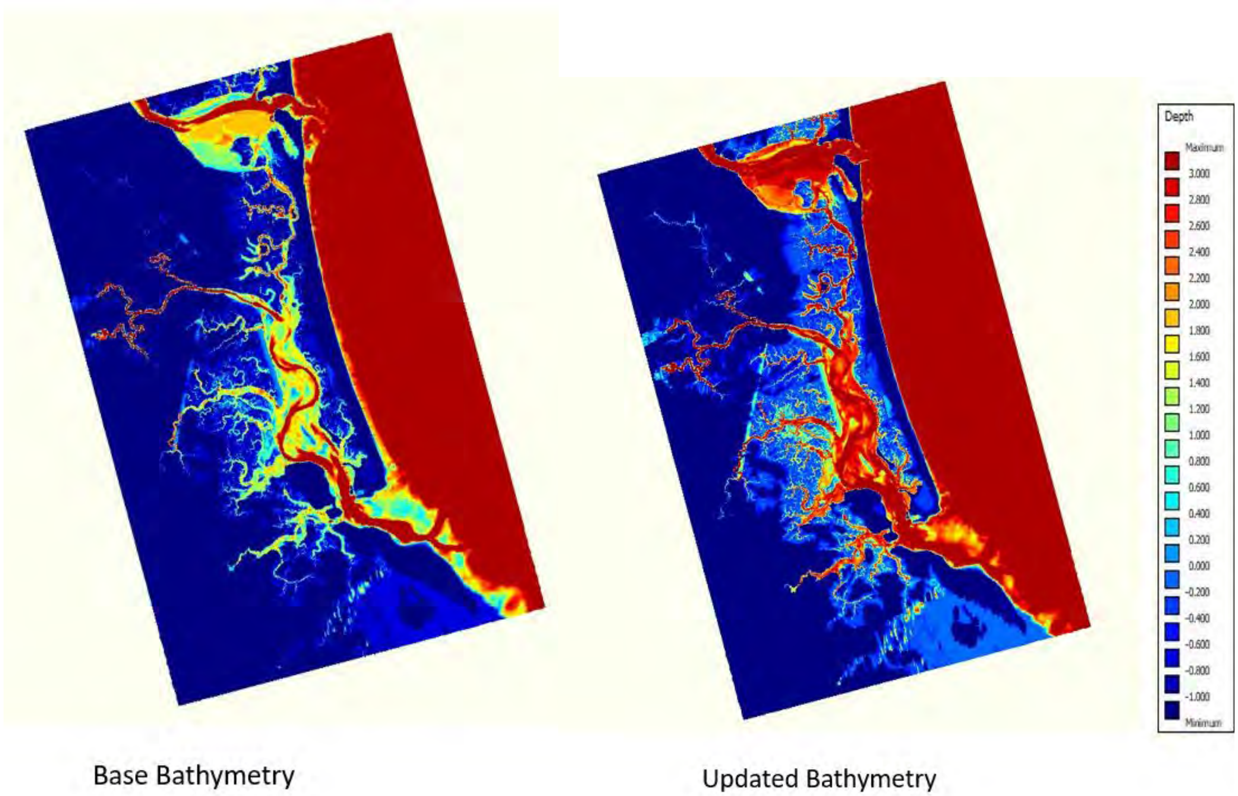

Figure 26. Initial bathymetry (present conditions) and updated bathymetry after incorporating SLR (future conditions).

Storm Characterization and analysis

To characterize storms and select which to run in the model, we used the Wave Information Studies (WIS) station 63045, located in 85 meters of water depth east-northeast of Plum Island. Figure 27 shows the US Army Corps of Engineers analysis at this station, with corresponding return period for the top ten events. Our analysis of all events in the record yielded similar results to those of the USACE. These events were based on Newbury exposure. Overall, the town of Newbury is exposed to storms with wind and waves from ~20-180 degree azimuth, with additional exposure to high fetch conditions from 20-135 degrees. The most frequent events occur from 78-145 degrees, and the top ten events on record from 61-101 degrees. Hence, we selected four of the top ten events to simulate for our analysis. For each of these events, the wind speed, direction, offshore wave height and wave period, and corresponding surge (obtained from the Northeast Atlantic Coastal Study (NACS)), was forced at the open boundary. For reference, we selected storm 4,5,6 and 7 from Figure 27, labeled in this report as C4, C5, C6, and C7, respectively.

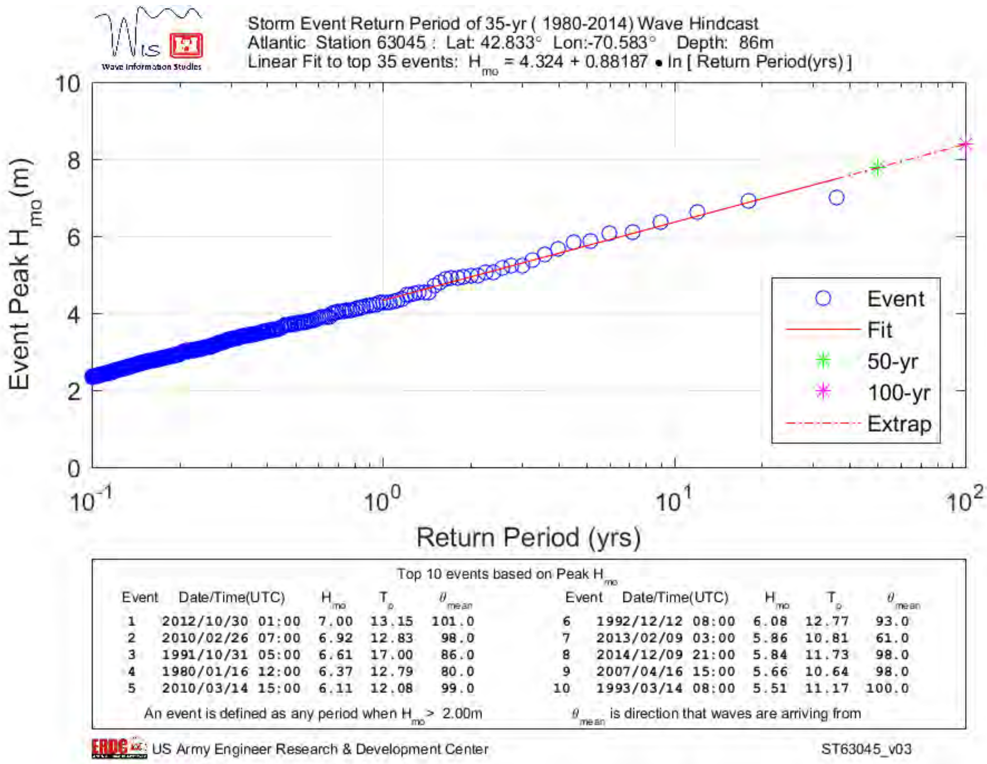

Figure 27. Storm event analysis conducted by the US Army Corps of Engineers at WIS station 63045. The table shows the top ten events with their corresponding return period

Field Measurements

The following figures show the processed wave data from select stations in the field study. For the shore station (first station on the marsh platform), the largest wave recorded was 0.15 m at the North transect (Transect #1). The max depth at the East and South (Transect #2 & 3, respectively) shore stations was 0.6 m, and at the North, it was 0.85 m. The average wave period was 1.4 s and 1.8 s for the East and South shore stations, respectively, and it was 2.5 s for the North shoreline station. The average orbital velocity for all stations was 0.05 m/s.

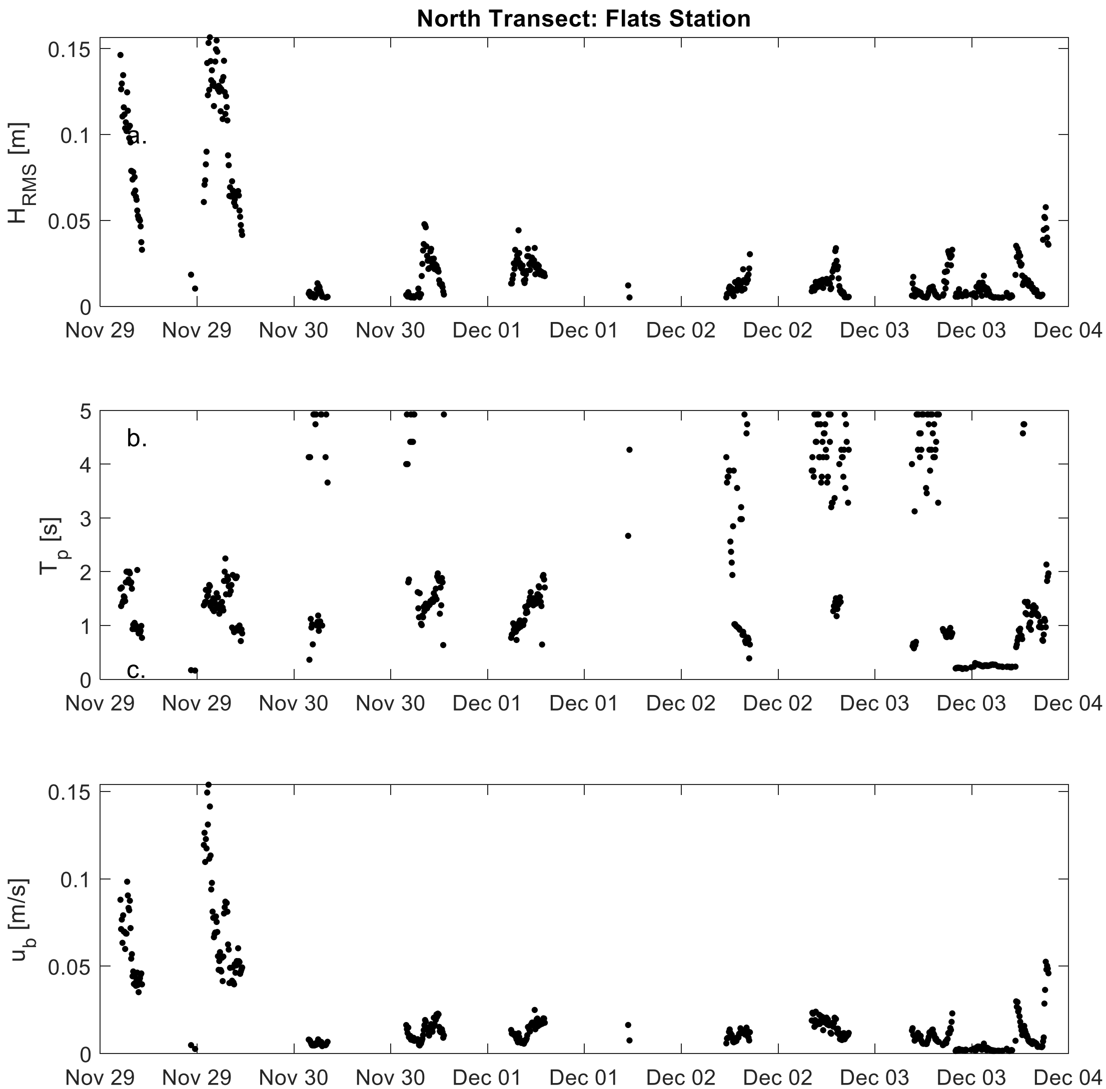

Figure 28. Wave statistics at the flats station in the North Transect. Each point represents the statistics for one instrument burst. Bursts of measurements occurred every 5 min. a) root-mean-square wave height (m). b) peak wave period (s). c) bottom wave-orbital velocity (m/s).

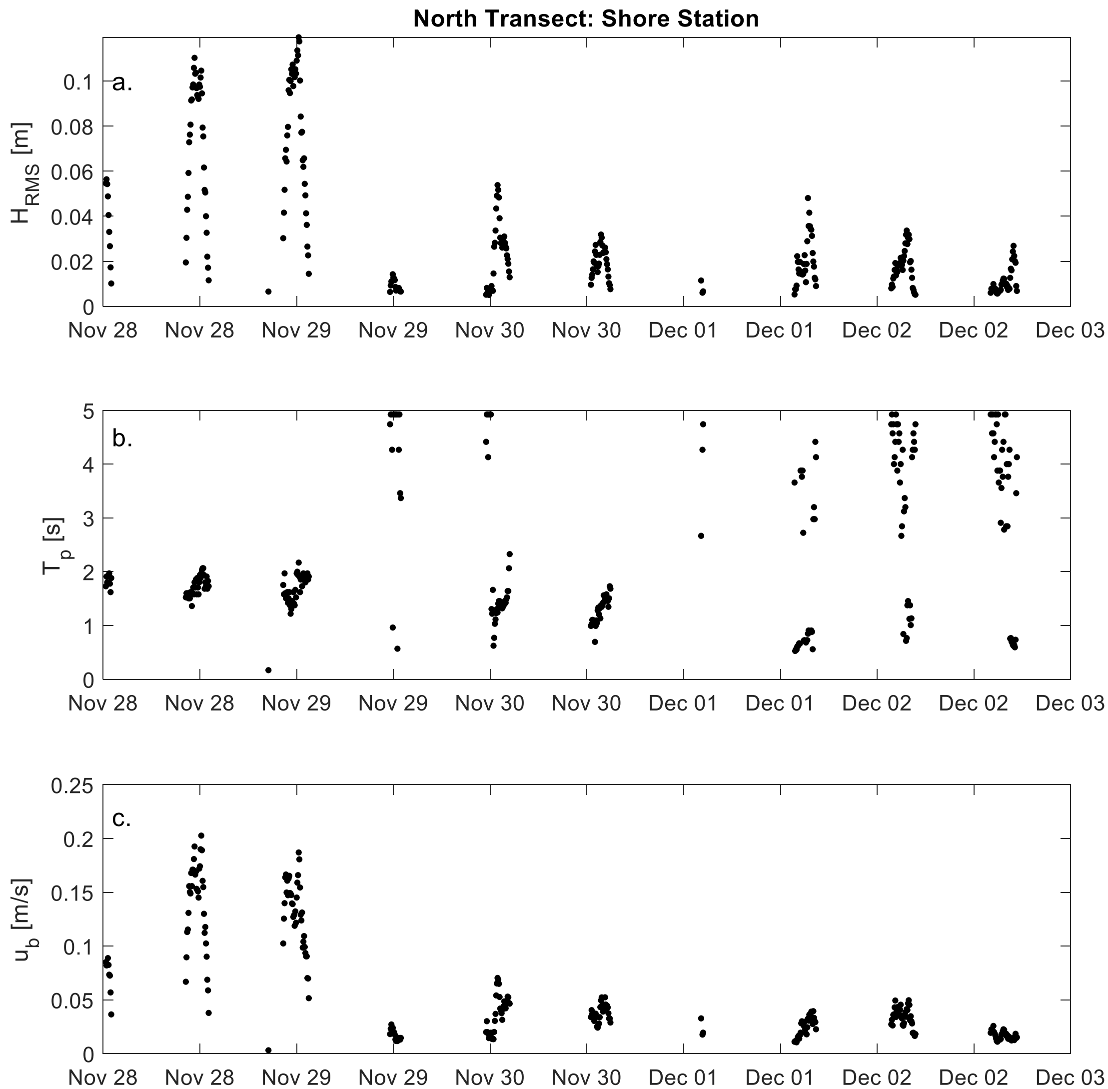

Figure 29. Wave statistics at the shore station in the North Transect. Each point represents the statistics for one instrument burst. Bursts occurred every 5 min. a) root-mean-square wave height (m). b) peak wave period (s). c) bottom wave-orbital velocity (m/s).

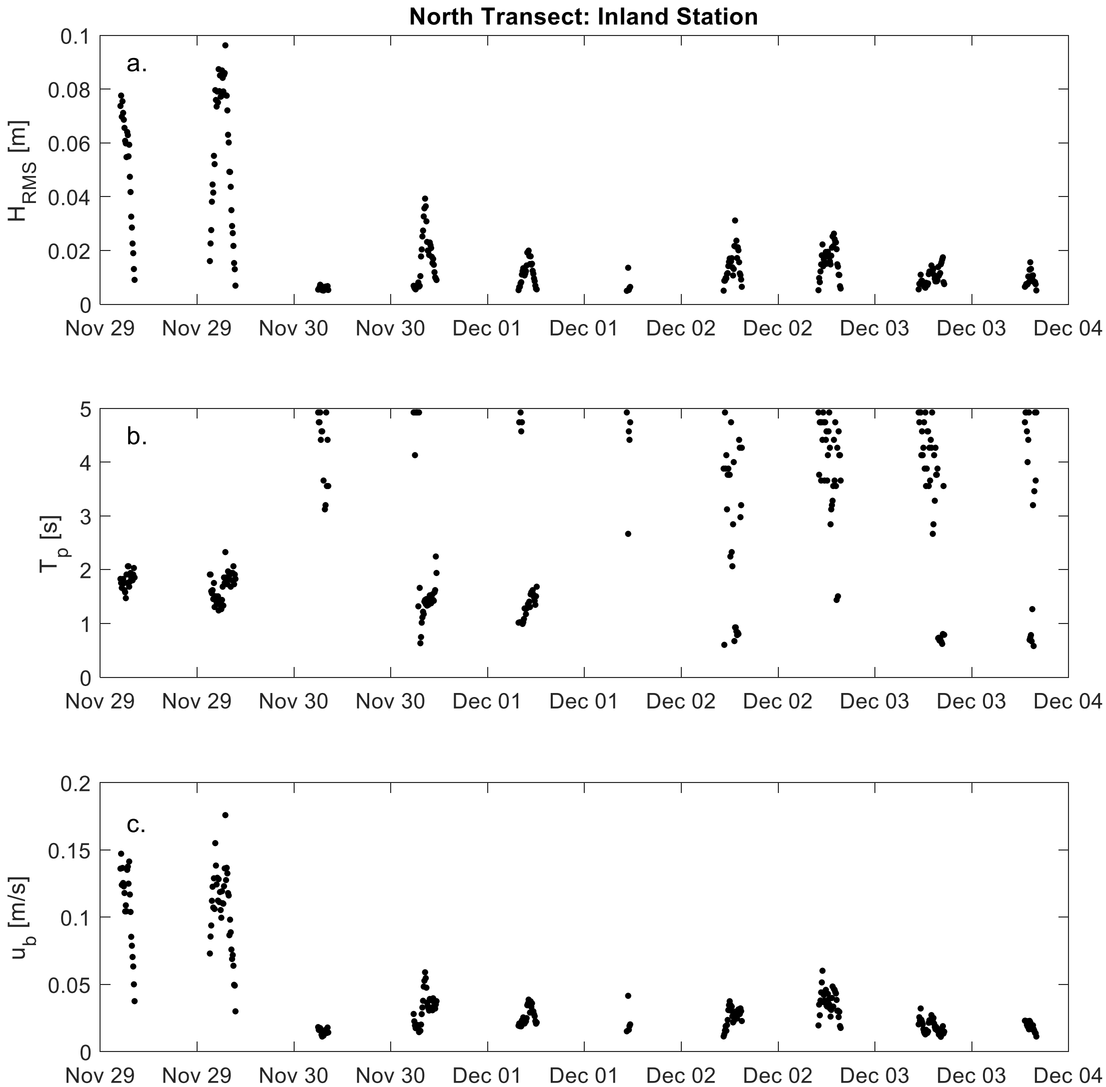

Figure 30. Wave statistics at the inland station in the North Transect. Each point represents the statistics for one instrument burst. Bursts occurred every 5 min. a) root-mean-square wave height (m). b) peak wave period (s). c) bottom wave-orbital velocity (m/s).

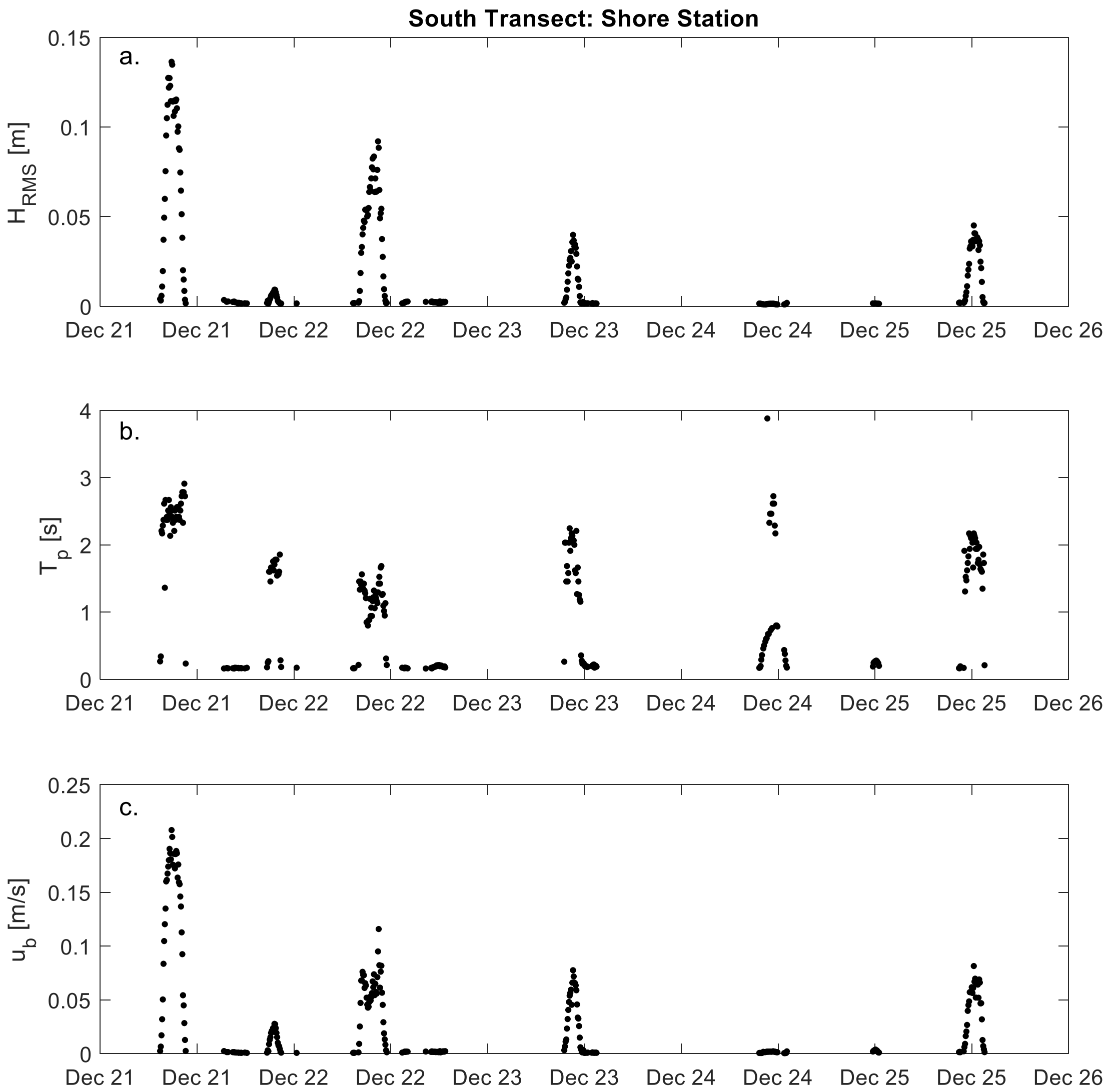

Figure 31. Wave statistics at the shore station in the south instrument transect. Each point represents the statistics for one instrument burst. Bursts occurred every 5 min. a) root-mean-square wave height (m). b) peak wave period (s). c) bottom wave-orbital velocity (m/s).

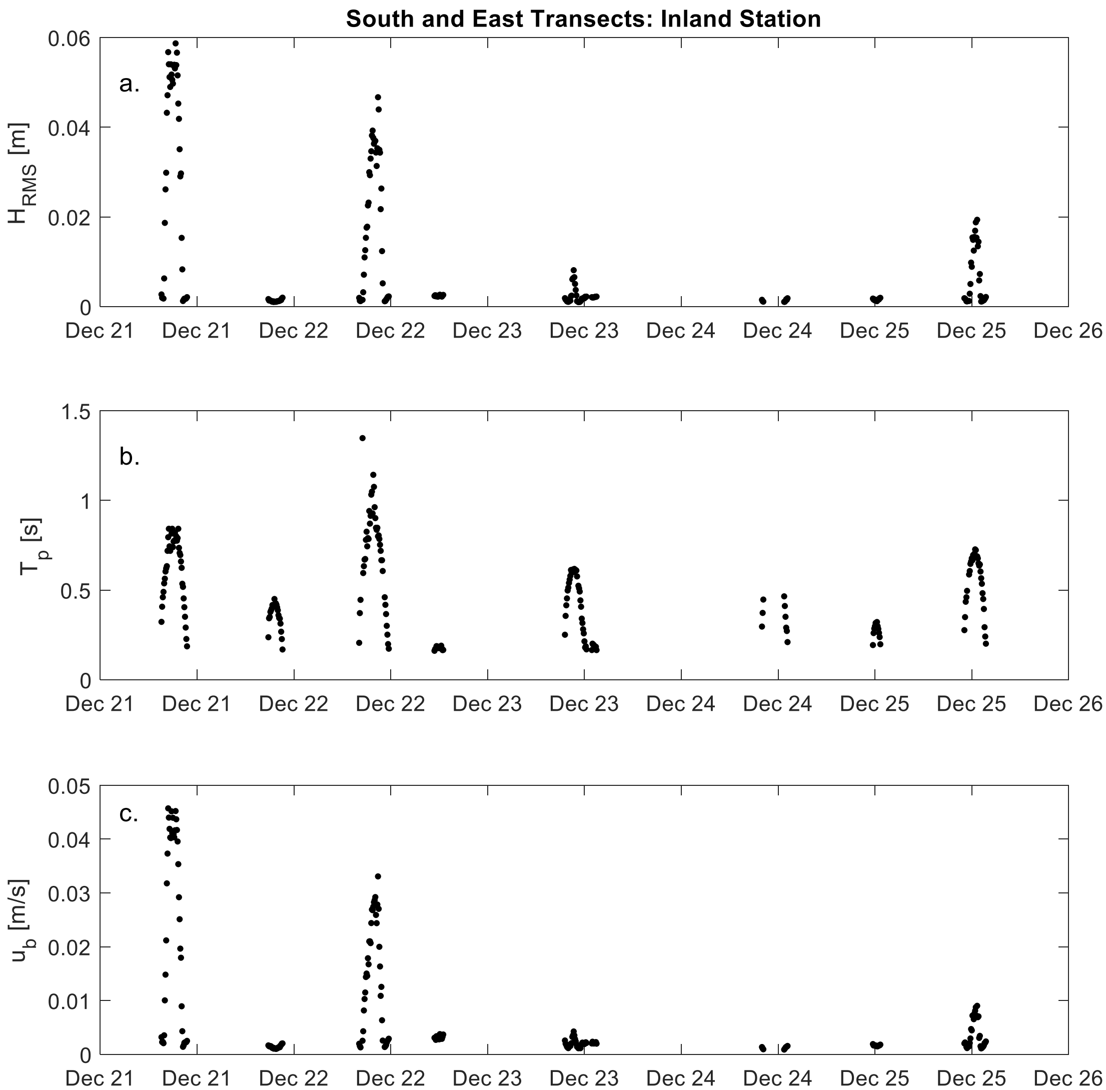

Figure 32. Wave statistics at the inland station in the south and east instrument transects. Each point represents the statistics for one instrument burst. Bursts occurred every 5 min. a) root-mean-square wave height (m). b) peak wave period (s). c) bottom wave-orbital velocity (m/s).

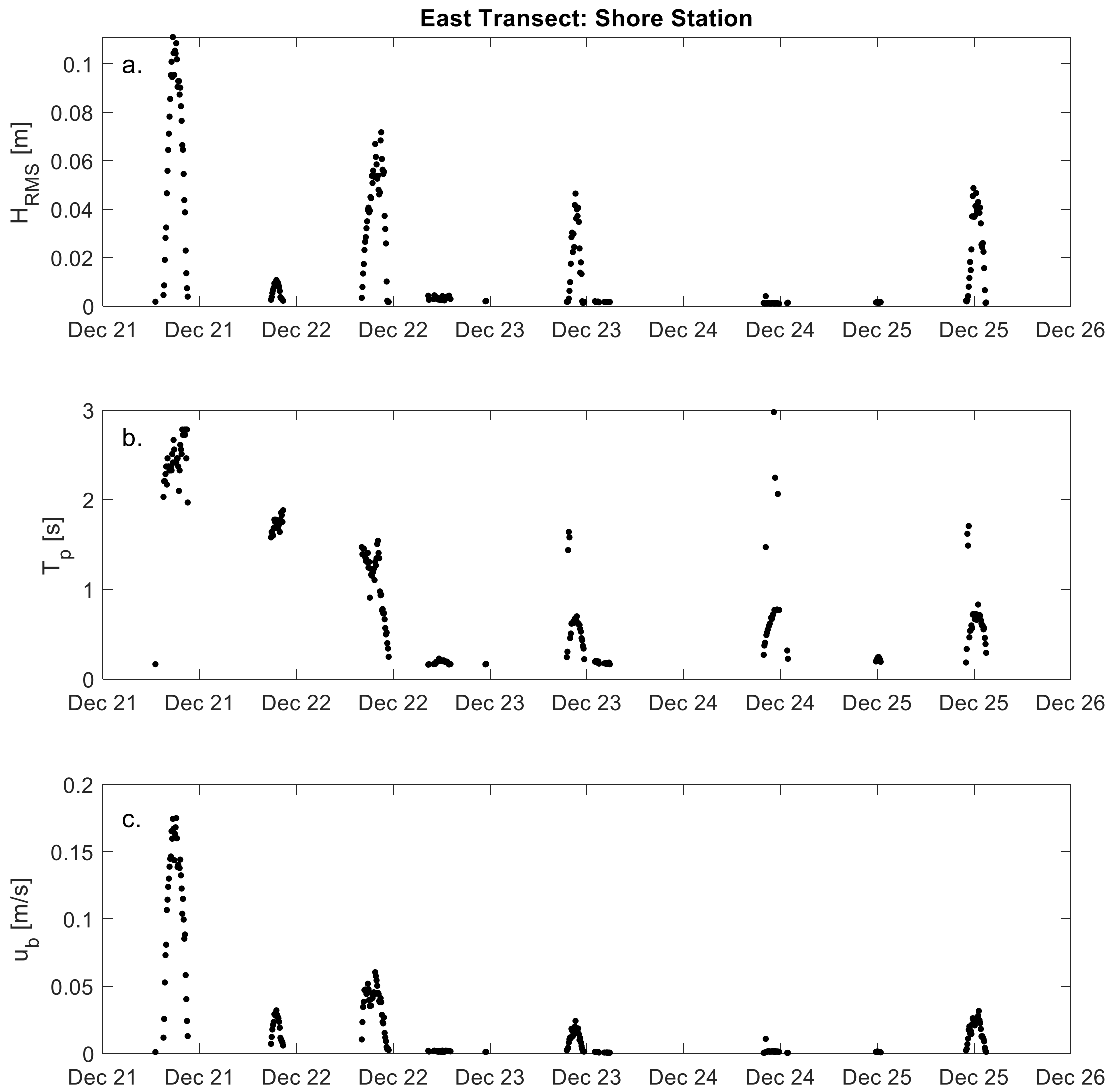

Figure 33. Wave statistics at the shore station in the east instrument transect. Each point represents the statistics for one instrument burst. Bursts occurred every 5 min. a) root-mean-square wave height (m). b) peak wave period (s). c) bottom wave-orbital velocity (m/s).

Due to the orientation of the transects, the waves are larger for different wind directions (Figure 35). Transects were oriented in the directions with larger fetch that are more exposed to wave action (north, east, and south). However, the dominant wind direction during the hydrodynamic measurements was from the northwest (Figure 34), which did not produce waves in the areas of interest on the marsh. The wind data is from the PIE LTER Marshview Farm weather station.

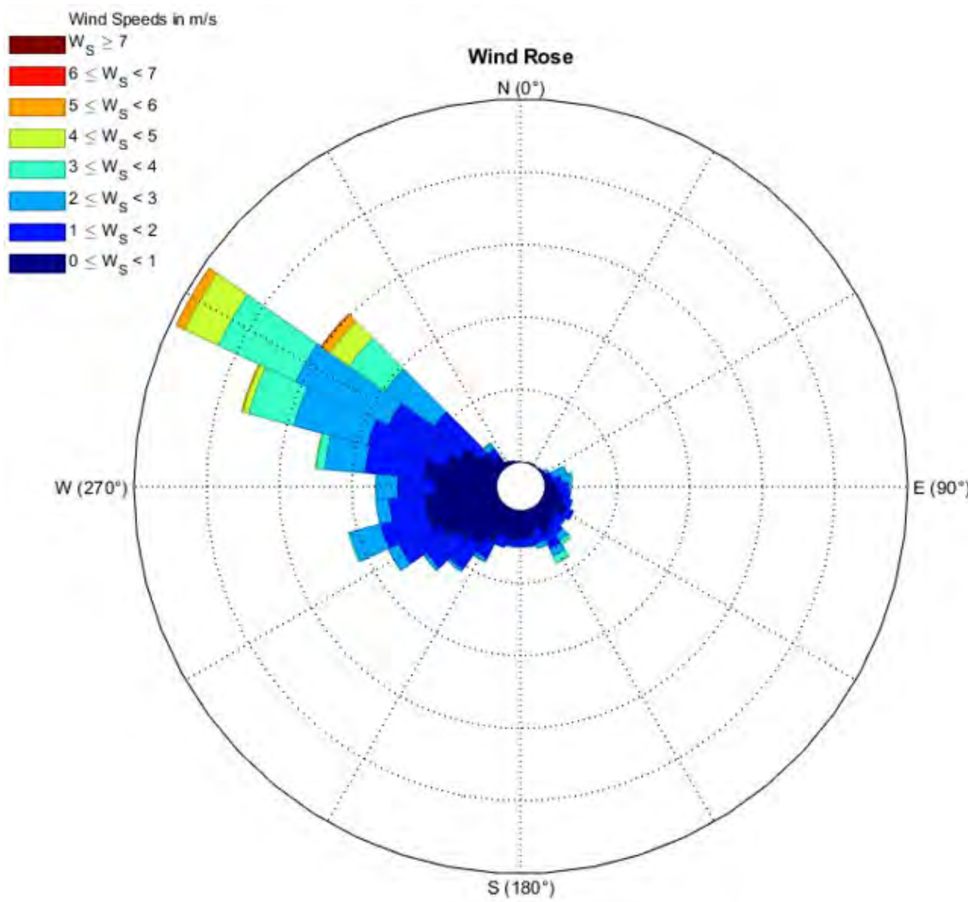

Figure 34. Wind rose showing the wind direction and speed over the course of the hydrodynamic field measurements. Data is from the PIE LTER Marshview Farm weather station.

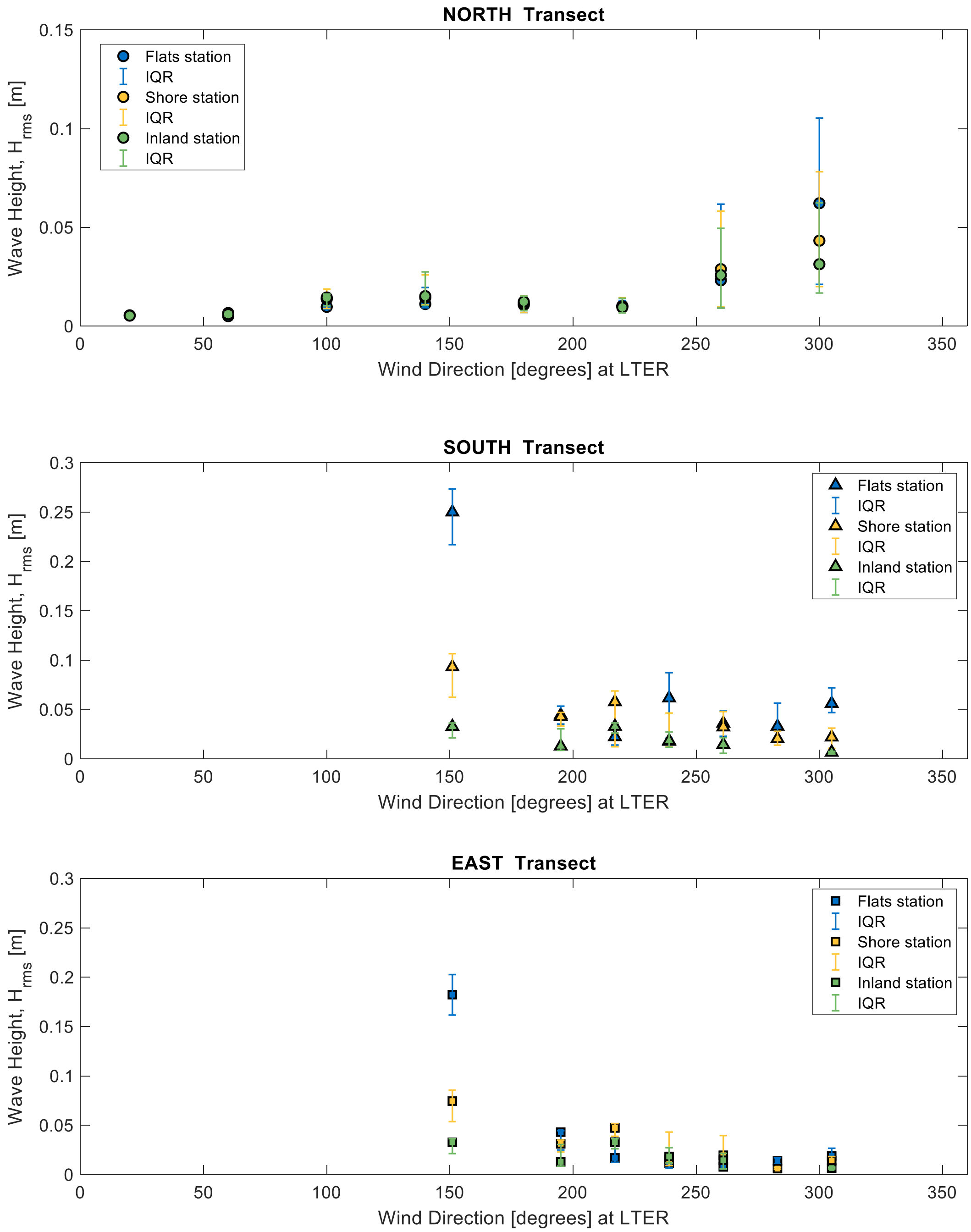

Figure 35. Wave height as a function of wind direction at each transect. Error bars are the interquartile range, and symbols mark the median value. Data is grouped into 8 bins. The wind data is from the Plum Island Long Term Ecological Research Center (LTER).

Exponential decay

The wave data was modeled as an exponential decay. This model is not process-based, but rather, provides information on the net wave transformation as a whole. The only the distance between the measurements is taken into account for better comparison. Following Equation 3, an exponential decay constant, k_i, was calculated for every simultaneous burst across the marsh.

The results follow a clear pattern with water depth. In Figure 36, the decay constants for each field transect are binned by water depth. The error bars show the interquartile range. With greater inundation, the decay constants are lower, meaning less attenuation. There is much greater scatter in the data from the North transect, likely due to the close proximity of the instruments. Negative decay constants indicate wave height amplification occurred.

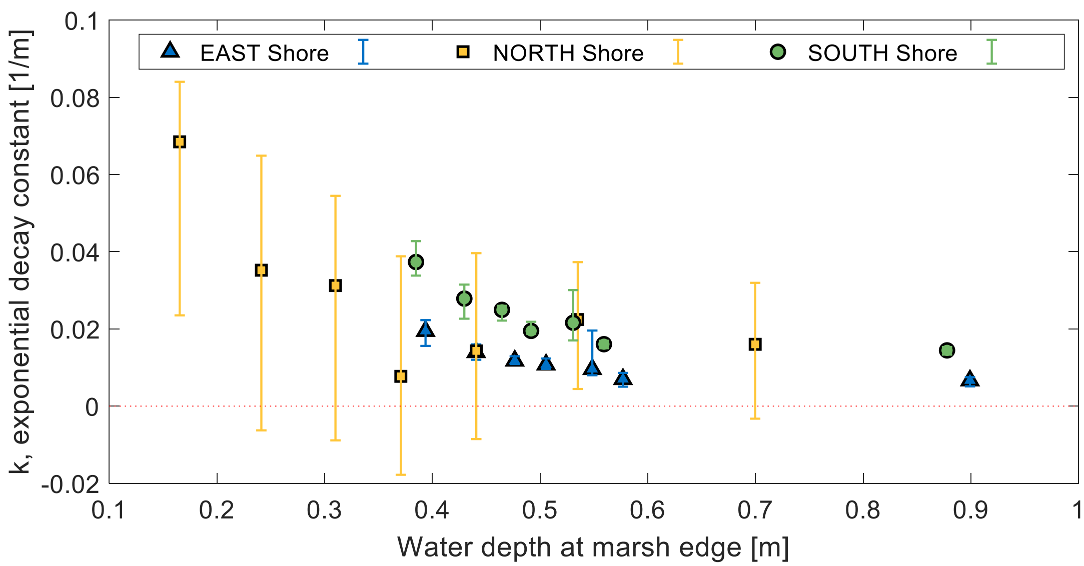

Figure 36. Results from the three transects in the field study. Exponential decay constants are binned by depth, where each "bin" has an equal number of data points. The error bars show the interquartile range of the data in each bin. Exponential decay constants less than 0 indicate wave height amplification occurred.

The calculated exponential decay constants can also be used to determine distances for equivalent attenuation. Using Equation 3 with a set k_i value and H/H_0 ratio, the x distance can be solved. Using averages from the field results, it was determined that with 40 cm of inundation, it took traversing about 46 m of marsh for a typical wave to lose 75% of its height. If the inundation is increased to 90 cm, it took 139 m of marsh to lose 75% of its height. This point is illustrated in Figure 37.

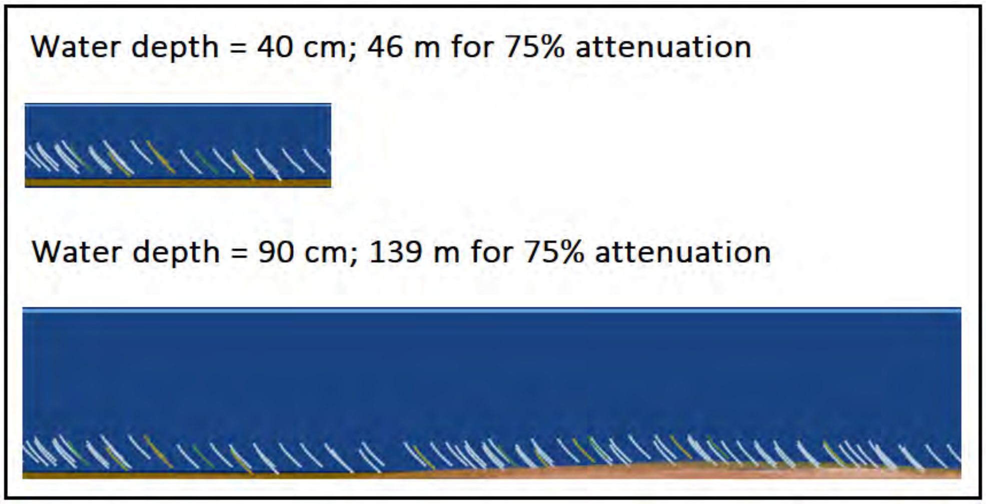

Figure 37. Illustrative example of how the exponential decay constants can be used to calculate distances of equivalent attenuation. The values for k_i for 40 cm and 90 cm of inundation are 0.03 and 0.01, respectively. These values are from the results of the field study.

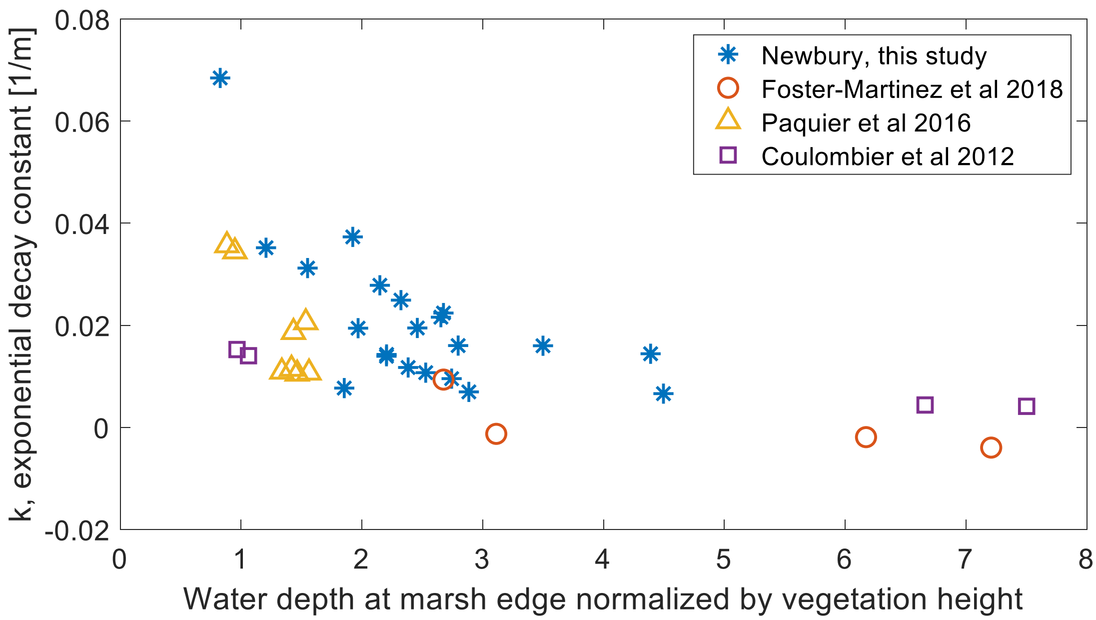

Figure 38. Comparison of the exponential decay results from the field measurements of this study to those conducted in other locations under similar conditions.

Comparison to other studies

The exponential decay constants calculated from the field measurements were compared to other field studies with similar conditions of low biomass (i.e. non-summer conditions, moderate to low wave heights). Paquier et al. (2016) present results from a wave attenuation study in Chesapeake Bay in a marsh dominated by *Spartina alterniflora* and *Spartina patens*. The results in Foster-Martinez et al (2018) are from a marsh with *Spartina foliosa* and *Salicornia pacifica* in

San Francisco Bay, and Coulombier et al (2012) are from a *Spartina alterniflora*-dominated marsh in the St. Lawrence Estuary. Comparing the decay constants removes potential discrepancies due to differences in how vegetation characteristics (i.e. stem count and stem width) were measured between the studies. The results do however account for the differences in height of the vegetation (Figure 38). The results are normalized for the vegetation height, meaning all points greater than 1 on the x-axis represent conditions when the vegetation is submerged (water depth is greater than vegetation height). The exponential decay constants from this study tend to be greater than other studies for all given normalized water depths, meaning there was greater wave attenuation in Newbury for similar inundation conditions. This result is likely due to the prevalence of senesced vegetation during the study period.

Marsh Transect Wave Attenuation Model

Using the MTWA model, results from different conditions, both marsh conditions and hydrodynamic conditions, were generated and evaluated. Complete attenuation is defined as the point when the wave height is 0.04 m or less. The distance from the start of the transect to complete attenuation was calculated and compared for the different conditions. For some conditions, complete attenuation was not reached. This occurred due to one of three reasons: the marsh was no longer inundated; the wave height never reached 0.04 m across the 1000 m transect; or the Delft3D output had no wave activity at that location.

Note for all figures in this section, the y-axis scale is consistent, but the x-axis scale changes to best show the results. The title contains information on the location of the transect. The transect locations can be seen in Figure 63, where the large numbers correspond to the areas of interest and the small numbers (within the hexagons) correspond to the transects with the area of interest. Tables of the complete attenuation distances, initial wave heights, and final wave heights can be found the Appendix 1: Marsh Transect Wave Attenuation Detailed Results.

Sea Level Rise

The results with sea level rise show greater inundation than those without, as expected. Greater inundation leads to less attenuation by vegetation. However, the Delft3D simulations show that the waves generated in the model with sea level rise tend to have longer wavelength (i.e. smaller wave number) and greater height. If all other conditions are held constant, vegetation attenuates waves with longer wavelengths to a greater degree than shorter wavelengths and attenuates larger wave heights more quickly than smaller wave heights (on a percentage basis). These effects are competing, and depending on the degree of difference in the inundation, wavelength, and wave height, the waves with sea level rise reach a height of 0.04 m closer or farther from the marsh edge than the waves without sea level rise. Numerous examples are provided in the following figures.

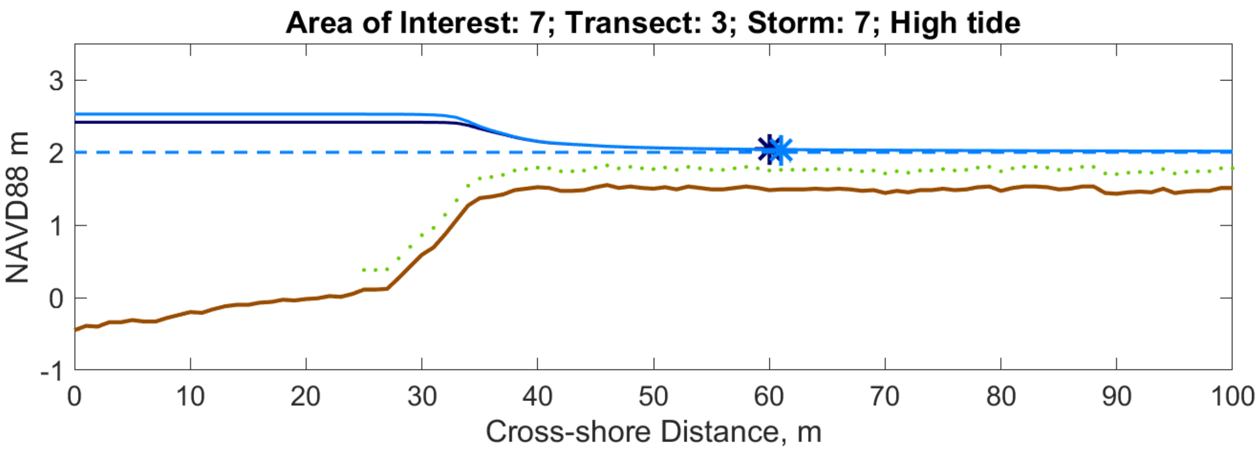

Figure 39. Wave height results with and without sea level rise (SLR).

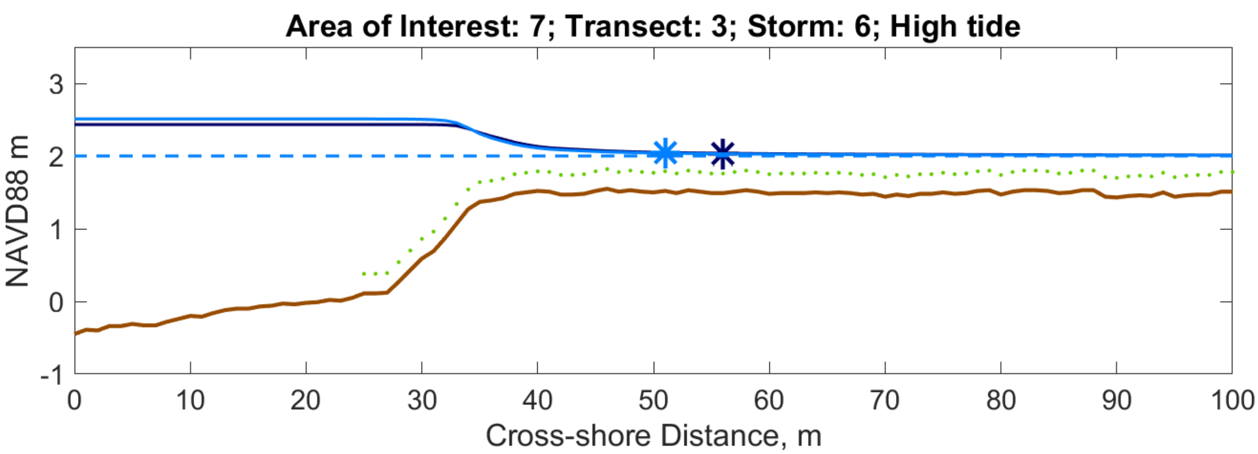

Figure 40. Wave height results with and without sea level rise (SLR). In all of these graphs, open-water is to left and upland is to the right, regardless of the true transect orientation.

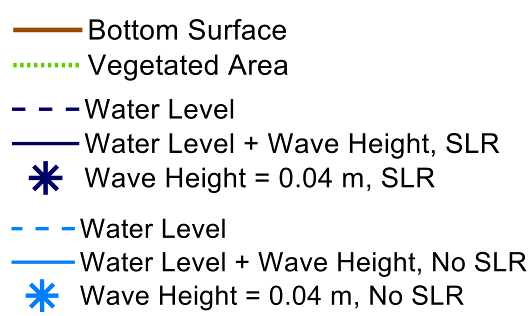

For the example in Figure 39, the wave without sea level rise (SLR) reaches complete attenuation (0.04 m) closer to shore than the wave with SLR. The reverse is true for the same transect but in a different storm simulation shown in Figure 40. Regardless, the magnitude of the difference is small. They are different by 1 m and 5 m in Figure 39 and Figure 40, respectively.

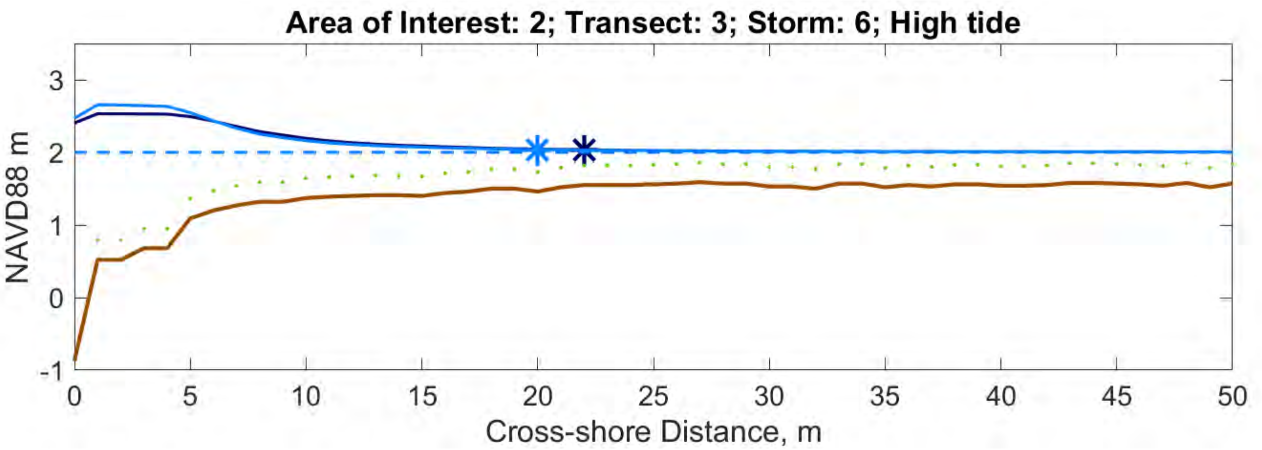

Figure 41. Wave height results with and without sea level rise (SLR). See Figure 40 for legend.

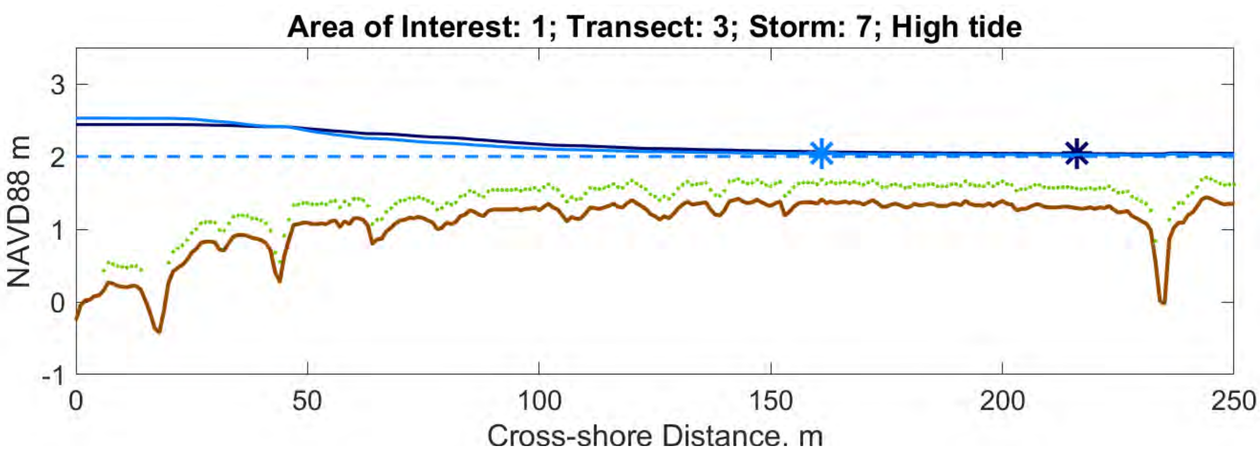

Figure 42. Wave height results with and without sea level rise (SLR). See Figure 40 for legend.

For both examples in Figure 41 and Figure 42 the wave with SLR reaches complete attenuation (0.04 m) closer to shore than the wave without SLR. The magnitude of the difference depends on the hydrodynamic conditions. In the top plot, the difference is small, 1m, whereas in the bottom example, the difference is 55 m.

Vegetation Type:

Spartina alterniflora and *Spartina patens* are two common marsh vegetation species with different morphologies. *Spartina patens* is shorter and has thinner stems in more dense stands of vegetation than *Spartina alterniflora*. Spartina alterniflora has two forms: a short form that grows on the marsh platform and a long form that grows at the mid-tide level and populates tidal creeks and tidal flats. Here, we see these differences impact the wave attenuation in different ways depending on the hydrodynamics. The drag coefficient is determined by the Reynolds number, and the Reynolds number is directly proportional to the stem width. Therefore, *Spartina patens* tends to have a lower Reynolds number and higher drag coefficient than *Spartina alterniflora.* In general, the waves on transects with *Spartina patens* reached complete attenuation over a shorter distance, but other factors are also present, causing the reverse to be true in some cases.

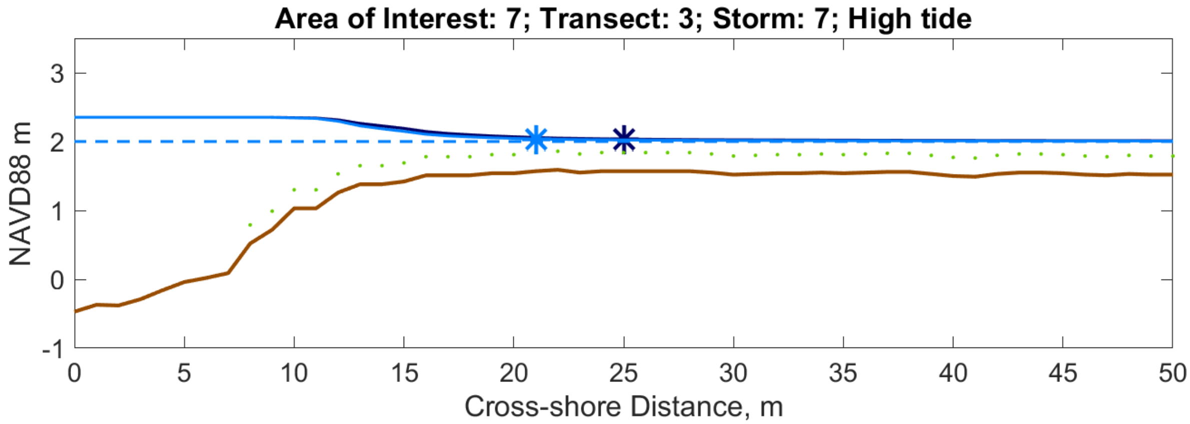

Figure 43. Wave height results with *Spartina alterniflora* and *Spartina patens*.

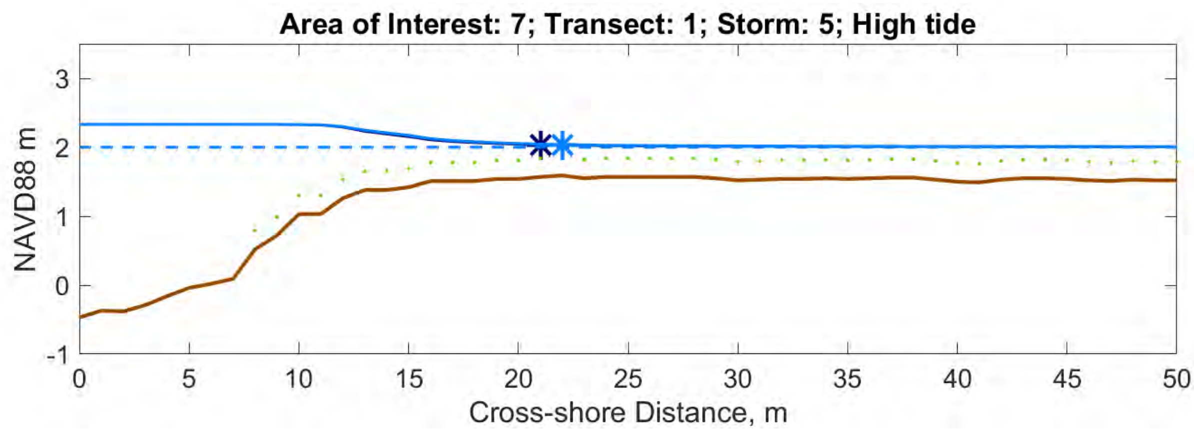

Figure 44. Wave height results with *Spartina alterniflora* and *Spartina patens*.

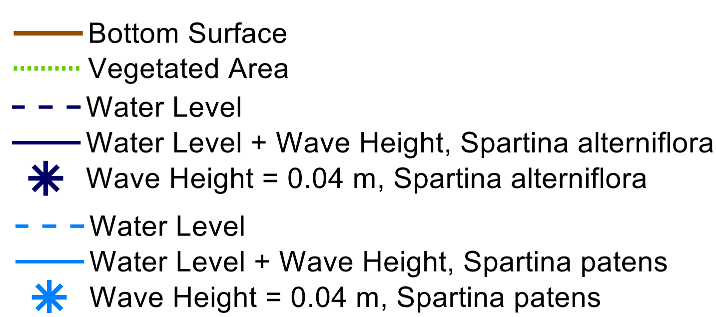

Examples in Figure 43 and Figure 44 show how similar transects can produce different results. In the two storms shown above, *Spartina alterniflora* reaches complete attenuation after *Spartina patens* in the top example and the reverse in the bottom example (Figure 44). The differences were small: 4 m and 1 m, top and bottom, respectively.

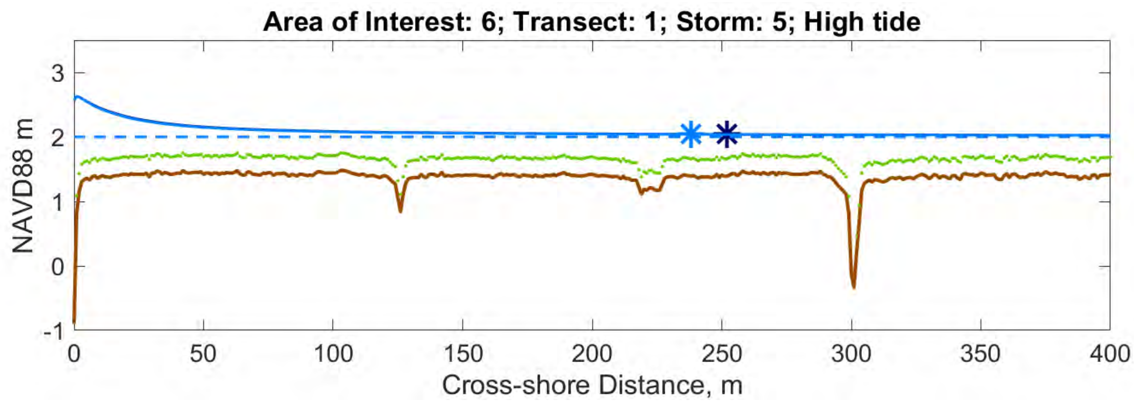

Figure 45. Wave height results with *Spartina alterniflora* and *Spartina patens*.

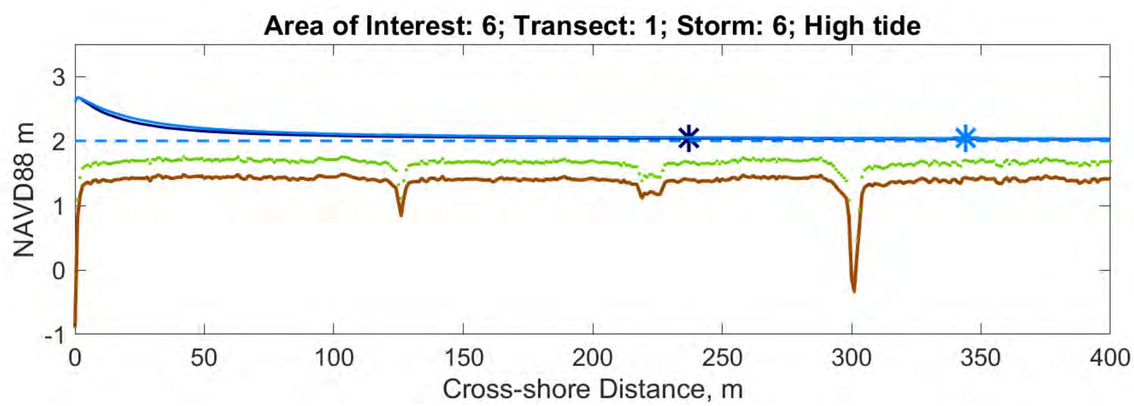

Figure 46. Wave height results with *Spartina alterniflora* and *Spartina patens*.

Examples in Figure 45 and Figure 46 show the dependence on hydrodynamic conditions. The same transect for two different storm conditions produces the same result, with *Spartina patens* reaching complete attenuation before *Spartina alterniflora* (short form), but to varying degrees of difference. In the top example, the difference is 14 m, whereas in the bottom example, the difference is 107 m.

Conversion to tidal flat

One of the major findings in our modeling is the importance of vegetation in attenuating wave storm energy. Removing drag due to vegetation from the model produced dramatically different results. Without vegetation 65% of the transects did not reach complete attenuation, whereas with vegetation only 15% did not reach complete attenuation across all four storms simulated. In the absence of vegetation, only drag due to bottom roughness reduces wave height.

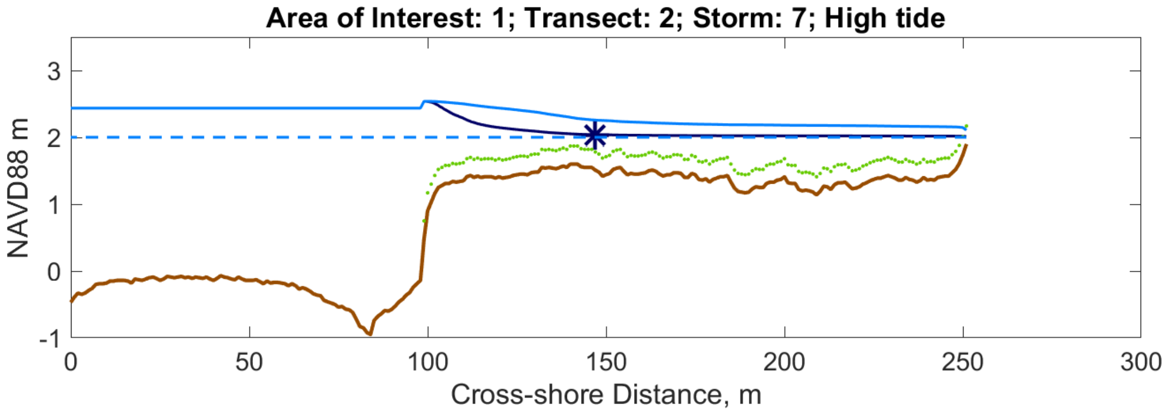

Figure 47. Wave height results with and without vegetation.

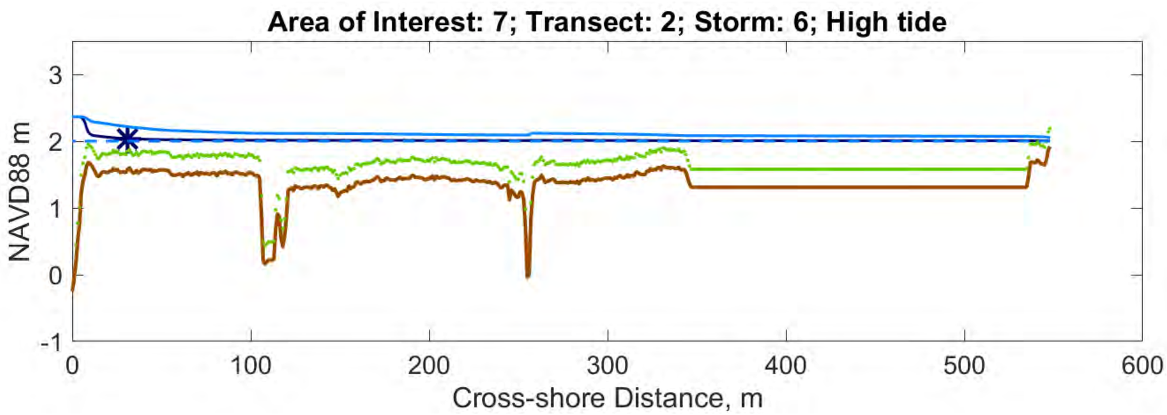

Figure 48. Wave height results with and without vegetation.

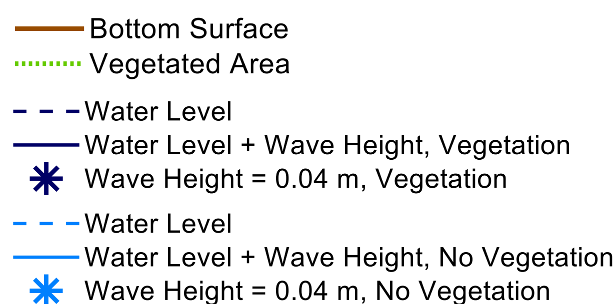

Both examples in Figure 47 and Figure 48 show instances where without vegetation, the wave height does not reach 0.04 m. For these cases, the transect ends because the marsh is no longer inundated. With vegetation, the wave height reaches 0.04 m after traversing 47 m (Figure 47) and 31 m (Figure 48).

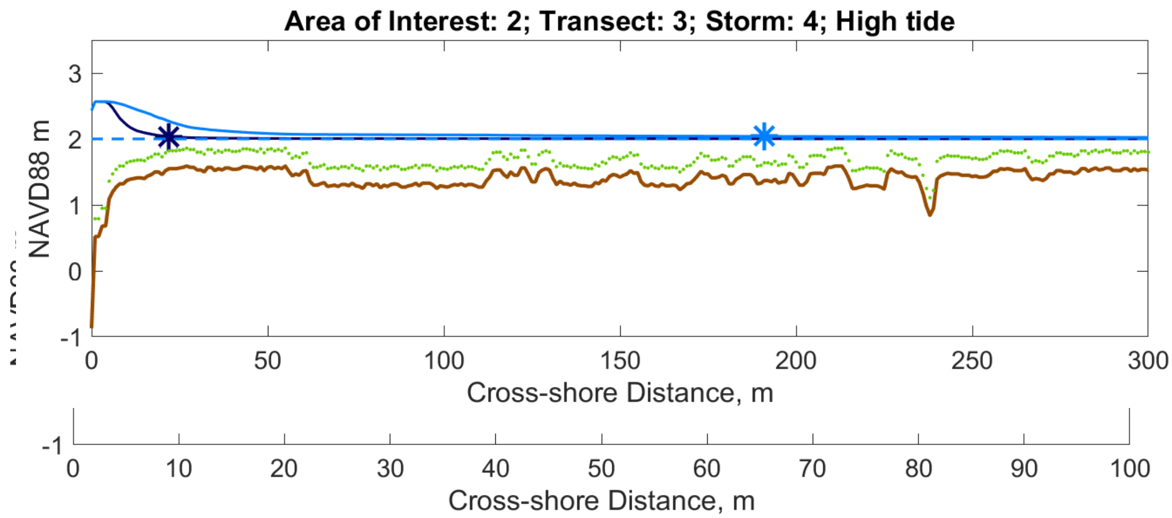

Figure 49. Wave height results with and without vegetation. Legend is the same as in Figure 48.

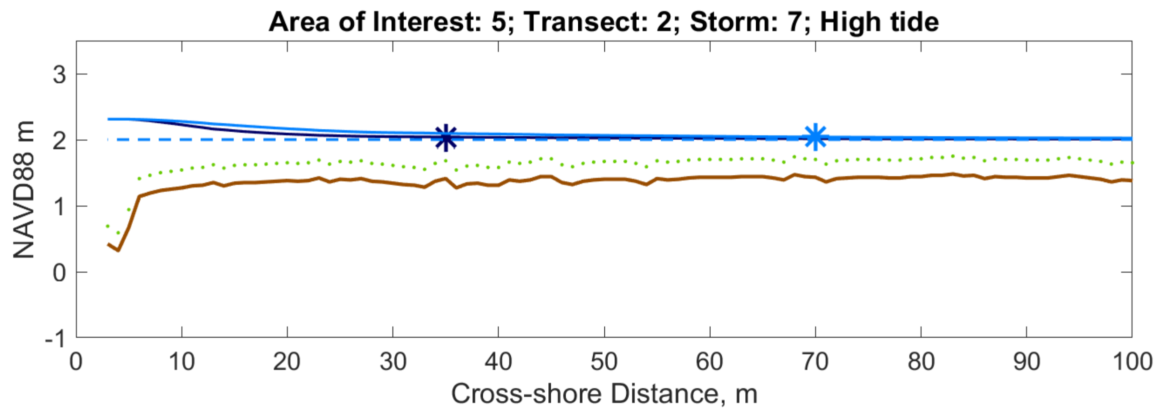

Figure 50. Wave height results with and without vegetation. Legend is the same as in Figure 48.

In the examples above, the drag due to bottom roughness is enough to cause the wave to reach complete attenuation; however, it requires a much longer distance to do so. In Figure 49, complete attenuation is reached in 22 m with vegetation and 191 m without. In the bottom example (Figure 50), the initial wave height is smaller, and therefore, there is less difference between the two cases. With vegetation, complete attenuation is reached in 35 m, and without reached in 70 m.

Lower platform elevation

Platform elevation has an important impact on wave energy. Lowering the marsh platform by 10% caused the waves to propagate farther inland for every transect and every storm simulation Lowering the elevation causes greater inundation, meaning the vegetation takes up a smaller portion of the water column and less impact on the wave height. Even though the same effect was observed elsewhere, the relative difference between distances required for complete attenuation changed depending on the hydrodynamic conditions. The examples in Figures 52 and 54 illustrate this point.

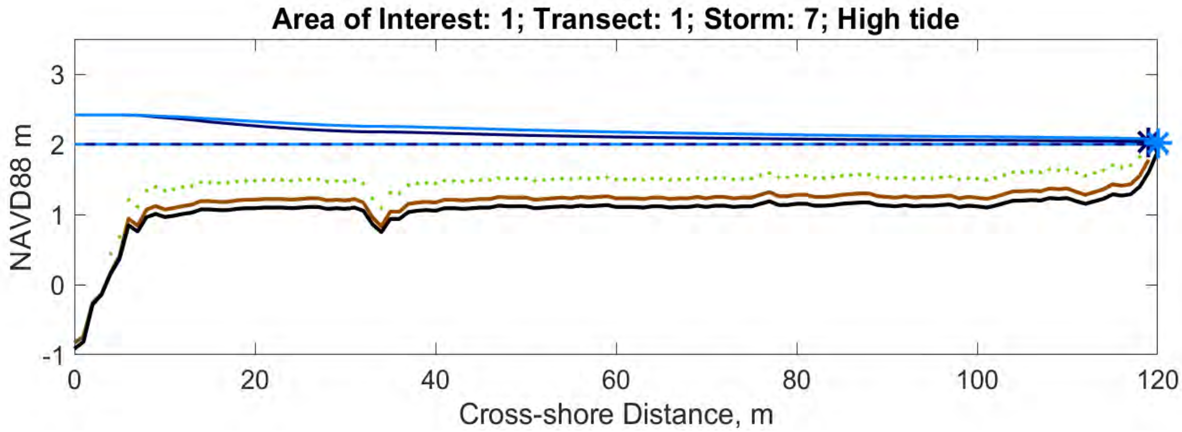

Figure 51. Wave height results with a normal marsh platform and with a lowered marsh platform. Note, the black line is the lowered marsh platform.

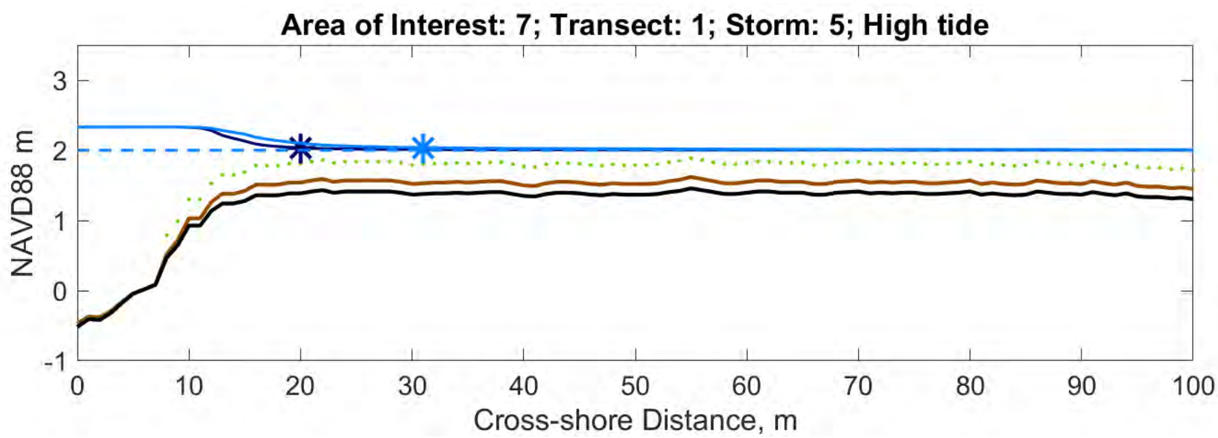

Figure 52. Wave height results with a normal marsh platform and with a lowered marsh platform. Note, the black line is the lowered marsh platform.

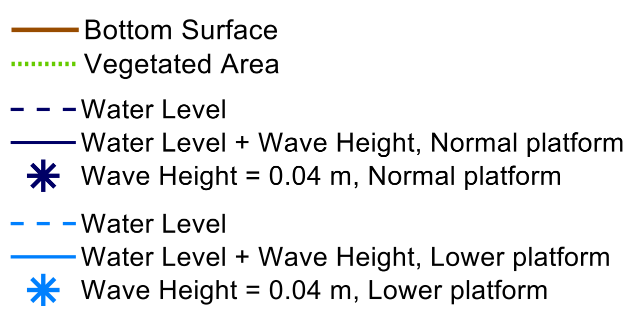

In the examples displayed in Figures 51 and 52, the differences between the complete attenuation point are smaller, relative to the other transects and storms. In Figure 51, lowering of the platforms causes an 11 m shift landward of the complete attenuation point, and in Figure 52, the attenuation point is the same (just before a non-inundation point is reached).

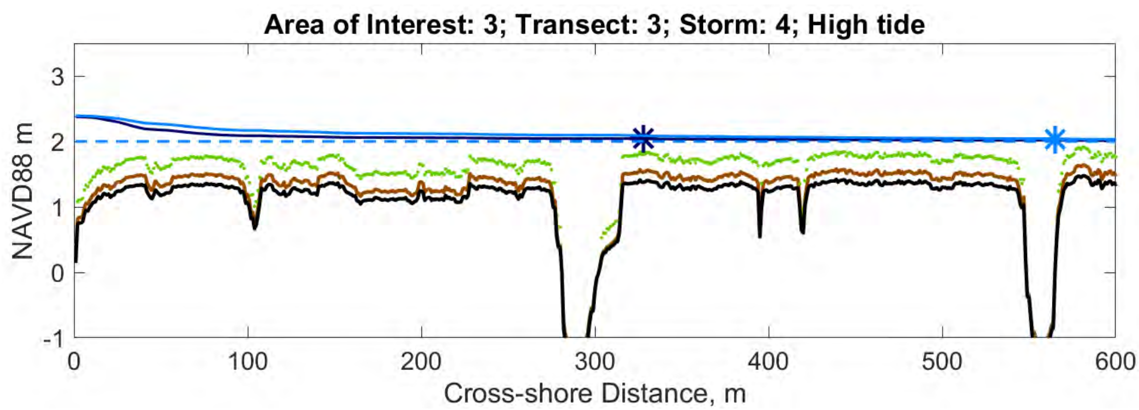

Figure 53. Wave height results with a normal marsh platform and with a lowered marsh platform. Note, the black line is the lowered marsh platform. Legend is the same as Figure 52.

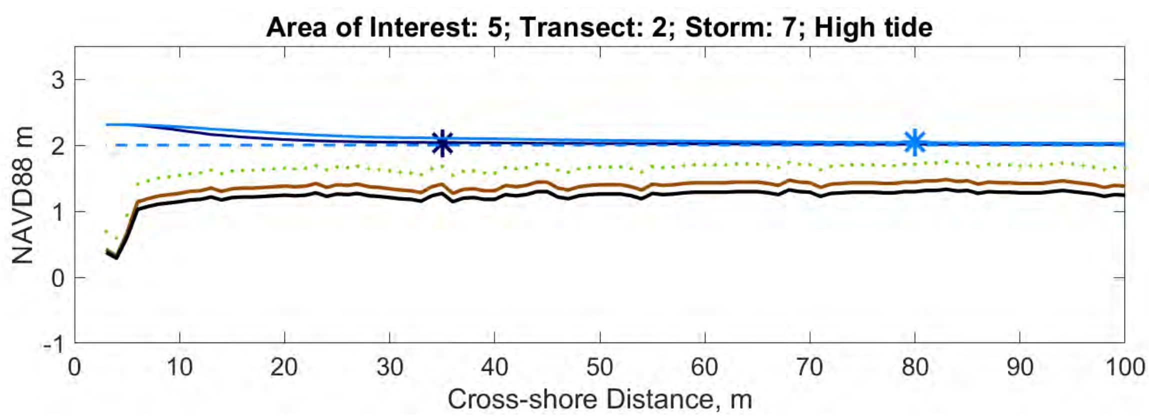

Figure 54. Wave height results with a normal marsh platform and with a lowered marsh platform. Note, the black line is the lowered marsh platform. Legend is the same as Figure 52.

The examples in Figure 53 show how the difference between them often scales with the distance to complete attenuation. In both plots, lowering the platform by 10% about doubles the distance needed to reach complete attenuation (Figure 54). The difference in the top plot is 237 m, and the difference in the bottom is 45 m.

Filling ditches

Filling ditches had a mixed effect on the wave heights depending on the width of the ditch, the number of ditches filled, and the hydrodynamic conditions. For the transects that were impacted by filling ditches, the effect tended to be small, with a median value of 3 m and an average of 30 m. Note, no transects ran along the ditches, but rather, cut across them. Also, the inundation patterns were not altered in the model to reflect the lack of flow conveyance from filled ditches; therefore, there may be effects that were not captured.

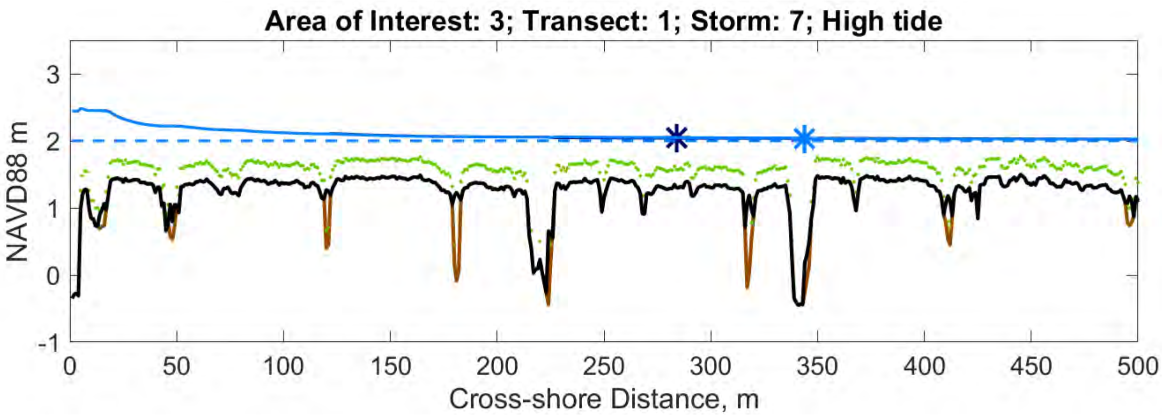

Figure 55. Wave height results for normal marsh platform and for platforms with ditches filled.

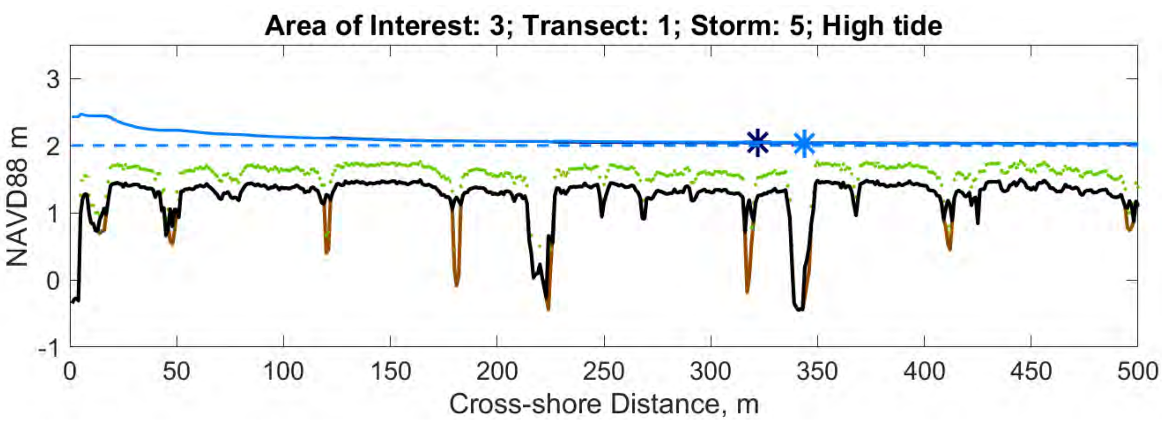

Figure 56. Wave height results for normal marsh platform and for platforms with ditches filled.

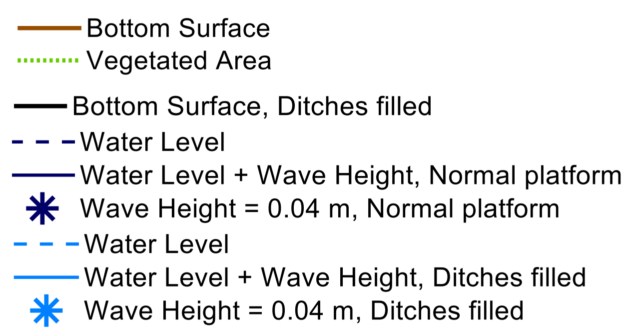

The transect in Figure 56 shows conditions where filling the ditches caused the complete attenuation point to move farther inland. The same transect is shown for two storms, allowing the impact of hydrodynamic conditions to be observed. In Figure 56, the difference between the complete attenuation points is 60 m, and in the bottom plot, it is 22 m.

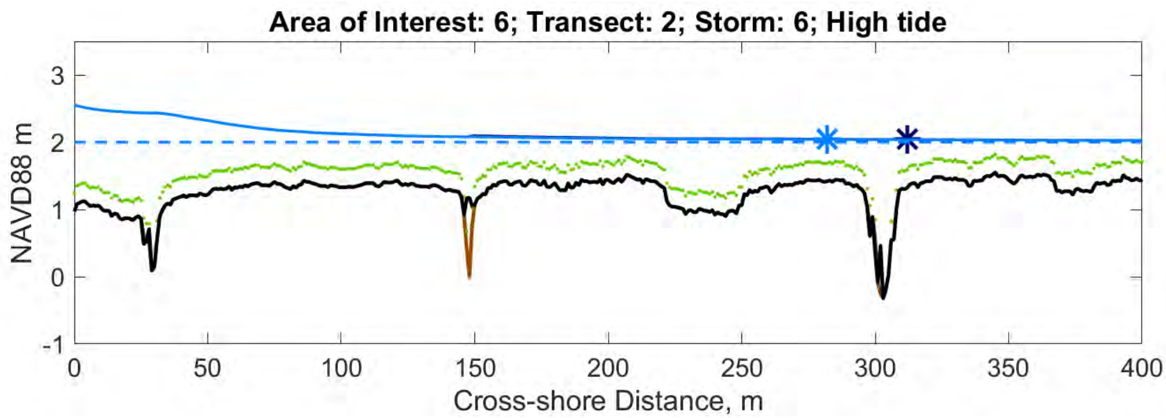

Figure 57. Wave height results for normal marsh platform and for platforms with ditches filled. Legend is the same as in Figure 56.

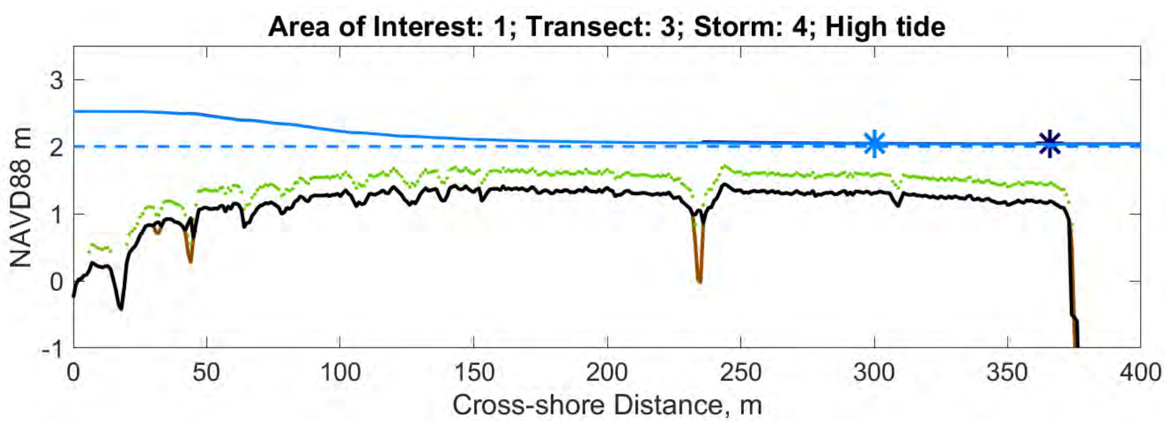

Figure 58. Wave height results for normal marsh platform and for platforms with ditches filled. Legend is the same as in Figure 56.

In the examples in Figures 57 and 58 filling ditches decreases the length of marsh required to reach complete attenuation. Filling the ditch prevents the inundation from increasing over those portions of the transects. Differences between the complete attenuation points are 30 m and 66 m, respectively.

Oyster reefs

The presence of oyster reefs had little effect on wave heights. They did, however, always decrease the distance required to the complete attenuation point, but this decrease was always less than 10 m. Oyster reefs have a greater impact on the waves when their height is comparable to the depth. Only conditions where the marsh was at least partially inundated were modeled here; therefore, the lower inundation conditions, where oyster reefs have a greater impact, were not modeled.

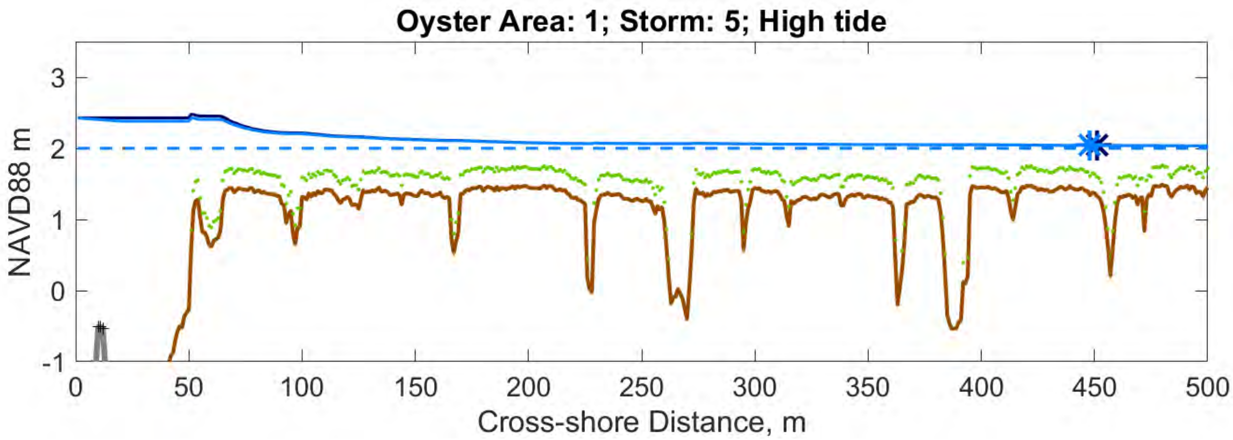

Figure 59. Wave height results for normal marsh and for a marsh with adjacent oyster reefs. Simulated oyster reef is shown by the gray mound.

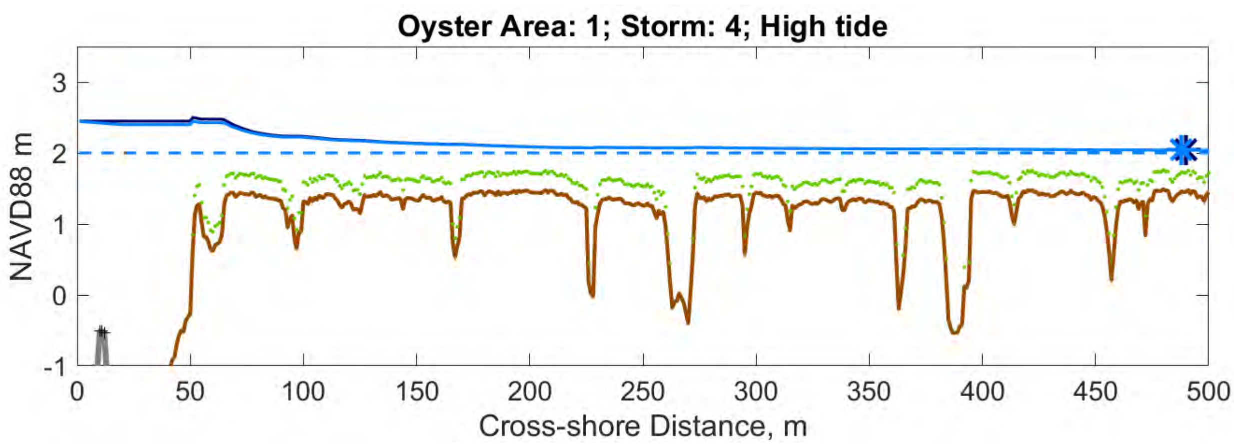

Figure 60. Wave height results for normal marsh and for a marsh with adjacent oyster reefs. Simulated oyster reef is shown by the gray mound.

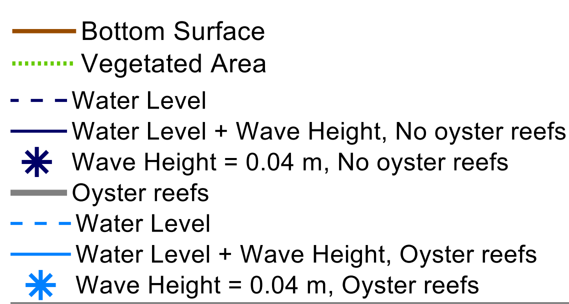

The same transect is shown for two storms in Figure 59 and Figure 60. The impact of the oyster reef is minimal, and the difference in the complete attention point is 3 m and 2 m, respectively.

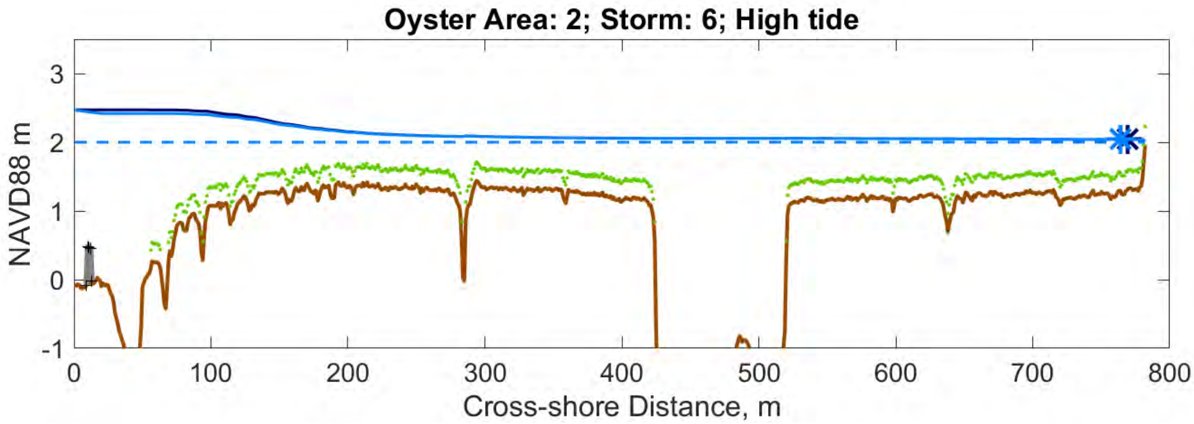

Figure 61. Wave height results for normal marsh and for a marsh with adjacent oyster reefs. Simulated oyster reef is shown by the gray mound.

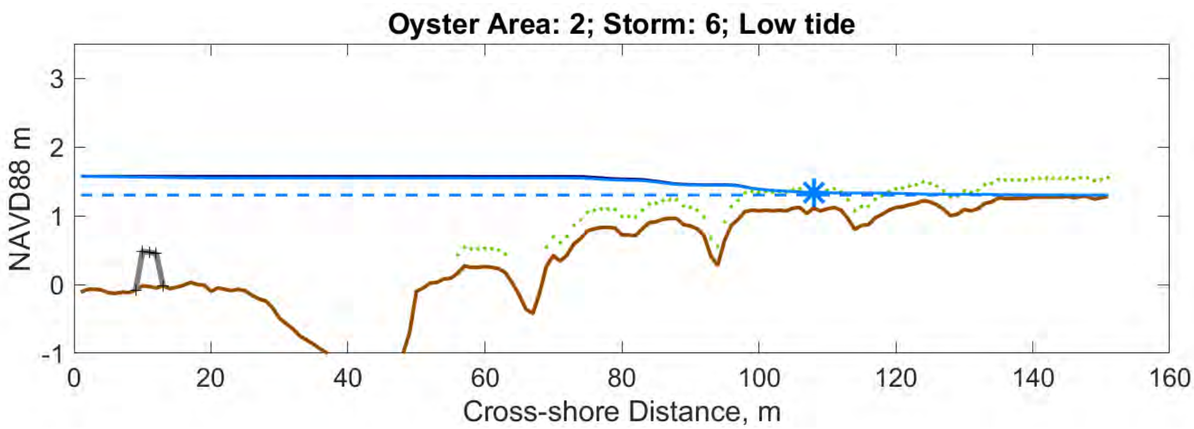

Figure 62. Wave height results for normal marsh and for a marsh with adjacent oyster reefs. Simulated oyster reef is shown by the gray mound.

The examples in Figures 61 and 62 show the difference between the higher tide case (spring high tide, Figure 61) and a lower tide case (neap high tide, Figure **62**). For the lower tide, the oyster reef does not change the position of the point of the complete attenuation (108 m). For the higher tide, the presence of the oyster reef causes a 5 m decrease in the distance to complete attenuation (764 m vs. 769 m).

CONCLUSIONS

Field Measurements

- Wave height time series measured at the three field transects (Figure 6) sites were sufficient for initializing the wave model and validating the modeled output. Although a major storm did not impact the area during the study area, the modeling allowed us to adequately scale storm conditions upward.

- The maximum waves measured at Transects #1, #2, and #3, observed were 0.17 m, 0.22 m, and 0.31 m, respectively. The maximum water depth measured on the marsh platform at Transect #2 and #3 was 0.57 m and 0.88 m at Transect #1. The median wave height at the edge of the marsh was 0.02 m for Transect #1 and #2 and 0.05 at Transect #3.

- Wave attenuation increased with decreasing water level. At the Transect #3, average percent attenuation was 74% for depths less than 0.5 m and 58% for depths greater than 0.5 m over a 50.2 m distance. For Transect #2, average attenuation was 64% for depths less than 0.5 m and 46% for depths greater than 0.5 m over a 74.6 m distance. At the Transect #1, the instruments were closer together. Over the 20.5 m distance, the average attenuation for depths greater than 0.5 m was 10% and 13% for depths less than 0.5 m.

Modeling Studies

- Wave attenuation across the marsh was modeled for four storms at two water levels using three transects across the marsh at each of the seven areas of interest (see seven sites in Figure 5). Conditions on the marsh platform were altered to test the impact of 10 different cases on wave attenuation. These results are largely summarized in Figures Figure **64**Figure 65.

- The distance to complete attenuation depends on the characteristics of the waves (wavelength and wave height) reaching the marsh and the topography of the marsh. These characteristics varied throughout the study area, and the distance to complete attenuation ranged from 20 m to 366 m for the base conditions.

- One of the major findings was that for the largest wave in each of the simulated storm at spring high tide, the waves were completely attenuated before reaching the upland surrounding the marsh. Two minor exceptions to this patterns occurred is areas 1 and 5, where wave heights were reduced from 0.53 m to 0.05 m and 0.26 m to 0.07 m, respectively. The resulting breaking waves against the shore were very small, but not completely attenuated, because the marsh is narrow at these sites.

- For the 10 cases studied, the most drastic change in attenuation occurred when the marsh platform was artificially lowered by 10% and/or the vegetation was completely removed. Under these circumstances, the bottom friction was reduced and thus, waves were not as greatly reduced in height compared to conditions of the present marsh system. When the marsh is lowered or the vegetation removed, waves never reached complete attenuation in 6 of the 7 areas with ensuing wave heights up to 0.27 breaking along the shoreline.

These findings emphasize the importance of maintaining a healthy marsh platform to attenuate breaking waves and shoreline erosion.

- Our regional modeling suggests that the topography of the marsh platform, with or without vegetation, does little to attenuate the storm surge, meaning that the water elevation along the shoreline during the storm is almost the same as it is in open water areas, such as in upper Plum Island Sound. It appears that during major storms, the entire backbarrier behaves as a large open-water pond. While some attenuation does occur as flooding from the sound enters the tidal creeks, once the marsh platform is flooded, storm winds push water against the high inland topography encompassing most of Newbury. At this stage, the storm setup acts to eliminate whatever attenuation existed initially. As expected, during intermediate storms, because storm surge inundation is lower, the marsh platform and vegetation produce high attenuation. During high inundation events, wind setup is of the order of 10-30 cm, while wave setup is negligible, likely because waves are attenuated rapidly. During lower inundation events wind, while attenuation can be higher, wind setup increases (~20-40 cm). Anecdotal observations of the marsh during major storm conditions tend to confirm this finding. Consequently, sea level rise will not appreciably increase storm surge height. However, as the marsh lowers the surge will impact the upland shoreline sooner during the storm impacts.

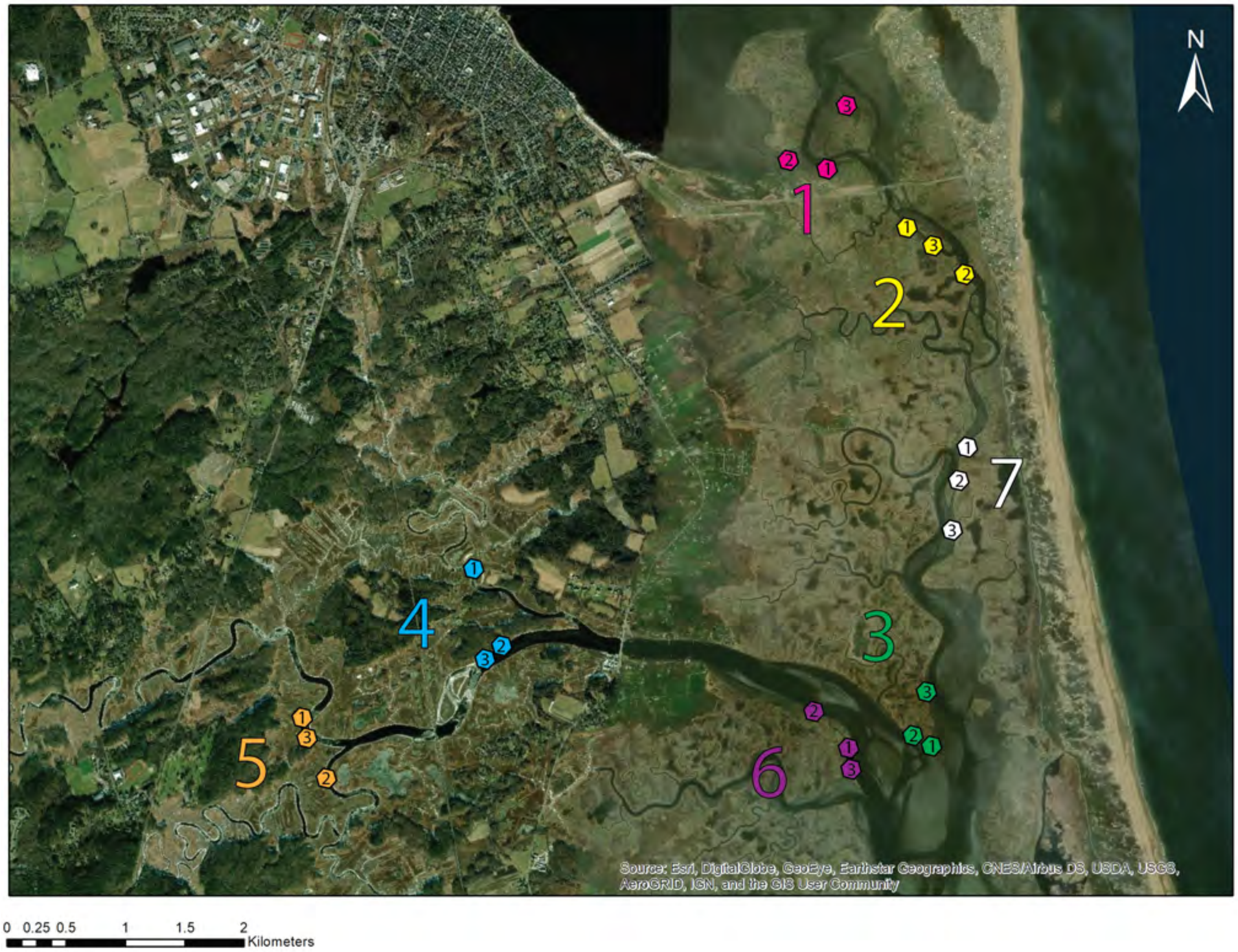

Figure 63. Location of the 7 Areas of Concern. Note that each site has three color-coded locations, indicating where the modeling outputs were collected along the transect across the marsh.

Figure 64. Schematic of Area #2 (see Figure 50 for location) illustrating that under moderate northeast storm conditions, maximum wave height along the marsh edge at the three sites varied from 0.2 to 0.8 cm, but after a distance of propagation across the marsh platform their heights reduce to 0.1 to 0.0 cm.

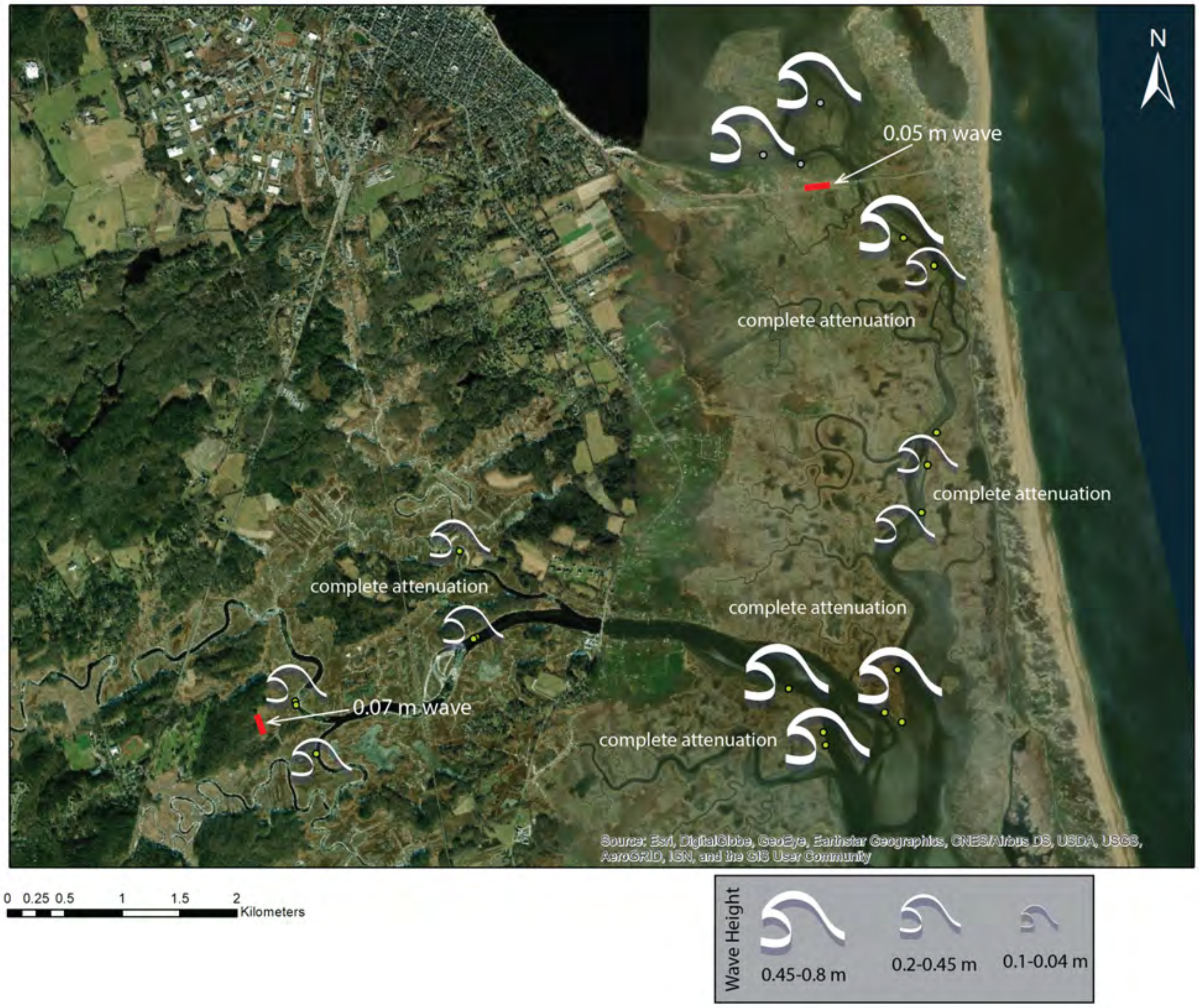

Figure 65. Summary diagram of maximum wave conditions for a variety of storm wind directions depending on the location of the station and its proximity to open water. The legend provides a range in wave heights for the maximum storm wind conditions. Note that all waves are attenuated except for sites at Kent Island and the Turnpike region where the marsh is particularly narrow.

Vegetation Trends

- The vegetation transect data demonstrates a lack of any overall trend between vegetation type and elevation. Because halophytic vegetation is closely tied to hydroperiod, this was finding was unexpected. One exception occurs at the Parker River transect where there is a slight correlation with percent *S. patens* (trend explains 30% of data). The overall lack of control by elevation indicates that the plants are responding to a variety of additional forcings, including hydroperiod, nutrient loading, peat characteristics, proximity to open water, and perhaps other factors (see below).

- At individual sites, natural expected relationships were blurred. Possible explanations include:

    a. **Plum Island Turnpike** is influenced by the restriction of the bridge and is far from Ipswich Bay. Therefore, salt water input to this region is low, resulting in a high diversity of saltmarsh vegetation on the high marsh rather than classic zonation patterns.
    b. **Kent Island** is heavily degraded as a result of increased inundation due to rising sea level. In addition, the presence of a berm for the railroad restricts tidal flow through this area. The observed vegetation appears in the initial phase of transition.
    c. **Parker River** is dominated by typical, healthy marsh vegetation. We observed a relationship between vegetation and elevation at this site. However, it is important to note that pannes have been drained over a large portion the site to improve native marsh habitat. Hence, the site is currently in a state of transition.

OUTREACH

Dialogue between the community and researchers has been an important part of this process. To help facilitate this dialogue, an informal presentation of the preliminary findings was held on May 31, 2019, at the Parker River Wildlife Refuge Headquarters. Presentation by project authors Zoe Hughes and Madeline Foster-Martinez was followed by a lively discussion, where community members and other stakeholders gave feedback and shared their own observations. This information was then incorporated into the modeling approach. For example, the MTWA model was run at a finer grid resolution.

The results of this study are relevant not only to Newbury, but also, to the broader applied scientific community working towards understanding coastal protection from living shorelines. Madeline Foster-Martinez has given two oral presentations at scientific conferences on the results from the field measurements. The first talk was titled Wave Attenuation across a salt marsh in Newbury, MA at the Coastal and Estuarine Research Federation. Mobile, AL on November 7, 2019. The second talk was given at the American Geophysical Union Fall Meeting in San Francisco, CA, on December 11, 2019, and focused on the results from the marsh scarp. The title was Role of marsh edge form in wave attenuation: field measurements in Newbury, MA. The material presented in these talks is currently in prep to be submitted to peer-reviewed journals.

DELIVERABLES

Task 1: Field Data Collection		
Sub-task 1.1 Vegetation transects, Summer	Characterization of marsh relief and vegetation	Vegetation Surveys, p. 37-42
Sub-task 1.2 Deploying marsh and PIS instruments	Time series of currents, tides, and waves	Field Measurements, p. 47-57
Sub-task 1.3 Late Fall vegetation survey	Characterization of marsh during dormant vegetation stage	Vegetation Surveys, p. 37-42
Task 2: Storm Characterization		
Sub-task 2.1 Compile existing storm data	Storm statistics	Storm characterization and analysis, p. 46-47
Sub-task 2.2 Data Analysis, Specify storm magnitude & frequency	Model storm inputs	Storm characterization and analysis, p. 46-47
Task 3: Defining Sea Level Positions		
Sub-task 3.1 Analyze sea level data	Discussion of SLR curves	Future Bathymetry adjustment due to sea level rise, p. 45 - 46
Sub-task 3.2 Specify future sea level positions for model	Specification of marsh positions for model	Future Bathymetry adjustment due to sea level rise, p. 45 - 46
Task 4: Hydrodynamic and Wave Modeling		
Sub-task 4.1 Implement initial conditions	Functioning hydrodynamic and wave model	Initial conditions, p. 19 Hydrodynamic and wave modeling, p.42 - 44
Sub-task 4.2 Validate and calibrate model	Calibrated model	Calibration/Validation, p. 20 Hydrodynamic and wave modeling, p.42 - 44
Sub-task 4.3 Run different storm conditions	Model output for different storm conditions	Storm characterization and analysis, p. 46-47, the storm output is used in all subsequent model runs (Sub-task 4.4 – Sun-task 5.4)
Sub-task 4.4 Run model for different SLR positions	Model output for different SLR conditions	Future Bathymetry adjustment due to sea level rise, p. 45 - 46 Sea level rise, p. 58-60
Task 5: Modeling Marsh Enhancements		
Sub-task 5.1 Run model for different marsh vegetation	Model output for different vegetation types	Vegetation type, p. 60-62
Sub-task 5.2 Run model for tidal flat conversion to marsh	Model output for marsh converted to tidal flat	Conversion to tidal flat, p. 63-64 Lower platform elevation, p. 65-66
Sub-task 5.3 Run model for ditch and channel filling	Model output for platform with reduced ditching	Filling ditches, p. 67-68
Sub-task 5.4 Run model for oyster and mussel reef	Model output for implementing oyster & mussel reefs	Oyster reefs, p. 69-70
Sub-task 5.5 Run model for thin layer deposition	Model output for raising marsh through TLD	No scientific consensus. MA agencies will not permit.

REFERENCES

Baptist, M.J., 2005, Modeling Floodplain Biogeomorphology. ISBN v. 90-407-2582-9.

Booij N., Ris, R.R.C., Holthuijsen, L.H.L., 1999. A third-generation wave model for coastal regions 1. Model description and validation. Journal of Geophysical Research 104, 7649–7666.

Caldwell, R. L., and D. A. Edmonds (2014) The effects of sediment properties on deltaic processes and morphologies: A numerical modeling study, J. Geophys. Res. Earth Surf., v. 119, p. 961-982.

Coulombier, T., Neumeier, U., & Bernatchez, P. (2012). Sediment transport in a cold climate saltmarsh (St. Lawrence Estuary, Canada), the importance of vegetation and waves. Estuarine, Coastal and Shelf Science, 101, 64–75. https://doi.org/10.1016/j.ecss.2012.02.014

DeConto, R.M., & Pollard, D., 2016. Contribution of Antarctica to past and future sea-level rise, Nature, p. 591-597.

Dean, R. G., & Dalrymple, R. A. (1991). Water wave mechanics for engineers and scientists (Vol. 2). world scientific publishing Co Inc.

Dietrich, J.C., et al (2011) Hurricane Gustav, 2008. Waves and storm surge: Hindcast, synoptic analysis, and validation in southern Louisiana. Mon. Weather Rev. 139 (2011), 2488–2522. https://doi.org/10.1175/2011MWR3611.1.

Fischbach, J.R., Johnson, D.R., Kuhn, K., Pollard, M., Stelzner, C., Costello, R., Molina, E., Sanchez, R., Syme, J., Roberts, H., & Cobell, Z., 2017. Coastal Master Plan Modeling: Version II. Baton Rouge, Louisiana: Coastal Protection and Restoration Authority, p. 1-216.

FitzGerald, D. M. (1993). Origin and Stability of Tidal Inlets in. Coastal and Estuarine Studies, 44, 1–61.

Fitzgerald, D. M., & Van Heteren, S. (1999). Classification of paraglacial barrier systems: coastal New England, USA. Sedimentology, 46(6), 1083–1108.

FitzGerald, D., Hughes, Z., Hein, C., and Georgiou, I., 2017, Hydrodynamic and Sediment Transport Modeling Leading to Restoration, Better Management, and Improved Sustainability of Great Marsh. National Wildlife Foundation, Final Report. 78 p

Foster-Martinez, M. R., Lacy, J. R., Ferner, M. C., & Variano, E. A. (2018). Wave attenuation across a tidal marsh in San Francisco Bay. Coastal Engineering, 136, 26–40. https://doi.org/10.1016/j.coastaleng.2018.02.001

Hanegan K., and Georgiou, I.Y., 2015, Tidal modulated flow and sediment flux through wax lake delta distributary channels: Implications for delta development. Proceedings of the International Association of Hydrological Sciences.

Hayes, M.O., 1979. Barrier island morphology as a function of wave and tide regime. In: Leatherman, S.P. (Ed.), Barrier Islands from the Gulf of St. Lawrence to the Gulf of Mexico. Academic Press, New York, NY, p. 1–29.

Hein, C.J., FitzGerald, D.M., Buynevich, I.V., van Heteren, S., and Kelley, J.T., 2014. Evolution of paraglacial coasts in response to changes in fluvial sediment supply. Geological Society, London, Special Publication, 388, 247-280.

Hein, C. J., FitzGerald, D. M., Carruthers, E. A., Stone, B. D., Barnhardt, W. A., & Gontz, A. M. (2012). Refining the model of barrier island formation along a paraglacial coast in the Gulf of Maine. Marine Geology, 307, 40–57.

Hopkinson CS, Morris JT, Fagherazzi S, Wollheim WM, Raymond PA. 2018. Lateral marsh edge erosion as a source of sediments for vertical marsh accretion. *J. Geophys. Res. Biogeosci.* 123:2444–65.

Hu K, Chen Q, Kimball SK (2012) Consistency in hurricane surface wind forecasting: an improved parametric model. Natural hazards v. 61, p. 1029-1050.

Kobayashi, N., Raichle, A. W., & Asano, T. (1993). Wave Attenuation by Vegetation. Journal of Waterway, Port, Coastal, and Ocean Engineering, 119(1), 30–48. https://doi.org/10.1061/(ASCE)0733-950X(1993)119:1(30)

Kopp, R.E., DeConto, R.M., Bader, D.A., Hay, C.C., Horton, R.M., Kulp, S., Oppenheimer, M., Pollard, D., and Strauss, B.H., 2017: Evolving understanding of Antarctic ice-sheet physics and ambiguity in probabilistic sea-level projections. Earth's Future, v 5, p. 1217-1233, doi:10.1002/2017EF000663.

Lesser, G., Roelvink, J., van Kester, J., and Stelling, G., 2004. Development and validation of a threedimensional morphological model. Coastal Engineering, v. 51, p. 883 - 915.

Liu K, Chen Q, Hu K, Xu K, Twilley RR (2018) Modeling hurricane-induced wetland-bay and bay-shelf sediment fluxes. Coastal Engineering, v. 135, p. 77-90.

Massachusetts Coastal Zone Management, 2013, Sea Level Rise: Understanding and Applying Trends and Future Scenarios for Analysis and Planning, Causeway Street, Suite 800, Boston, MA 18 p.

Millette, T.L., Argow, B.A., Marcano, E., Hayward, C., Hopkinson, C.S., and Valentine, V., *2010*, Salt Marsh Geomorphological Analyses *via*Integration of Multitemporal Multispectral Remote Sensing with LIDAR and GIS. Journal of Coastal Research: 26: 809 – 816.

Möller, I. 2006. Quantifying saltmarsh vegetation and its effect on wave height dissipation: Results from a UK East coast saltmarsh. Estuarine, Coastal and Shelf Science v. 69, p. 337–351.

Mukai A.Y., Westerink J.J., Luettich Jr R.A., Mark D., 2002, Eastcoast 2001, a tidal constituent database for western North Atlantic, Gulf of Mexico, and Caribbean Sea (No. ERDC/CHL-TR-02-24). Engineer Research and Development Center Vicksburg MS Coastal and Hydraulics lab.

National Flood Insurance Program, 2014, Policy Statistics for Massachusetts, https://www.iii.org/fact-statistic/facts-statistics-flood-insurance.

NOAA. 2017. Habitat Blueprint: Living Shorelines. https://www.habitatblueprint.noaa.gov/livingshorelines/

NOAA, 2018, Sea Level Rise Viewer, Office of Coastal Management DIGITALCOAST, https://coast.noaa.gov/digitalcoast/tools/slr

Paquier, A.-E., Haddad, J., Lawler, S., & Ferreira, C. M. (2016). Quantification of the Attenuation of Storm Surge Components by a Coastal Wetland of the US Mid Atlantic. Estuaries and Coasts. https://doi.org/10.1007/s12237-016-0190-1

Sammel, E. A. (1967). Water resources of the Parker and Rowley river basins, Massachusetts.

Shawler, J.L., Hein, C.J., Canuel, E.A., Kaste, J.M., Fitzsimons, G.G., Georgiou, I.Y., Willard, D.A., 2019. Tidal erosion and upstream sediment trapping modulate records of land-use change in a formerly glaciated New England estuary. *Anthropocene Coasts*, 2: 340-361, doi: 10.1139/anc-2018-0034

Simcox, A. C. (1992). Water resources of Massachusetts. Water-Resources Investigations Report, 90, 4144

Stark, J., Plancke, Y., Ides, S., Meire, P., and Temmerman, S., 2015, Storm surge attenuation in a large intertidal marsh: impact of marsh geomorphology, Proc. of the 36th IAHR World Congress. p. 325-341.

Stone, B.D., Stone, J.R., DiGiacomo-Cohen, M.L., 2006. Surficial Geologic Map of the Salem-Newburyport East-Wilmington-Rockport 16 Quadrangle Area in Northeast Massachusetts, U.S. Geological Survey Open-File Report, 2006-1260-B.

Sullivan JC, Torres R, Garrett A, Blanton J, Alexander C, Robinson M, Moore T, Amft J, Hayes D (2015) Complexity in salt marsh circulation for a semienclosed basin. Journal of Geophysical Research-Earth Surfaces 120: 1973–1989.

UMass Boston, 2016, Climate Ready Boston: Climate Change and Sea Level Rise Projections for Boston, Boston, MA. 60 p.

Valentine, V., & Hopkinson Jr, C. (2005). NCALM LIDAR: Plum Island, Massachusetts, USA: 18-19 April 2005. Elevation Data and Products Produced by NSF-Supported National Center for Airborne Laser Mapping (NCALM) for Plum Island Ecosystems Long Term Ecological Research (PIE-LTER) Project.

Vallino, J.J., Hopkinson Jr., C.S., 1998. Estimation of dispersion and characteristic mixing times in Plum Island Sound estuary. Estuarine Coastal and Shelf Science 46: 333–350.

Wade, c., 2018, Officials tally storm damage, the daily news. New york, NY, p.1-3.

Wiberg, P. L., & Sherwood, C. R. (2008). Calculating wave-generated bottom orbital velocities from surface-wave parameters. Computers & Geosciences, 34(10), 1243–1262. https://doi.org/10.1016/j.cageo.2008.02.010

Wilson, C., Hughes, Z.J., FitzGerald, D.M., Hopkinson, C.S., Valentine, V.J., Kolker, A.S., 2014. Marsh pool and tidal creek morphodynamics: dynamic equilibrium of northern saltmarshes? Geomorph., 213: 99-115.

Woods Hole Group, 2017, Living Shorelines in New England: State of the Practice, East Falmouth MA, 55 p.

Wu, W., Zhang, M., Ozeren Y., and Wren, D., 2013, Analysis of Vegetation Effect on Waves Using a Vertical 2D RANS Model: Journal of Coastal Research, 29: 383-397.

Yang, S. L., Shi B. W., Bouma, T. J., Ysebaert, T., and Luo, X. X., 2012, Wave Attenuation at a Salt Marsh Margin: A Case Study of an Exposed Coast on the Yangtze Estuary Estuaries and Coasts, v. 35, p. 169– 182,. DOI 10.1007/s12237-011-9424-4.

Zhao, L., Changsheng, C., Vallino, J., Hopkinson, C., Beardsley, R.C., Huichan, L., Lerczak, J., 2010. Wetland–estuarine–shelf interactions in the Plum Island Sound and Merrimack River in the Massachusetts coast. Journal of Geophysical Research 115, C10039.

.

.

APPENDIX 1: MARSH TRANSECT WAVE ATTENUATION DETAILED RESULTS

The following tables contain the full results from the Marsh Transect Wave Attenuation (MTWA) model. The naming convention is consistent through the tables and is as follows:

[T5]_[Sub-Task]_[Run]_C0[Storm Number]_[Tide case]_[Sea level rise case]

The descriptions of each naming element are found in the tables below.

Table 2. Descriptions of sub-task and run values used in the results naming convention.

Sub-Task	Run	Description
0	0	Base conditions
1	1	Vegetation changed to *Spartina alterniflora*
1	2	Vegetation changed to *Spartina patens*
2	1	No vegetation
2	2	No vegetation, lower platform elevation
2	3	Vegetation, lower platform elevation
3	0	Ditches filled
4	1	Oyster reefs present
4	2	No oyster reefs

Table 3. Descriptions of storm number, tide case, and sea level rise case short hands used in the results naming convention.

Storm Number	Description
4	Army Corps of Engineers (ACE) storm event analysis, #4 (Figure 27)
5	ACE storm event analysis, #5 (Figure 27)
6	ACE storm event analysis, #6 (Figure 27)
7	ACE storm event analysis, #7 (Figure 27)
Tide Case	**Description**
H	Water level simulates a spring high tide
L	Water level simulates a neap high tide
Sea Level Rise Case	**Description**
Base	No sea level rise included
SLR	Sea level rise effects included

For example, “T5_2_2_C04_H_Base” refers to the results from Storm C04 with no vegetation, lower marsh platform, spring high tide, and no sea level rise (Sub-task = 2; Run = 2; Storm number = 4; Tide case = H; Sea level rise case = Base).

Each column the following tables corresponds to one transect. The transect locations can be seen in Figure 63, where the large numbers correspond to the areas of interest and the small numbers (within the hexagons) correspond to the transects with the area of interest.

Table 4. Distance (m) to complete attenuation (wave height less than 0.04 m) for each transect. “7777” = The wave reached non-inundated land before the wave height decreased below 0.04m. “8889” = There was no wave at that location for the given storm and condition. “9999” = The wave height remained greater than 0.04 m for 1000 m.

Areas of Interest:	**1**	**1**	**1**	**2**	**2**	**2**	**3**	**3**	**3**	**4**	**4**	**4**	**5**	**5**	**5**	**6**	**6**	**6**	**7**	**7**	**7**
Transect Numbers:	**1**	**2**	**3**	**1**	**2**	**3**	**1**	**2**	**3**	**1**	**2**	**3**	**1**	**2**	**3**	**1**	**2**	**3**	**1**	**2**	**3**
T5_0_0_C04_H_Base	7777	198	366	73	38	22	138	196	80	35	61	51	7777	29	7777	187	326	196	20	30	53
T5_0_0_C04_L_Base	11	103	60	6	7	5	6	8	11	9	31	7777	8888	6	8888	7777	35	3	10	5	34
T5_0_0_C05_H_Base	119	161	202	64	35	20	108	177	69	36	63	58	7777	32	7777	179	322	190	20	21	48
T5_0_0_C05_L_Base	9	103	50	5	7	5	6	7	10	9	31	32	8888	6	8888	7777	35	3	10	5	33
T5_0_0_C06_H_Base	119	177	298	65	40	22	166	153	89	34	64	61	7777	29	7777	169	312	182	21	31	56
T5_0_0_C06_L_Base	9	103	51	6	7	5	7	7	11	9	31	32	8888	6	8888	7777	35	3	10	5	33
T5_0_0_C07_H_Base	119	147	216	69	47	24	193	157	91	36	65	63	7777	35	7777	180	328	193	22	33	60
T5_0_0_C07_L_Base	9	102	49	5	7	5	7	8	10	9	31	32	8888	6	8888	7777	35	3	10	5	33
T5_0_0_C04_H_SLR	116	156	172	46	28	18	81	421	56	30	58	45	7777	23	297	167	283	181	19	21	48
T5_0_0_C04_L_SLR	11	103	50	5	6	5	6	8	10	9	31	7777	7777	6	17	7777	35	3	10	5	34
T5_0_0_C05_H_SLR	91	142	151	35	27	18	67	212	47	31	58	45	7777	21	288	165	367	179	19	13	45
T5_0_0_C05_L_SLR	9	103	47	5	6	5	6	8	9	9	31	32	7777	6	17	7777	35	3	10	5	33
T5_0_0_C06_H_SLR	101	152	159	45	33	20	101	142	66	31	58	45	7777	22	269	159	280	173	20	22	51
T5_0_0_C06_L_SLR	9	103	49	5	7	5	6	8	10	9	31	32	7777	6	17	7777	35	3	10	5	34
T5_0_0_C07_H_SLR	99	142	161	55	41	24	116	143	76	34	60	48	7777	23	334	166	396	180	22	30	61
T5_0_0_C07_L_SLR	9	102	47	5	7	5	7	8	11	9	31	32	7777	6	17	7777	40	3	11	5	34

Table 5. Distance (m) to complete attenuation (wave height less than 0.04 m) for each transect. “7777” = The wave reached non-inundated land before the wave height decreased below 0.04m. “8889” = There was no wave at that location for the given storm and condition. “9999” = The wave height remained greater than 0.04 m for 1000 m.

Areas of Interest:	**1**	**1**	**1**	**2**	**2**	**2**	**3**	**3**	**3**	**4**	**4**	**4**	**5**	**5**	**5**	**6**	**6**	**6**	**7**	**7**	**7**
Transect Numbers:	**1**	**2**	**3**	**1**	**2**	**3**	**1**	**2**	**3**	**1**	**2**	**3**	**1**	**2**	**3**	**1**	**2**	**3**	**1**	**2**	**3**
T5_1_1_C04_H_Base	7777	251	732	87	45	25	195	378	128	38	62	56	7777	38	7777	262	385	242	22	44	62
T5_1_1_C04_L_Base	12	103	74	6	8	6	7	8	12	9	31	7777	8888	6	8888	7777	38	7777	11	5	34
T5_1_1_C05_H_Base	7777	233	344	78	40	23	154	366	90	39	64	61	7777	42	7777	252	374	235	21	30	54
T5_1_1_C05_L_Base	10	103	53	6	7	5	6	8	11	9	31	32	8888	6	8888	7777	38	7777	10	5	33
T5_1_1_C06_H_Base	7777	251	636	80	49	25	261	338	149	37	65	62	7777	38	7777	237	362	227	23	45	66
T5_1_1_C06_L_Base	10	103	55	6	8	6	7	8	12	9	31	32	8888	6	8888	7777	38	7777	10	5	33
T5_1_1_C07_H_Base	7777	173	470	84	59	27	331	342	152	40	66	63	7777	44	7777	254	389	238	25	49	75
T5_1_1_C07_L_Base	9	103	51	6	8	5	7	8	11	9	31	32	8888	6	8888	7777	38	7777	10	5	34
T5_1_2_C04_H_Base	106	140	165	54	32	22	73	63	53	41	63	58	7777	44	7777	265	194	149	22	18	47
T5_1_2_C04_L_Base	9	103	49	5	7	5	6	7	9	9	31	7777	8888	6	8888	7777	8	3	11	5	33
T5_1_2_C05_H_Base	89	137	150	49	32	23	63	62	42	41	65	62	7777	47	7777	238	179	137	22	12	46
T5_1_2_C05_L_Base	9	102	47	5	6	5	6	7	9	9	31	32	8888	6	8888	7777	7	3	11	5	33
T5_1_2_C06_H_Base	95	139	156	46	33	21	81	101	54	40	66	63	7777	44	7777	344	195	164	22	18	48
T5_1_2_C06_L_Base	9	102	47	5	7	5	6	7	9	9	31	32	8888	6	8888	7777	9	3	11	5	33
T5_1_2_C07_H_Base	92	135	150	49	37	21	85	81	56	41	67	64	7777	50	7777	215	179	135	21	19	50
T5_1_2_C07_L_Base	8	102	47	5	7	5	6	7	9	9	31	32	8888	6	8888	7777	6	3	11	5	33

Table 6. Distance (m) to complete attenuation (wave height less than 0.04 m) for each transect. “7777” = The wave reached non-inundated land before the wave height decreased below 0.04m. “8889” = There was no wave at that location for the given storm and condition. “9999” = The wave height remained greater than 0.04 m for 1000 m.

Areas of Interest:	**1**	**1**	**1**	**2**	**2**	**2**	**3**	**3**	**3**	**4**	**4**	**4**	**5**	**5**	**5**
Transect Numbers:	**1**	**2**	**3**	**1**	**2**	**3**	**1**	**2**	**3**	**1**	**2**	**3**	**1**	**2**	**3**
T5_2_1_C04_H_Base	7777	7777	7777	577	464	191	930	9999	632	25	38	35	7777	92	7777
T5_2_1_C04_L_Base	21	104	86	8	11	7	7	8	14	8	31	32	8888	7	8888
T5_2_1_C05_H_Base	7777	7777	7777	414	400	79	870	9999	573	28	38	35	7777	70	7777
T5_2_1_C05_L_Base	19	104	85	8	10	6	7	8	14	9	31	32	8888	6	8888
T5_2_1_C06_H_Base	7777	7777	7777	493	506	180	9999	9999	662	38	48	36	7777	81	7777
T5_2_1_C06_L_Base	19	104	85	8	11	7	7	8	14	9	31	32	8888	7	8888
T5_2_1_C07_H_Base	7777	7777	7777	554	594	258	9999	9999	688	26	33	33	7777	70	7777
T5_2_1_C07_L_Base	15	104	84	8	11	7	7	8	14	9	31	32	8888	6	8888
T5_2_2_C04_H_Base	7777	296	7777	9999	9999	657	9999	9999	7777	41	49	39	7777	261	7777
T5_2_2_C04_L_Base	57	111	116	16	17	9	20	11	25	9	32	32	8888	9	8888
T5_2_2_C05_H_Base	7777	296	7777	9999	9999	333	9999	9999	7777	45	51	39	7777	194	7777
T5_2_2_C05_L_Base	45	111	102	14	16	8	20	11	25	9	31	32	8888	8	8888
T5_2_2_C06_H_Base	7777	296	7777	9999	9999	442	9999	9999	7777	89	59	46	7777	224	7777
T5_2_2_C06_L_Base	46	111	103	16	18	9	20	11	25	10	31	32	8888	8	8888
T5_2_2_C07_H_Base	7777	295	7777	9999	9999	763	9999	9999	7777	43	48	36	7777	202	7777
T5_2_2_C07_L_Base	28	110	101	13	18	8	20	11	25	9	31	32	8888	7	8888
T5_2_3_C04_H_Base	120	253	7777	146	148	36	229	596	177	70	69	64	7777	68	359
T5_2_3_C04_L_Base	15	106	84	7	9	6	18	10	14	9	32	32	8888	6	8888
T5_2_3_C05_H_Base	120	252	648	108	69	31	192	525	131	78	70	65	7777	75	359
T5_2_3_C05_L_Base	13	105	58	6	9	6	8	10	13	9	31	32	8888	6	8888
T5_2_3_C06_H_Base	120	253	728	104	150	34	295	457	198	63	70	65	7777	67	359
T5_2_3_C06_L_Base	13	105	60	7	9	6	19	10	14	9	31	32	8888	6	8888
T5_2_3_C07_H_Base	120	250	653	115	260	39	384	467	215	82	70	65	7777	80	359
T5_2_3_C07_L_Base	11	103	56	6	9	6	19	10	13	9	31	32	8888	6	8888

Table 7. Distance (m) to complete attenuation (wave height less than 0.04 m) for each transect. “7777” = The wave reached non-inundated land before the wave height decreased below 0.04m. “8889” = There was no wave at that location for the given storm and condition. “9999” = The wave height remained greater than 0.04 m for 1000 m.

Areas of Interest:	**6**	**6**	**6**	**7**	**7**	**7**
Transect Numbers:	**1**	**2**	**3**	**1**	**2**	**3**
T5_2_1_C04_H_Base	9999	9999	7777	71	7777	386
T5_2_1_C04_L_Base	7777	51	7777	12	7777	34
T5_2_1_C05_H_Base	9999	9999	7777	35	548	288
T5_2_1_C05_L_Base	7777	51	7777	12	7777	34
T5_2_1_C06_H_Base	9999	9999	7777	78	7777	413
T5_2_1_C06_L_Base	7777	51	7777	12	7777	34
T5_2_1_C07_H_Base	9999	9999	7777	121	7777	484
T5_2_1_C07_L_Base	7777	51	7777	12	7777	34
T5_2_2_C04_H_Base	9999	9999	958	293	554	674
T5_2_2_C04_L_Base	13	68	11	13	6	35
T5_2_2_C05_H_Base	9999	9999	958	99	553	644
T5_2_2_C05_L_Base	13	68	11	12	6	35
T5_2_2_C06_H_Base	9999	9999	958	316	554	674
T5_2_2_C06_L_Base	15	68	11	12	6	35
T5_2_2_C07_H_Base	9999	9999	958	509	554	674
T5_2_2_C07_L_Base	13	67	11	13	6	35
T5_2_3_C04_H_Base	396	844	360	31	166	93
T5_2_3_C04_L_Base	5	46	7	12	6	34
T5_2_3_C05_H_Base	367	509	333	31	80	79
T5_2_3_C05_L_Base	5	46	7	12	5	34
T5_2_3_C06_H_Base	333	482	306	32	158	91
T5_2_3_C06_L_Base	5	46	7	12	5	34
T5_2_3_C07_H_Base	372	858	342	36	167	105
T5_2_3_C07_L_Base	5	46	7	12	5	34

Table 8. Distance (m) to complete attenuation (wave height less than 0.04 m) for each transect. “7777” = The wave reached non-inundated land before the wave height decreased below 0.04m. “8889” = There was no wave at that location for the given storm and condition. “9999” = The wave height remained greater than 0.04 m for 1000 m.

Areas of Interest:	**1**	**1**	**1**	**2**	**2**	**2**	**3**	**3**	**3**	**4**	**4**	**4**	**5**	**5**	**5**	**6**	**6**	**6**	**7**	**7**	**7**
Transect Numbers:	**1**	**2**	**3**	**1**	**2**	**3**	**1**	**2**	**3**	**1**	**2**	**3**	**1**	**2**	**3**	**1**	**2**	**3**	**1**	**2**	**3**
T5_3_0_C04_H_Base	7777	198	300	73	38	22	133	196	80	36	61	51	7777	29	7777	187	312	196	20	30	53
T5_3_0_C04_L_Base	11	103	60	6	7	5	6	8	11	9	32	32	8888	6	8888	7777	35	3	10	5	34
T5_3_0_C05_H_Base	119	161	202	64	35	20	107	177	69	37	63	58	7777	32	7777	179	291	190	20	21	48
T5_3_0_C05_L_Base	9	103	49	5	7	5	6	7	10	9	32	32	8888	6	8888	7777	35	3	10	5	33
T5_3_0_C06_H_Base	119	177	256	65	40	22	161	153	89	35	64	61	7777	29	7777	169	282	182	21	31	56
T5_3_0_C06_L_Base	9	103	50	6	7	5	7	7	11	9	32	32	8888	6	8888	7777	35	3	10	5	33
T5_3_0_C07_H_Base	119	147	215	69	47	24	186	156	91	37	65	63	7777	35	7777	180	315	192	22	33	60
T5_3_0_C07_L_Base	9	102	48	5	7	5	7	8	10	9	32	32	8888	6	8888	7777	35	3	10	5	33

Table 9. Initial wave height (m) for each transect.

Areas of Interest:	**1**	**1**	**1**	**2**	**2**	**2**	**3**	**3**	**3**	**4**	**4**	**4**
Transect Numbers:	**1**	**2**	**3**	**1**	**2**	**3**	**1**	**2**	**3**	**1**	**2**	**3**
T5_0_0_C04_H_Base	0.53	0.52	0.52	0.46	0.36	0.43	0.55	0.52	0.54	0.30	0.33	0.33
T5_0_0_C04_L_Base	0.42	0.44	0.47	0.40	0.31	0.37	0.48	0.32	0.47	0.27	0.33	0.33
T5_0_0_C05_H_Base	0.46	0.49	0.44	0.40	0.31	0.37	0.50	0.51	0.50	0.28	0.28	0.28
T5_0_0_C05_L_Base	0.35	0.39	0.38	0.35	0.27	0.32	0.43	0.35	0.43	0.26	0.27	0.27
T5_0_0_C06_H_Base	0.47	0.52	0.48	0.44	0.36	0.40	0.56	0.56	0.54	0.31	0.27	0.27
T5_0_0_C06_L_Base	0.34	0.39	0.38	0.37	0.30	0.34	0.48	0.41	0.45	0.29	0.26	0.26
T5_0_0_C07_H_Base	0.42	0.44	0.44	0.41	0.35	0.39	0.55	0.54	0.51	0.27	0.24	0.24
T5_0_0_C07_L_Base	0.27	0.32	0.34	0.32	0.27	0.30	0.47	0.42	0.40	0.26	0.22	0.22
T5_0_0_C04_H_SLR	0.64	0.64	0.59	0.51	0.39	0.47	0.61	0.63	0.61	0.39	0.41	0.41
T5_0_0_C04_L_SLR	0.54	0.53	0.53	0.46	0.35	0.43	0.56	0.51	0.54	0.29	0.34	0.34
T5_0_0_C05_H_SLR	0.54	0.58	0.51	0.45	0.34	0.41	0.56	0.59	0.56	0.34	0.38	0.38
T5_0_0_C05_L_SLR	0.45	0.49	0.45	0.41	0.31	0.37	0.51	0.51	0.50	0.28	0.28	0.28
T5_0_0_C06_H_SLR	0.57	0.61	0.55	0.49	0.42	0.47	0.62	0.65	0.60	0.36	0.40	0.40
T5_0_0_C06_L_SLR	0.47	0.52	0.48	0.44	0.36	0.40	0.57	0.55	0.54	0.31	0.27	0.27
T5_0_0_C07_H_SLR	0.54	0.54	0.53	0.49	0.43	0.49	0.62	0.62	0.60	0.30	0.33	0.33
T5_0_0_C07_L_SLR	0.40	0.43	0.43	0.40	0.34	0.38	0.56	0.54	0.51	0.27	0.24	0.24

Table 10: Initial wave height (m) for each transect.

Areas of Interest:	5	5	5	6	6	6	7	7	7
Transect Numbers:	**1**	**2**	**3**	**1**	**2**	**3**	**1**	**2**	**3**
T5_0_0_C04_H_Base	0.26	0.36	0.25	0.59	0.57	0.62	0.39	0.38	0.43
T5_0_0_C04_L_Base	0.00	0.35	0.00	0.43	0.36	0.51	0.32	0.24	0.31
T5_0_0_C05_H_Base	0.24	0.33	0.24	0.56	0.53	0.59	0.33	0.34	0.38
T5_0_0_C05_L_Base	0.00	0.30	0.00	0.43	0.34	0.49	0.25	0.20	0.27
T5_0_0_C06_H_Base	0.24	0.35	0.24	0.61	0.55	0.63	0.36	0.37	0.43
T5_0_0_C06_L_Base	0.00	0.31	0.00	0.45	0.35	0.52	0.24	0.21	0.28
T5_0_0_C07_H_Base	0.22	0.31	0.22	0.54	0.49	0.56	0.35	0.35	0.42
T5_0_0_C07_L_Base	0.00	0.26	0.00	0.42	0.32	0.47	0.23	0.21	0.26
T5_0_0_C04_H_SLR	0.41	0.47	0.41	0.70	0.70	0.71	0.45	0.47	0.51
T5_0_0_C04_L_SLR	0.24	0.35	0.23	0.61	0.44	0.63	0.38	0.37	0.42
T5_0_0_C05_H_SLR	0.37	0.43	0.38	0.65	0.63	0.66	0.39	0.40	0.44
T5_0_0_C05_L_SLR	0.22	0.31	0.22	0.58	0.41	0.61	0.33	0.33	0.37
T5_0_0_C06_H_SLR	0.39	0.46	0.39	0.69	0.65	0.71	0.43	0.44	0.51
T5_0_0_C06_L_SLR	0.23	0.33	0.22	0.63	0.43	0.65	0.36	0.36	0.43
T5_0_0_C07_H_SLR	0.34	0.40	0.34	0.63	0.60	0.65	0.42	0.43	0.53
T5_0_0_C07_L_SLR	0.20	0.29	0.20	0.55	0.43	0.58	0.35	0.34	0.41

Table 11. Initial wave height (m) for each transect.

Areas of Interest:	**1**	**1**	**1**	**2**	**2**	**2**	**3**	**3**	**3**	**4**	**4**	**4**
Transect Numbers:	**1**	**2**	**3**	**1**	**2**	**3**	**1**	**2**	**3**	**1**	**2**	**3**
T5_1_1_C05_H_Base	0.46	0.49	0.44	0.40	0.31	0.37	0.50	0.51	0.50	0.28	0.28	0.28
T5_1_1_C05_L_Base	0.35	0.39	0.38	0.35	0.27	0.32	0.43	0.35	0.43	0.26	0.27	0.27
T5_1_1_C06_H_Base	0.47	0.52	0.48	0.44	0.36	0.40	0.56	0.56	0.54	0.31	0.27	0.27
T5_1_1_C06_L_Base	0.34	0.39	0.38	0.37	0.30	0.34	0.48	0.41	0.45	0.29	0.26	0.26
T5_1_1_C07_H_Base	0.42	0.44	0.44	0.41	0.35	0.39	0.55	0.54	0.51	0.27	0.24	0.24
T5_1_1_C07_L_Base	0.27	0.32	0.34	0.32	0.27	0.30	0.47	0.42	0.40	0.26	0.22	0.22
T5_1_2_C04_H_Base	0.53	0.52	0.52	0.46	0.36	0.43	0.55	0.52	0.54	0.30	0.33	0.33
T5_1_2_C04_L_Base	0.42	0.44	0.47	0.40	0.31	0.37	0.48	0.32	0.47	0.27	0.33	0.33
T5_1_2_C05_H_Base	0.46	0.49	0.44	0.40	0.31	0.37	0.50	0.51	0.50	0.28	0.28	0.28
T5_1_2_C05_L_Base	0.35	0.39	0.38	0.35	0.27	0.32	0.43	0.35	0.43	0.26	0.27	0.27
T5_1_2_C06_H_Base	0.47	0.52	0.48	0.44	0.36	0.40	0.56	0.56	0.54	0.31	0.27	0.27
T5_1_2_C06_L_Base	0.34	0.39	0.38	0.37	0.30	0.34	0.48	0.41	0.45	0.29	0.26	0.26
T5_1_2_C07_H_Base	0.42	0.44	0.44	0.41	0.35	0.39	0.55	0.54	0.51	0.27	0.24	0.24
T5_1_2_C07_L_Base	0.27	0.32	0.34	0.32	0.27	0.30	0.47	0.42	0.40	0.26	0.22	0.22
T5_2_1_C04_H_Base	0.53	0.52	0.52	0.46	0.36	0.43	0.55	0.52	0.54	0.30	0.33	0.33
T5_2_1_C04_L_Base	0.42	0.44	0.47	0.40	0.31	0.37	0.48	0.32	0.47	0.27	0.33	0.33
T5_2_1_C05_H_Base	0.46	0.49	0.44	0.40	0.31	0.37	0.50	0.51	0.50	0.28	0.28	0.28
T5_2_1_C05_L_Base	0.35	0.39	0.38	0.35	0.27	0.32	0.43	0.35	0.43	0.26	0.27	0.27
T5_2_1_C06_H_Base	0.47	0.52	0.48	0.44	0.36	0.40	0.56	0.56	0.54	0.31	0.27	0.27
T5_2_1_C06_L_Base	0.34	0.39	0.38	0.37	0.30	0.34	0.48	0.41	0.45	0.29	0.26	0.26
T5_2_1_C07_H_Base	0.42	0.44	0.44	0.41	0.35	0.39	0.55	0.54	0.51	0.27	0.24	0.24
T5_2_1_C07_L_Base	0.27	0.32	0.34	0.32	0.27	0.30	0.47	0.42	0.40	0.26	0.22	0.22

Table 12: Initial wave height (m) for each transect.

Areas of Interest:	5	5	5	6	6	6	7	7	7
Transect Numbers:	**1**	**2**	**3**	**1**	**2**	**3**	**1**	**2**	**3**
T5_1_1_C05_H_Base	0.24	0.33	0.24	0.56	0.53	0.59	0.33	0.34	0.38
T5_1_1_C05_L_Base	0.00	0.30	0.00	0.43	0.34	0.49	0.25	0.20	0.27
T5_1_1_C06_H_Base	0.24	0.35	0.24	0.61	0.55	0.63	0.36	0.37	0.43
T5_1_1_C06_L_Base	0.00	0.31	0.00	0.45	0.35	0.52	0.24	0.21	0.28
T5_1_1_C07_H_Base	0.22	0.31	0.22	0.54	0.49	0.56	0.35	0.35	0.42
T5_1_1_C07_L_Base	0.00	0.26	0.00	0.42	0.32	0.47	0.23	0.21	0.26
T5_1_2_C04_H_Base	0.26	0.36	0.25	0.59	0.57	0.62	0.39	0.38	0.43
T5_1_2_C04_L_Base	0.00	0.35	0.00	0.43	0.36	0.51	0.32	0.24	0.31
T5_1_2_C05_H_Base	0.24	0.33	0.24	0.56	0.53	0.59	0.33	0.34	0.38
T5_1_2_C05_L_Base	0.00	0.30	0.00	0.43	0.34	0.49	0.25	0.20	0.27
T5_1_2_C06_H_Base	0.24	0.35	0.24	0.61	0.55	0.63	0.36	0.37	0.43
T5_1_2_C06_L_Base	0.00	0.31	0.00	0.45	0.35	0.52	0.24	0.21	0.28
T5_1_2_C07_H_Base	0.22	0.31	0.22	0.54	0.49	0.56	0.35	0.35	0.42
T5_1_2_C07_L_Base	0.00	0.26	0.00	0.42	0.32	0.47	0.23	0.21	0.26
T5_2_1_C04_H_Base	0.26	0.36	0.25	0.59	0.57	0.62	0.39	0.38	0.43
T5_2_1_C04_L_Base	0.00	0.35	0.00	0.43	0.36	0.51	0.32	0.24	0.31
T5_2_1_C05_H_Base	0.24	0.33	0.24	0.56	0.53	0.59	0.33	0.34	0.38
T5_2_1_C05_L_Base	0.00	0.30	0.00	0.43	0.34	0.49	0.25	0.20	0.27
T5_2_1_C06_H_Base	0.24	0.35	0.24	0.61	0.55	0.63	0.36	0.37	0.43
T5_2_1_C06_L_Base	0.00	0.31	0.00	0.45	0.35	0.52	0.24	0.21	0.28
T5_2_1_C07_H_Base	0.22	0.31	0.22	0.54	0.49	0.56	0.35	0.35	0.42
T5_2_1_C07_L_Base	0.00	0.26	0.00	0.42	0.32	0.47	0.23	0.21	0.26

Table 13. Initial wave height (m) for each transect.

Areas of Interest:	**1**	**1**	**1**	**2**	**2**	**2**	**3**	**3**	**3**	**4**	**4**	**4**
Transect Numbers:	**1**	**2**	**3**	**1**	**2**	**3**	**1**	**2**	**3**	**1**	**2**	**3**
T5_2_2_C05_H_Base	0.46	0.49	0.44	0.40	0.31	0.37	0.50	0.51	0.50	0.28	0.28	0.28
T5_2_2_C05_L_Base	0.35	0.39	0.38	0.35	0.27	0.32	0.43	0.35	0.43	0.26	0.27	0.27
T5_2_2_C06_H_Base	0.47	0.52	0.48	0.44	0.36	0.40	0.56	0.56	0.54	0.31	0.27	0.27
T5_2_2_C06_L_Base	0.34	0.39	0.38	0.37	0.30	0.34	0.48	0.41	0.45	0.29	0.26	0.26
T5_2_2_C07_H_Base	0.42	0.44	0.44	0.41	0.35	0.39	0.55	0.54	0.51	0.27	0.24	0.24
T5_2_2_C07_L_Base	0.27	0.32	0.34	0.32	0.27	0.30	0.47	0.42	0.40	0.26	0.22	0.22
T5_2_3_C04_H_Base	0.53	0.52	0.52	0.46	0.36	0.43	0.55	0.52	0.54	0.30	0.33	0.33
T5_2_3_C04_L_Base	0.42	0.44	0.47	0.40	0.31	0.37	0.48	0.32	0.47	0.27	0.33	0.33
T5_2_3_C05_H_Base	0.46	0.49	0.44	0.40	0.31	0.37	0.50	0.51	0.50	0.28	0.28	0.28
T5_2_3_C05_L_Base	0.35	0.39	0.38	0.35	0.27	0.32	0.43	0.35	0.43	0.26	0.27	0.27
T5_2_3_C06_H_Base	0.47	0.52	0.48	0.44	0.36	0.40	0.56	0.56	0.54	0.31	0.27	0.27
T5_2_3_C06_L_Base	0.34	0.39	0.38	0.37	0.30	0.34	0.48	0.41	0.45	0.29	0.26	0.26
T5_2_3_C07_H_Base	0.42	0.44	0.44	0.41	0.35	0.39	0.55	0.54	0.51	0.27	0.24	0.24
T5_2_3_C07_L_Base	0.27	0.32	0.34	0.32	0.27	0.30	0.47	0.42	0.40	0.26	0.22	0.22
'T5_3_0_C04_H_Base	0.53	0.52	0.52	0.46	0.36	0.43	0.55	0.52	0.54	0.30	0.33	0.33
T5_3_0_C04_L_Base	0.42	0.44	0.47	0.40	0.31	0.37	0.48	0.32	0.47	0.27	0.33	0.33
T5_3_0_C05_H_Base	0.46	0.49	0.44	0.40	0.31	0.37	0.50	0.51	0.50	0.28	0.28	0.28
T5_3_0_C05_L_Base	0.35	0.39	0.38	0.35	0.27	0.32	0.43	0.35	0.43	0.26	0.27	0.27
T5_3_0_C06_H_Base	0.47	0.52	0.48	0.44	0.36	0.40	0.56	0.56	0.54	0.31	0.27	0.27
T5_3_0_C06_L_Base	0.34	0.39	0.38	0.37	0.30	0.34	0.48	0.41	0.45	0.29	0.26	0.26
T5_3_0_C07_H_Base	0.42	0.44	0.44	0.41	0.35	0.39	0.55	0.54	0.51	0.27	0.24	0.24
T5_3_0_C07_L_Base	0.27	0.32	0.34	0.32	0.27	0.30	0.47	0.42	0.40	0.26	0.22	0.22

Table 14. Initial wave height (m) for each transect.

Areas of Interest:	**5**	**5**	**5**	**6**	**6**	**6**	**7**	**7**	**7**
Transect Numbers:	**1**	**2**	**3**	**1**	**2**	**3**	**1**	**2**	**3**
T5_2_2_C05_H_Base	0.24	0.33	0.24	0.56	0.53	0.59	0.33	0.34	0.38
T5_2_2_C05_L_Base	0.00	0.30	0.00	0.43	0.34	0.49	0.25	0.20	0.27
T5_2_2_C06_H_Base	0.24	0.35	0.24	0.61	0.55	0.63	0.36	0.37	0.43
T5_2_2_C06_L_Base	0.00	0.31	0.00	0.45	0.35	0.52	0.24	0.21	0.28
T5_2_2_C07_H_Base	0.22	0.31	0.22	0.54	0.49	0.56	0.35	0.35	0.42
T5_2_2_C07_L_Base	0.00	0.26	0.00	0.42	0.32	0.47	0.23	0.21	0.26
T5_2_3_C04_H_Base	0.26	0.36	0.25	0.59	0.57	0.62	0.39	0.38	0.43
T5_2_3_C04_L_Base	0.00	0.35	0.00	0.43	0.36	0.51	0.32	0.24	0.31
T5_2_3_C05_H_Base	0.24	0.33	0.24	0.56	0.53	0.59	0.33	0.34	0.38
T5_2_3_C05_L_Base	0.00	0.30	0.00	0.43	0.34	0.49	0.25	0.20	0.27
T5_2_3_C06_H_Base	0.24	0.35	0.24	0.61	0.55	0.63	0.36	0.37	0.43
T5_2_3_C06_L_Base	0.00	0.31	0.00	0.45	0.35	0.52	0.24	0.21	0.28
T5_2_3_C07_H_Base	0.22	0.31	0.22	0.54	0.49	0.56	0.35	0.35	0.42
T5_2_3_C07_L_Base	0.00	0.26	0.00	0.42	0.32	0.47	0.23	0.21	0.26
'T5_3_0_C04_H_Base	0.26	0.36	0.25	0.59	0.57	0.62	0.39	0.38	0.43
T5_3_0_C04_L_Base	0.00	0.35	0.00	0.43	0.36	0.51	0.32	0.24	0.31
T5_3_0_C05_H_Base	0.24	0.33	0.24	0.56	0.53	0.59	0.33	0.34	0.38
T5_3_0_C05_L_Base	0.00	0.30	0.00	0.43	0.34	0.49	0.25	0.20	0.27
T5_3_0_C06_H_Base	0.24	0.35	0.24	0.61	0.55	0.63	0.36	0.37	0.43
T5_3_0_C06_L_Base	0.00	0.31	0.00	0.45	0.35	0.52	0.24	0.21	0.28
T5_3_0_C07_H_Base	0.22	0.31	0.22	0.54	0.49	0.56	0.35	0.35	0.42
T5_3_0_C07_L_Base	0.00	0.26	0.00	0.42	0.32	0.47	0.23	0.21	0.26

Table 15. Final wave height (m) for each transect.

Areas of Interest:	1	1	1	2	2	2	3	3	3
Transect Numbers:	**1**	**2**	**3**	**1**	**2**	**3**	**1**	**2**	**3**
T5_0_0_C04_H_Base	0.048	0.021	0.008	0.002	0.001	0.001	0.004	0.011	0.003
T5_0_0_C04_L_Base	0.000	0.003	0.001	0.000	0.000	0.000	0.002	0.002	0.000
T5_0_0_C05_H_Base	0.031	0.016	0.004	0.001	0.001	0.000	0.003	0.010	0.002
T5_0_0_C05_L_Base	0.000	0.002	0.000	0.000	0.000	0.000	0.001	0.001	0.000
T5_0_0_C06_H_Base	0.037	0.019	0.007	0.001	0.001	0.001	0.006	0.009	0.004
T5_0_0_C06_L_Base	0.000	0.001	0.000	0.000	0.000	0.000	0.002	0.001	0.000
T5_0_0_C07_H_Base	0.031	0.012	0.005	0.001	0.002	0.001	0.007	0.009	0.004
T5_0_0_C07_L_Base	0.000	0.001	0.000	0.000	0.000	0.000	0.003	0.001	0.000
T5_0_0_C04_H_SLR	0.032	0.015	0.004	0.001	0.001	0.000	0.002	0.015	0.002
T5_0_0_C04_L_SLR	0.000	0.002	0.000	0.000	0.000	0.000	0.001	0.001	0.000
T5_0_0_C05_H_SLR	0.021	0.010	0.003	0.001	0.000	0.000	0.002	0.011	0.001
T5_0_0_C05_L_SLR	0.000	0.001	0.000	0.000	0.000	0.000	0.001	0.001	0.000
T5_0_0_C06_H_SLR	0.025	0.013	0.004	0.001	0.001	0.001	0.003	0.009	0.002
T5_0_0_C06_L_SLR	0.000	0.001	0.000	0.000	0.000	0.000	0.002	0.001	0.000
T5_0_0_C07_H_SLR	0.024	0.010	0.004	0.001	0.002	0.001	0.004	0.009	0.003
T5_0_0_C07_L_SLR	0.000	0.001	0.000	0.000	0.000	0.001	0.002	0.001	0.000
T5_1_1_C04_H_Base	0.072	0.035	0.014	0.002	0.002	0.001	0.007	0.015	0.005
T5_1_1_C04_L_Base	0.000	0.004	0.002	0.000	0.000	0.001	0.003	0.001	0.001
T5_1_1_C05_H_Base	0.046	0.025	0.007	0.002	0.001	0.001	0.005	0.014	0.004
T5_1_1_C05_L_Base	0.000	0.002	0.000	0.000	0.000	0.001	0.002	0.002	0.000
T5_1_1_C06_H_Base	0.055	0.031	0.011	0.002	0.002	0.001	0.010	0.012	0.006
T5_1_1_C06_L_Base	0.000	0.002	0.000	0.000	0.000	0.001	0.004	0.002	0.001
T5_1_1_C07_H_Base	0.045	0.018	0.009	0.002	0.003	0.001	0.012	0.013	0.006
T5_1_1_C07_L_Base	0.000	0.001	0.000	0.000	0.000	0.001	0.006	0.002	0.000

Table 16. Final wave height (m) for each transect.

Areas of Interest:	4	4	4	5	5	5	6	6	6	7	7	7
Transect Numbers:	**1**	**2**	**3**	**1**	**2**	**3**	**1**	**2**	**3**	**1**	**2**	**3**
T5_0_0_C04_H_Base	0.002	0.002	0.006	0.075	0.000	0.055	0.011	0.014	0.007	0.001	0.004	0.001
T5_0_0_C04_L_Base	0.001	0.002	0.040	0.000	0.000	0.000	0.082	0.005	0.032	0.001	0.008	0.001
T5_0_0_C05_H_Base	0.002	0.002	0.006	0.086	0.000	0.058	0.010	0.014	0.007	0.001	0.003	0.001
T5_0_0_C05_L_Base	0.001	0.002	0.036	0.000	0.000	0.000	0.082	0.005	0.033	0.000	0.002	0.000
T5_0_0_C06_H_Base	0.002	0.001	0.006	0.085	0.000	0.056	0.010	0.013	0.007	0.001	0.004	0.001
T5_0_0_C06_L_Base	0.001	0.002	0.036	0.000	0.000	0.000	0.085	0.005	0.034	0.000	0.002	0.000
T5_0_0_C07_H_Base	0.002	0.001	0.005	0.120	0.000	0.097	0.010	0.015	0.007	0.001	0.004	0.001
T5_0_0_C07_L_Base	0.001	0.001	0.031	0.000	0.000	0.000	0.081	0.005	0.033	0.000	0.004	0.000
T5_0_0_C04_H_SLR	0.001	0.002	0.005	0.054	0.000	0.032	0.009	0.012	0.006	0.000	0.003	0.001
T5_0_0_C04_L_SLR	0.001	0.003	0.041	0.077	0.000	0.006	0.105	0.005	0.035	0.001	0.011	0.001
T5_0_0_C05_H_SLR	0.001	0.002	0.005	0.053	0.000	0.031	0.009	0.018	0.006	0.000	0.002	0.000
T5_0_0_C05_L_SLR	0.001	0.002	0.037	0.072	0.000	0.006	0.102	0.005	0.035	0.001	0.007	0.001
T5_0_0_C06_H_SLR	0.001	0.002	0.005	0.051	0.000	0.029	0.009	0.012	0.006	0.001	0.003	0.001
T5_0_0_C06_L_SLR	0.001	0.002	0.038	0.074	0.000	0.006	0.107	0.006	0.036	0.001	0.012	0.001
T5_0_0_C07_H_SLR	0.002	0.002	0.005	0.060	0.000	0.036	0.009	0.020	0.006	0.001	0.004	0.001
T5_0_0_C07_L_SLR	0.001	0.001	0.034	0.056	0.000	0.004	0.099	0.009	0.035	0.001	0.014	0.001
T5_1_1_C04_H_Base	0.003	0.002	0.008	0.089	0.001	0.068	0.014	0.019	0.009	0.001	0.006	0.001
T5_1_1_C04_L_Base	0.001	0.003	0.042	0.000	0.000	0.000	0.088	0.007	0.043	0.001	0.012	0.001
T5_1_1_C05_H_Base	0.003	0.002	0.008	0.100	0.001	0.071	0.014	0.019	0.009	0.001	0.004	0.001
T5_1_1_C05_L_Base	0.001	0.003	0.036	0.000	0.000	0.000	0.089	0.007	0.044	0.000	0.003	0.000
T5_1_1_C06_H_Base	0.002	0.002	0.008	0.099	0.001	0.069	0.013	0.018	0.009	0.001	0.006	0.001
T5_1_1_C06_L_Base	0.001	0.002	0.036	0.000	0.000	0.000	0.092	0.007	0.044	0.000	0.004	0.001
T5_1_1_C07_H_Base	0.003	0.002	0.007	0.130	0.001	0.111	0.014	0.019	0.009	0.001	0.007	0.002
T5_1_1_C07_L_Base	0.001	0.001	0.031	0.000	0.000	0.000	0.088	0.007	0.043	0.000	0.007	0.001

Table 17. Final wave height (m) for each transect.

Areas of Interest:	1	1	1	2	2	2	3	3	3
Transect Numbers:	**1**	**2**	**3**	**1**	**2**	**3**	**1**	**2**	**3**
T5_1_2_C05_H_Base	0.019	0.007	0.002	0.001	0.001	0.001	0.002	0.005	0.001
T5_1_2_C05_L_Base	0.000	0.001	0.000	0.000	0.000	0.000	0.001	0.001	0.000
T5_1_2_C06_H_Base	0.021	0.008	0.003	0.001	0.001	0.001	0.002	0.007	0.002
T5_1_2_C06_L_Base	0.000	0.001	0.000	0.000	0.000	0.000	0.001	0.001	0.000
T5_1_2_C07_H_Base	0.019	0.006	0.003	0.001	0.001	0.001	0.002	0.006	0.002
T5_1_2_C07_L_Base	0.000	0.000	0.000	0.000	0.000	0.000	0.001	0.001	0.000
T5_2_1_C04_H_Base	0.275	0.143	0.062	0.021	0.016	0.008	0.038	0.073	0.030
T5_2_1_C04_L_Base	0.003	0.020	0.005	0.002	0.001	0.006	0.013	0.007	0.004
T5_2_1_C05_H_Base	0.223	0.125	0.046	0.015	0.012	0.005	0.033	0.069	0.026
T5_2_1_C05_L_Base	0.002	0.015	0.003	0.001	0.001	0.004	0.011	0.008	0.003
T5_2_1_C06_H_Base	0.241	0.135	0.057	0.018	0.019	0.008	0.041	0.074	0.032
T5_2_1_C06_L_Base	0.002	0.014	0.003	0.002	0.001	0.006	0.015	0.011	0.004
T5_2_1_C07_H_Base	0.214	0.109	0.051	0.020	0.024	0.011	0.043	0.073	0.033
T5_2_1_C07_L_Base	0.001	0.009	0.002	0.001	0.001	0.004	0.016	0.012	0.003
T5_2_2_C04_H_Base	0.219	0.034	0.246	0.053	0.057	0.024	0.077	0.142	0.074
T5_2_2_C04_L_Base	0.002	0.001	0.001	0.000	0.000	0.000	0.005	0.001	0.011
T5_2_2_C05_H_Base	0.168	0.030	0.217	0.042	0.048	0.016	0.067	0.129	0.062
T5_2_2_C05_L_Base	0.001	0.001	0.000	0.000	0.000	0.000	0.004	0.001	0.009
T5_2_2_C06_H_Base	0.188	0.033	0.219	0.043	0.057	0.022	0.077	0.131	0.071
T5_2_2_C06_L_Base	0.001	0.001	0.000	0.000	0.000	0.000	0.005	0.001	0.011
T5_2_2_C07_H_Base	0.156	0.024	0.210	0.048	0.067	0.030	0.081	0.130	0.073
T5_2_2_C07_L_Base	0.001	0.000	0.000	0.000	0.000	0.000	0.006	0.001	0.010

Table 18. Final wave height (m) for each transect.

Areas of Interest:	4	4	4	5	5	5	6	6	6	7	7	7
Transect Numbers:	**1**	**2**	**3**	**1**	**2**	**3**	**1**	**2**	**3**	**1**	**2**	**3**
T5_1_2_C05_H_Base	0.003	0.003	0.010	0.077	0.001	0.052	0.013	0.007	0.005	0.001	0.002	0.000
T5_1_2_C05_L_Base	0.001	0.003	0.037	0.000	0.000	0.000	0.097	0.003	0.029	0.001	0.002	0.000
T5_1_2_C06_H_Base	0.003	0.002	0.009	0.079	0.001	0.052	0.018	0.008	0.006	0.001	0.002	0.001
T5_1_2_C06_L_Base	0.001	0.003	0.037	0.000	0.000	0.000	0.097	0.003	0.039	0.000	0.002	0.000
T5_1_2_C07_H_Base	0.004	0.002	0.008	0.098	0.001	0.075	0.012	0.007	0.004	0.001	0.002	0.001
T5_1_2_C07_L_Base	0.001	0.001	0.031	0.000	0.000	0.000	0.096	0.002	0.028	0.001	0.003	0.000
T5_2_1_C04_H_Base	0.000	0.000	0.000	0.180	0.002	0.179	0.099	0.097	0.057	0.007	0.046	0.010
T5_2_1_C04_L_Base	0.000	0.000	0.018	0.000	0.002	0.000	0.113	0.036	0.225	0.006	0.091	0.010
T5_2_1_C05_H_Base	0.000	0.000	0.000	0.174	0.001	0.173	0.093	0.091	0.055	0.002	0.034	0.007
T5_2_1_C05_L_Base	0.000	0.000	0.017	0.000	0.001	0.000	0.112	0.036	0.224	0.001	0.041	0.004
T5_2_1_C06_H_Base	0.000	0.000	0.000	0.176	0.002	0.173	0.098	0.096	0.060	0.007	0.046	0.013
T5_2_1_C06_L_Base	0.001	0.000	0.027	0.000	0.001	0.000	0.118	0.039	0.246	0.001	0.046	0.005
T5_2_1_C07_H_Base	0.000	0.000	0.000	0.170	0.001	0.184	0.092	0.092	0.055	0.010	0.048	0.015
T5_2_1_C07_L_Base	0.000	0.000	0.023	0.000	0.000	0.000	0.111	0.033	0.217	0.003	0.071	0.006
T5_2_2_C04_H_Base	0.000	0.000	0.000	0.198	0.008	0.064	0.168	0.150	0.001	0.004	0.000	0.000
T5_2_2_C04_L_Base	0.000	0.000	0.000	0.000	0.000	0.000	0.001	0.001	0.002	0.001	0.030	0.004
T5_2_2_C05_H_Base	0.000	0.000	0.000	0.186	0.005	0.060	0.155	0.139	0.001	0.001	0.000	0.000
T5_2_2_C05_L_Base	0.000	0.000	0.000	0.000	0.000	0.000	0.001	0.001	0.002	0.000	0.011	0.002
T5_2_2_C06_H_Base	0.000	0.000	0.000	0.188	0.007	0.062	0.158	0.143	0.001	0.005	0.000	0.000
T5_2_2_C06_L_Base	0.000	0.000	0.000	0.000	0.000	0.000	0.001	0.001	0.002	0.000	0.012	0.002
T5_2_2_C07_H_Base	0.000	0.000	0.000	0.173	0.005	0.051	0.153	0.141	0.000	0.007	0.000	0.000
T5_2_2_C07_L_Base	0.000	0.000	0.000	0.000	0.000	0.000	0.001	0.000	0.002	0.001	0.022	0.002

Table 19. Final wave height (m) for each transect.

Areas of Interest:	**1**	**1**	**1**	**2**	**2**	**2**	**3**	**3**	**3**
Transect Numbers:	**1**	**2**	**3**	**1**	**2**	**3**	**1**	**2**	**3**
T5_2_3_C05_H_Base	0.020	0.003	0.029	0.003	0.004	0.002	0.007	0.021	0.006
T5_2_3_C05_L_Base	0.000	0.000	0.000	0.000	0.000	0.000	0.000	0.000	0.001
T5_2_3_C06_H_Base	0.024	0.004	0.036	0.003	0.005	0.002	0.011	0.018	0.008
T5_2_3_C06_L_Base	0.000	0.000	0.000	0.000	0.000	0.000	0.001	0.000	0.001
T5_2_3_C07_H_Base	0.018	0.002	0.031	0.004	0.006	0.002	0.013	0.018	0.009
T5_2_3_C07_L_Base	0.000	0.000	0.000	0.000	0.000	0.000	0.001	0.000	0.001
'T5_3_0_C04_H_Base	0.048	0.021	0.008	0.002	0.001	0.001	0.004	0.012	0.003
T5_3_0_C04_L_Base	0.000	0.003	0.001	0.000	0.000	0.000	0.002	0.002	0.000
T5_3_0_C05_H_Base	0.031	0.016	0.005	0.001	0.001	0.000	0.003	0.011	0.002
T5_3_0_C05_L_Base	0.000	0.002	0.000	0.000	0.000	0.000	0.001	0.001	0.000
T5_3_0_C06_H_Base	0.037	0.019	0.007	0.001	0.002	0.001	0.006	0.010	0.004
T5_3_0_C06_L_Base	0.000	0.001	0.000	0.000	0.000	0.000	0.002	0.001	0.000
T5_3_0_C07_H_Base	0.031	0.012	0.006	0.001	0.002	0.001	0.006	0.010	0.004
T5_3_0_C07_L_Base	0.000	0.001	0.000	0.000	0.000	0.000	0.003	0.001	0.000

Table 20. Final wave height (m) for each transect.

Areas of Interest:	**4**	**4**	**4**	**5**	**5**	**5**	**6**	**6**	**6**	**7**	**7**	**7**
Transect Numbers:	**1**	**2**	**3**	**1**	**2**	**3**	**1**	**2**	**3**	**1**	**2**	**3**
T5_2_3_C05_H_Base	0.000	0.001	0.000	0.157	0.002	0.007	0.019	0.024	0.000	0.000	0.000	0.000
T5_2_3_C05_L_Base	0.000	0.000	0.000	0.000	0.000	0.000	0.000	0.000	0.000	0.000	0.000	0.000
T5_2_3_C06_H_Base	0.000	0.001	0.000	0.157	0.002	0.007	0.017	0.022	0.000	0.000	0.000	0.000
T5_2_3_C06_L_Base	0.000	0.000	0.000	0.000	0.000	0.000	0.000	0.000	0.000	0.000	0.001	0.000
T5_2_3_C07_H_Base	0.000	0.001	0.000	0.167	0.002	0.004	0.020	0.026	0.000	0.001	0.000	0.000
T5_2_3_C07_L_Base	0.000	0.000	0.000	0.000	0.000	0.000	0.000	0.000	0.000	0.000	0.001	0.000
'T5_3_0_C04_H_Base	0.002	0.002	0.006	0.075	0.000	0.055	0.011	0.014	0.007	0.001	0.004	0.001
T5_3_0_C04_L_Base	0.001	0.003	0.031	0.000	0.000	0.000	0.082	0.005	0.032	0.001	0.008	0.001
T5_3_0_C05_H_Base	0.002	0.002	0.006	0.086	0.000	0.058	0.010	0.014	0.007	0.001	0.002	0.000
T5_3_0_C05_L_Base	0.001	0.002	0.025	0.000	0.000	0.000	0.082	0.005	0.033	0.000	0.002	0.000
T5_3_0_C06_H_Base	0.002	0.001	0.006	0.085	0.000	0.056	0.009	0.013	0.007	0.001	0.004	0.001
T5_3_0_C06_L_Base	0.001	0.002	0.025	0.000	0.000	0.000	0.085	0.005	0.034	0.000	0.002	0.000
T5_3_0_C07_H_Base	0.002	0.001	0.005	0.120	0.000	0.097	0.010	0.014	0.007	0.001	0.004	0.001
T5_3_0_C07_L_Base	0.001	0.001	0.021	0.000	0.000	0.000	0.081	0.005	0.033	0.000	0.004	0.000

Table 21. Distance (m) to complete attenuation (wave height less than 0.04 m) for each transect for oyster reef placement simulation.

Oyster Transect	1	2
T5_4_1_C04_H_Base	489	782
T5_4_1_C04_L_Base	53	151
T5_4_1_C05_H_Base	448	782
T5_4_1_C05_L_Base	53	151
T5_4_1_C06_H_Base	53	782
T5_4_1_C06_L_Base	53	151
T5_4_1_C07_H_Base	490	782
T5_4_1_C07_L_Base	53	151
T5_4_2_C04_H_Base	451	782
T5_4_2_C04_L_Base	53	151
T5_4_2_C05_H_Base	490	782
T5_4_2_C05_L_Base	53	151
T5_4_2_C06_H_Base	418	782
T5_4_2_C06_L_Base	53	151
T5_4_2_C07_H_Base	433	782
T5_4_2_C07_L_Base	53	151

Table 22. Initial wave height (m) for each transect for oyster reef placement simulation.

Oyster Transect	1	2
T5_4_1_C04_L_Base	0.27	0.26
T5_4_1_C05_H_Base	0.43	0.44
T5_4_1_C05_L_Base	0.28	0.26
T5_4_1_C06_H_Base	0.47	0.47
T5_4_1_C06_L_Base	0.31	0.27
T5_4_1_C07_H_Base	0.44	0.44
T5_4_1_C07_L_Base	0.29	0.26
T5_4_2_C04_H_Base	0.44	0.47
T5_4_2_C04_L_Base	0.27	0.26
T5_4_2_C05_H_Base	0.43	0.44
T5_4_2_C05_L_Base	0.28	0.26
T5_4_2_C06_H_Base	0.47	0.47
T5_4_2_C06_L_Base	0.31	0.27
T5_4_2_C07_H_Base	0.44	0.44
T5_4_2_C07_L_Base	0.29	0.26

Table 23. Final wave height (m) for each transect for oyster reef placement simulation.

Oyster Transect	1	2
T5_4_1_C04_L_Base	0.003	0.000
T5_4_1_C05_H_Base	0.012	0.014
T5_4_1_C05_L_Base	0.002	0.000
T5_4_1_C06_H_Base	0.010	0.014
T5_4_1_C06_L_Base	0.002	0.000
T5_4_1_C07_H_Base	0.011	0.014
T5_4_1_C07_L_Base	0.002	0.000
T5_4_2_C04_H_Base	0.013	0.014
T5_4_2_C04_L_Base	0.003	0.000
T5_4_2_C05_H_Base	0.012	0.014
T5_4_2_C05_L_Base	0.002	0.000
T5_4_2_C06_H_Base	0.010	0.014
T5_4_2_C06_L_Base	0.002	0.000
T5_4_2_C07_H_Base	0.011	0.014
T5_4_2_C07_L_Base	0.002	0.000